

AD-A135 609

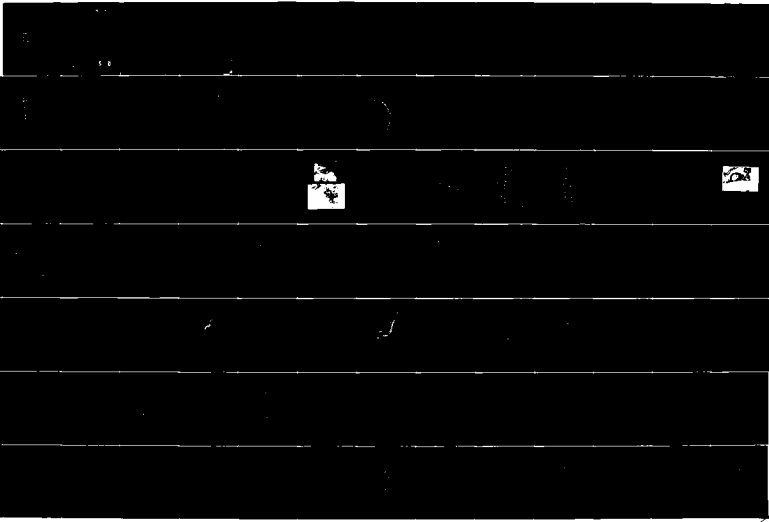
OBSERVATIONS OF A MIDLATITUDE SQUALL LINE BOUNDARY
LAYER WAKEUP AIR FORCE INST OF TECH WRIGHT-PATTERSON
AFB OH P HAMILTON 1987 AFIT/CI/NR-87-451

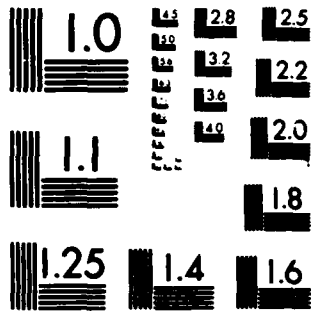
1/2

UNCLASSIFIED

F 1 4/2

NL





MICROCOPY RESOLUTION TEST CHART
NATIONAL BUREAU OF STANDARDS-1963-A

①

DTIC FILE COPY 4/5

AD-A185 609

THESIS

OBSERVATIONS OF A MIDLATITUDE SQUALL LINE BOUNDARY LAYER WAKE

Submitted by
Paul Hamilton
Department of Atmospheric Science

In partial fulfillment of the requirements
for the degree of Master of Science
Colorado State University
Fort Collins, Colorado
Summer, 1987

DTIC
ELECTE
OCT 27 1987
S H D

DISTRIBUTION STATEMENT A
Approved for public release;
Distribution Unlimited

REPORT DOCUMENTATION PAGE		READ INSTRUCTIONS BEFORE COMPLETING FORM
1. REPORT NUMBER AFIT/CI/NR 87- 45T	2. GOVT ACCESSION NO.	3. RECIPIENT'S CATALOG NUMBER
4. TITLE (and Subtitle) Observations of a Midlatitude Squall Line Boundary Layer Wake		5. TYPE OF REPORT & PERIOD COVERED THESIS/DISSERTATION
		6. PERFORMING ORG. REPORT NUMBER
7. AUTHOR(s) Paul Hamilton		8. CONTRACT OR GRANT NUMBER(s)
9. PERFORMING ORGANIZATION NAME AND ADDRESS AFIT STUDENT AT: Colorado State University		10. PROGRAM ELEMENT, PROJECT, TASK AREA & WORK UNIT NUMBERS
11. CONTROLLING OFFICE NAME AND ADDRESS AFIT/NR WPAFB OH 45433-6583		12. REPORT DATE 1987
		13. NUMBER OF PAGES 93
14. MONITORING AGENCY NAME & ADDRESS (if different from Controlling Office)		15. SECURITY CLASS. (of this report) UNCLASSIFIED
		15a. DECLASSIFICATION/DOWNGRADING SCHEDULE
16. DISTRIBUTION STATEMENT (of this Report) APPROVED FOR PUBLIC RELEASE; DISTRIBUTION UNLIMITED		
17. DISTRIBUTION STATEMENT (of the abstract entered in Block 20, if different from Report)		
18. SUPPLEMENTARY NOTES APPROVED FOR PUBLIC RELEASE: IAW AFR 190-1		Lynn E. Wolaver Dean for Research and Professional Development AFIT/NR
19. KEY WORDS (Continue on reverse side if necessary and identify by block number)		
20. ABSTRACT (Continue on reverse side if necessary and identify by block number) ATTACHED		

45

ABSTRACT OF THESIS

OBSERVATIONS OF A MIDLATITUDE SQUALL LINE BOUNDARY LAYER WAKE

Mesoscale pressure perturbations frequently observed with mesoscale convective systems (MCS) are examined with special emphasis on the characteristics, structure, lifecycle and driving mechanism of the "wake depression" found in the wake region of the convection. A severe squall line which traversed the OK PRE-STORM surface and upper air mesonet-work on 10-11 June 1985 is the focus of this observational study. Extensive surface, upper air and digitized radar data collected during the OK PRE-STORM field experiment were used for analysis.

Various mesoanalyses of this squall line at the surface and aloft have allowed for intensive examination of three pressure features observed with this squall line: the mesohigh, wake depression and pre-squall mesolow. Their relationship to and interaction with other meteorological parameters such as precipitation, temperature, potential temperature and moisture are explored. Furthermore, the mesoscale system-relative "jets" observed with midlatitude squall lines are examined for their possible influence on the pressure field.

The mesohigh develops quickly during the early growth of the squall line and precedes the wake depression by several hours. The predominant mesohigh is linked to the formation of a large cold pool which developed as a result of widespread hail and intense rainfall from a supercell ahead of the young squall line.

Analyses show the wake depression not to be a uniform, stagnant feature behind the mesohigh but appears to have embedded small-scale features, a distinct lifecycle and can undergo rapid intensification. The wake depression also is related with some aspects of the squall line's precipitation pattern. The low consistently "hugs" the back edge of the



Per	
Ad	<input checked="" type="checkbox"/>
lon	<input type="checkbox"/>
on/	
ity Codes	

Dist	Avail and/or Special
A-1	

stratiform precipitation and is observed to split into two separate lows as the convective line splits. Additionally, the wake depression is a hydrostatic response to a layer of warm, dry air (produced by subsidence) found just above the surface. It is suggested that the wake depression is in part a surface manifestation of forced subsidence by the descending rear inflow jet.

Paul Hamilton
Department of Atmospheric Science
Colorado State University
Fort Collins, Colorado 80523
Summer, 1987

COLORADO STATE UNIVERSITY

May 13, 1987

We hereby recommend that the Thesis OBSERVATIONS OF A MIDLATITUDE SQUALL LINE BOUNDARY LAYER WAKE prepared under our supervision by Paul Hamilton be accepted as fulfilling in part requirements for the degree of Master of Science.

Committee on Graduate Work

Committee Member

Donald F. Meyer

Committee Member

Wayne H. Schubert

Committee Member

Richard H. Johnson

Adviser

Department Head

ABSTRACT OF THESIS

OBSERVATIONS OF A MIDLATITUDE SQUALL LINE BOUNDARY LAYER WAKE

Mesoscale pressure perturbations frequently observed with mesoscale convective systems (MCS) are examined with special emphasis on the characteristics, structure, lifecycle and driving mechanism of the "wake depression" found in the wake region of the convection. A severe squall line which traversed the OK PRE-STORM surface and upper air mesonet-work on 10-11 June 1985 is the focus of this observational study. Extensive surface, upper air and digitized radar data collected during the OK PRE-STORM field experiment were used for analysis.

Various mesoanalyses of this squall line at the surface and aloft have allowed for intensive examination of three pressure features observed with this squall line: the mesohigh, wake depression and pre-squall mesolow. Their relationship to and interaction with other meteorological parameters such as precipitation, temperature, potential temperature and moisture are explored. Furthermore, the mesoscale system-relative "jets" observed with midlatitude squall lines are examined for their possible influence on the pressure field.

The mesohigh develops quickly during the early growth of the squall line and precedes the wake depression by several hours. The predominant mesohigh is linked to the formation of a large cold pool which developed as a result of widespread hail and intense rainfall from a supercell ahead of the young squall line.

Analyses show that the wake depression is not a uniform, stagnant feature behind the mesohigh but has embedded small-scale features, a distinct lifecycle and can undergo rapid intensification. The wake depression also is related to some aspects of the squall line's precipitation pattern. The low consistently "hugs" the back edge of the stratiform

precipitation and is observed to split into two separate lows as the convective line splits. Additionally, the wake depression is a hydrostatic response to a layer of warm, dry air (produced by subsidence) found just above the surface. It is suggested that the wake depression is in part a surface manifestation of forced subsidence by the descending rear inflow jet.

Paul Hamilton
Department of Atmospheric Science
Colorado State University
Fort Collins, Colorado 80523
Summer, 1987

ACKNOWLEDGEMENTS

I wish to extend sincere gratitude to my advisor, Dr. Richard H. Johnson, whose guidance made this research a success. His "open-door" policy and personal interest in weather combined to make this a unique working experience. My appreciation to the other committee members, Dr. Wayne Schubert and Dr. Howard Frisinger.

Special thanks to Jim Toth who took much of his time to introduce me to the Atmospheric Science Department's computer system and answered question after question and never grew impatient. I have learned much from him and will be forever grateful.

Many thanks to Gail Cordova for typing the manuscript and to Judy Sorbie for drafting some of the figures. I would also like to thank Greg Stumpf and Tammy Taylor for their assistance.

I acknowledge and thank the Air Force Institute of Technology who funded much of this research and made this experience possible. This research was supported by the National Science Foundation (NSF) Grant No. ATM-8507961.

TABLE OF CONTENTS

1	Introduction	1
2	Background	6
2.1	The Mesohigh	6
2.2	The Wake Depression	9
2.3	The Pre-Squall Mesolow	11
3	Oklahoma-Kansas PRE-STORM	13
3.1	Data Sources	13
3.2	Data Analysis Procedures	15
4	Synoptic Overview	19
5	Results of Surface Analyses of the 10- 11 June Squall Line	29
5.1	The Storm's Precipitation Pattern	29
5.2	Temperature and Dewpoint Analyses	36
5.3	Mesoanalysis of the Surface Pressure	41
5.4	Surface Analyses of Potential and Equivalent Potential Temperatures	59
6	Time Series for Selected PAM stations	65
7	Results of Lower Tropospheric Analyses for the 10-11 June Squall Line	71
8	Summary and Discussion	87
	References	90

LIST OF FIGURES

Fig. 1. Vertical cross section normal to 22 May 1976 squall line	2
Fig. 2. Schematic of mesoscale surface pressure and streamlines in vicinity of a squall line	5
Fig. 3. Schematic section through a squall line illustrating the thunderstorm high and wake depression	8
Fig. 4. Illustration of a cumulonimbus cloud and vertical motion downwind of cloud.	12
Fig. 5. The OK PRE-STORM surface mesonet network showing the positions of the eighty automated surface observing stations	14
Fig. 6. Locations of the rawinsonde stations in the immediate OK PRE-STORM network	16
Fig. 7. Approximate tracks of the 19 MCSs which passed over the OK PRE-STORM mesonet network in June 1985	20
Fig. 8. Visible (upper) and IR (lower) images of the forming squall line at 2100 GMT, 10 June 1985	21
Fig. 9. Surface mesoanalysis at 2100 GMT, 10 June 1985	23
Fig. 10. 850 mb (a), 700 mb (b), 500 mb (c) and 300 mb (d) height and temperature analyses for 0000 GMT, 11 June 1985	24,25
Fig. 11. Pre-squall sounding from Pratt (PTT), KS at 2330 GMT, 10 June 1985	26
Fig. 12. IR image of mature squall line at 0300 GMT, 11 June 1985	28
Fig. 13. Diagonal displays of composited low-level reflectivity at hourly intervals	30
Fig. 14. Isochrone analysis of gust front position	33
Fig. 15. Analyses of Total Rainfall (a), Stratiform Rainfall (b) and Stratiform Rain Fraction (c) for the 10-11 June squall line over the PAM network	34,35

Fig. 16. Surface temperature (a) and dewpoint (b) analyses for 2300 GMT, 10 June 1985 over the PRE-STORM network	37
Fig. 17. As in Fig. 16 except for 0300 GMT, 11 June 1985	38
Fig. 18. As in Fig. 16 except for 0700 GMT, 11 June 1985	39
Fig. 19. Pressure analysis at 518 m ASL at 2300 GMT, 10 June 1985	42
Fig. 20. As in Fig. 19 except for 0100 GMT, 11 June 1985	44
Fig. 21. Severe weather events in southwest Kansas during the late afternoon on 10 June 1985	45
Fig. 22. As in Fig. 19 except for 0200 GMT, 11 June 1985	47
Fig. 23. As in Fig. 19 except for 0300 GMT, 11 June 1985	49
Fig. 24. As in Fig. 19 except for 0400 GMT, 11 June 1985	50
Fig. 25. As in Fig. 19 except for 0500 GMT, 11 June 1985	52
Fig. 26. As in Fig. 19 except for 0600 GMT, 11 June 1985	53
Fig. 27. As in Fig. 19 except for 0700 GMT, 11 June 1985	54
Fig. 28. As in Fig. 19 except for 0725 GMT, 11 June 1985	56
Fig. 29. Surface divergence field ($\times 10^{-5} \text{ s}^{-1}$) over PAM network at 0720 GMT, 11 June 1985	57
Fig. 30. Tracks of surface mesohigh (H) and wake depression (L)	58
Fig. 31. Analyses of potential temperature (a) and equivalent potential temperature (b) at 2300 GMT, 10 June 1985	60
Fig. 32. As in Fig. 31 except for 0230 GMT, 11 June 1985	62
Fig. 33. As in Fig. 31 except for 0725 GMT, 11 June 1985	63
Fig. 34. Time series of pressure (mb) and accumulated rainfall (mm) in (a) and pressure, temperature ($^{\circ}\text{C}$) and dewpoint ($^{\circ}\text{C}$) in (b) at PAM station 10	66
Fig. 35. As in Fig. 34 except for PAM station 41	68
Fig. 36. Time series of maximum wind gust (m s^{-1}), pressure (mb) and accumulated rainfall (mm) at PAM station 23	69
Fig. 37. Wake region "onion" sounding from Wichita (IAB), KS at 2100 GMT, 10 June 1985	72

Fig. 38. As in Fig. 37 except for 0624 GMT, 11 June 1985	74
Fig. 39. Composite 850 mb relative humidity (%) with reflectivity at 0600 GMT, 11 June 1985	76
Fig. 40. Same as Fig. 39 except for potential temperatures (θ)	77
Fig. 41. Same as Fig. 40 except for equivalent potential temperatures (θ_e)	78
Fig. 42. Composite 700 mb relative humidity (%) with reflectivity	81
Fig. 43. Composite cross section of potential temperature (K) and relative humidity (%) at 0600 GMT, 11 June 1985	82
Fig. 44. Vertical cross sections reconstructed from radar volume scan conducted at 0345-0353 GMT, 11 June 1985	84
Fig. 45. Vertical composite cross section of system-relative flow ($m\ s^{-1}$) and relative humidity (%) at 0600 GMT, 11 June 1985	86

Chapter 1

INTRODUCTION

Mesoscale Convective Systems (MCS) such as tropical and midlatitude squall lines and Mesoscale Convective Complexes (MCC) as defined by Maddox (1980) have increasingly become the focus of research in the field of mesoscale meteorology. Many extensive studies of squall lines have been performed using a myriad of data sets or procedures that include conventional and Doppler radar, satellite imagery, atmospheric sounders, wind profilers, surface networks and numerical modelling techniques. These studies have not only raised new and challenging questions but have given further insight to the answers. However, answers to many questions regarding the dynamical and thermodynamical structure in both the vertical and horizontal and the surface characteristics of these systems remain elusive.

Figure 1 shows a simplified two-dimensional schematic of a midlatitude squall line (from Smull and Houze, 1986a). The structure of this squall line is quite similar to those observed over the tropics. The storm is most notably characterized by a narrow line, approximately 10 to 50 km in width, of intense convective cells which leads the system. The convective cells are frequently observed to extend well into the upper troposphere and even to push through the tropopause. The remainder of the storm is characterized by a large anvil region at the middle to upper tropospheric level. The leading portion of this anvil may extend more than 50 km ahead of the convective line (Newton, 1966) while the trailing anvil may reach rearward of the convective line for over 150 km and is often observed to be quite thick (up to 10 km). To feed the system, a flow of warm, moist and unstable air enters the individual convective cells at low levels, rises through these towers as convective-scale updrafts, and diverges forward/rearward into the leading/trailing anvil.

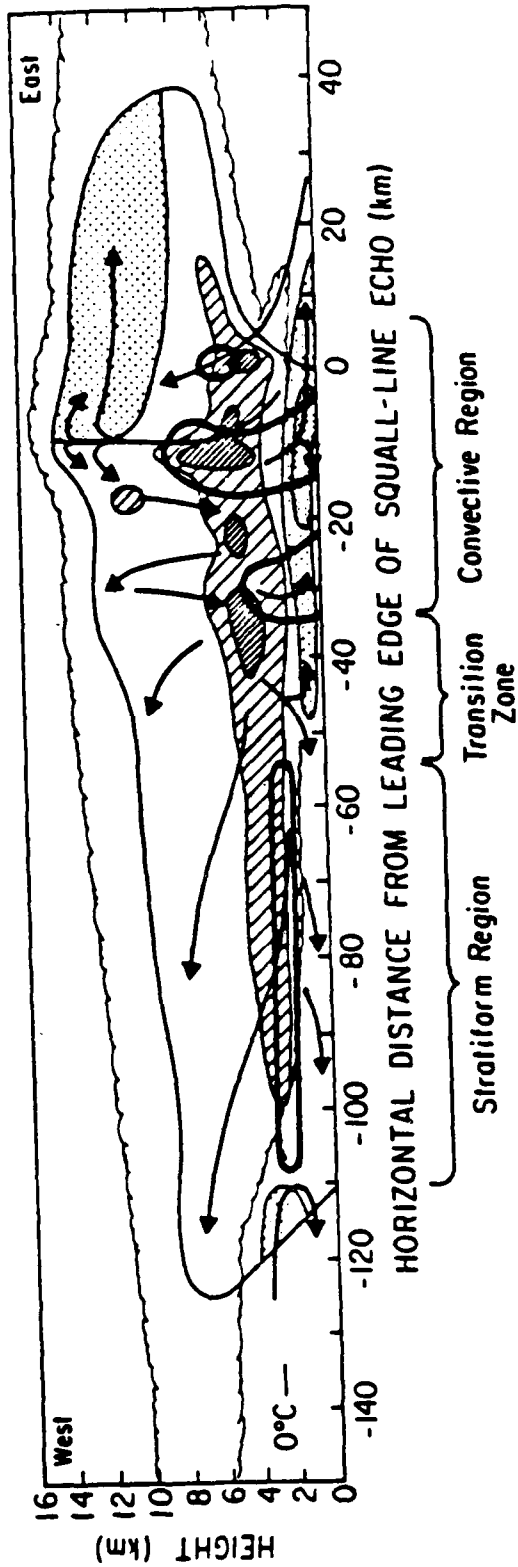


Fig. 1. Vertical cross section normal to 22 May 1976 squall line. Scalloped line marks extent of cloud. Outermost solid contour marks boundary of precipitation echo, while heavy solid lines enclose more intense echoes. Stippling indicates areas of system-relative rear to front flow (left to right), with darker stippling representing stronger flow. System-relative front to rear flow is indicated likewise but with hatching. Streamlines show two dimensional relative flow. (from Smull and Houze, 1986a).

The convective cells also develop strong evaporatively driven downdrafts which support and advance the gust front.

A topic of considerable research and debate in recent years has been of the system-relative front-to-rear and rear-to-front "jets" or flows accompanying the squall line. These jets are vaguely apparent in the figure. Extensive studies by Smull and Houze (1985, 1986a, 1986b) have verified these features in the squall lines they studied. This circulation feature is also evident in Newton's (1966) study. The front-to-rear jet is a strong current of air flowing horizontally rearward through the convective line and into the trailing anvil at midlevels. The rear-to-front jet enters the system from the rear and has been observed to descend through the melting level and into the convective line at low levels (Smull and Houze, 1985; Augustine and Zipser, 1986; Smull and Houze, 1986b). At the leading line of convection, the rear inflow has been hypothesized to join with the convective downdrafts and reinforce the gust front (Smull and Houze, 1985; Roux, 1987). This paper will not discuss the reasons or causes for these mesoscale jet features; however, we will use their presence to draw conclusions.

Intense rainfall is often associated with the passage of a squall line. The precipitation field accompanying the storm has been recently categorized into three often distinct regions (Smull and Houze, 1985): the convective line, the transition zone and the stratiform region. The primary precipitation maximum is observed to coincide with the leading convective line. Here the rainfall can exceed 100 mm h^{-1} . A secondary precipitation maximum is coupled with the trailing anvil. This region of stratiform rainfall can account for 30-40% of the total measured precipitation in tropical squall lines (Cheng and Houze, 1979). Situated between these two precipitation maxima and parallel to the convective line is the transition zone where little, if any, rain is recorded at the surface. This zone of precipitation minimum is sometimes quite distinct on a radar depiction of the storm and is denoted by a minimum of low-level reflectivity between the convective line and the stratiform regions.

Of considerable interest to this research project is the surface pressure field associated with the squall line. The most notable feature is the pressure jump coinciding with

the passage at the surface of a mesohigh caused largely by evaporative cooling at the convective line. The pressure jump occurs concurrently with or just before the passage of the gust front (Fujita, 1963). Frequently extending several hundred kilometers in length, the mesohigh is a dominant feature on surface mesoscale analyses. Approximately, 100 km to the rear of this mesohigh is another mesoscale pressure feature common to squall lines - a mesolow or "wake" depression. The "wake" depression may or may not be widespread like the mesohigh. Its horizontal extent may range from 50-400 km (Schaefer *et al.*, 1985). Also, a second region of low pressure is commonly found just ahead of the convective line and the surface mesohigh. Figure 2 illustrates all three of these surface pressure features (from Schaefer *et al.*, 1985). A more complete discussion of the probable causes of the mesohigh and the mesolows as explained by previous studies is delayed until the next section.

Many of the previous papers on the mesoscale pressure patterns associated with the squall lines have focused on the more dominant mesohigh or pre-squall mesolow instead of the "wake" depression. As stated by Atkinson (1981), "the wake low is far less well documented than the high." The specific goals of this research then are to investigate the surface features of midlatitude squall lines concentrating especially on the mesohigh and the "wake" depression. Specifically, what are the characteristics of the "wake" depression and how is it developed and maintained? Also, we will research the lower tropospheric environment to include the boundary layer of squall lines.

The Oklahoma-Kansas PRE-STORM (Preliminary Regional Experiment for STORM-Central) experiment conducted during the spring of 1985 gives us an excellent opportunity to investigate these questions and much more. An unprecedented database collected during this two month experiment will provide ample information to explore the surface and lower tropospheric features of midlatitude squall lines.

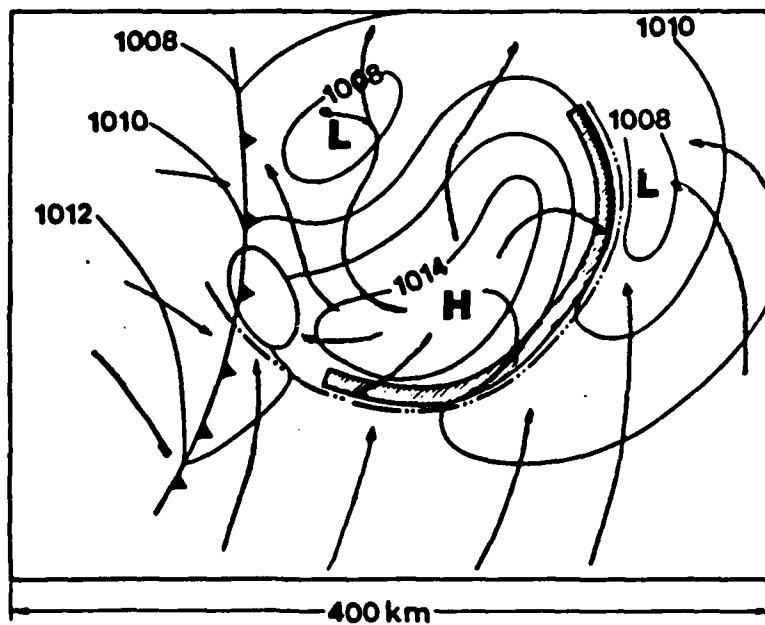


Fig. 2. Schematic of mesoscale surface pressure and streamlines in vicinity of a squall line. The mesohigh and mesolows are denoted with a L and H, respectively. Pressures are labeled in millibars. The squall line is denoted by a dashed and double-dotted line. A cold front is denoted with a pointed solid line. (from Schaefer *et al.*, 1985).

Chapter 2

BACKGROUND

Significant variations in atmospheric pressure exist both in the sub-cloud environment and within the cloud mass of tropical and midlatitude squall lines. As mentioned previously, three primary pressure features (see Fig. 2) are commonly observed at the surface: the mesohigh, the wake depression and the pre-squall mesolow. With weaker squall lines, the wake depression and the pre-squall mesolow may appear in a diminished state. Mesoscale "highs" and "lows" have been documented to occur at the low to middle levels within the storm. Research by LeMone (1983) and LeMone et al (1984) reveal the presence of a mesolow above the surface mesohigh at an altitude of approximately 1 to 1.5 km AGL (or some 500 m or more above cloud base) and about 10 km to the rear of the storm's leading edge. Moncrieff (1986) has also shown the presence of a mesohigh above the wake depression within the trailing anvil.

The following sections represent a review of past investigations into the structure and hypothesized causes of the surface mesohigh, the wake depression and lastly the pre-squall mesolow:

2.1 The Mesohigh

Various terms have been used by authors when referring to the region of high pressure found underneath the raining downdrafts of individual or multi-cellular thunderstorms: mesohigh (Zipser, 1977), thunderstorm high (Fujita, 1955), and "bubble" high (Darkow and Livingston, 1975) to name a few. We choose to adopt the former in this paper.

Among the early works on the pressure perturbation field associated with convective storms was that performed by Levine (1942). His analyses led him to conclude that the mesohigh was a result of the dynamic effect of downward accelerating air from the

convective downdrafts impacting the ground. Later, research by Sawyer (1946) based on the work by Humphreys (1929) made calculations showing that evaporative processes played an important role in the formation of the mesohigh. A hypothetical column of unsaturated air would evaporate some of the precipitation falling into it causing the air to cool and contract. This leaves the top of the column with relatively less air and therefore a region of low pressure develops. Air from the surrounding environment would then flow into this region of lower pressure increasing the total mass of the column. It is this increase in mass of the column which was suggested to cause the mesohigh observed at the surface.

Tepper (1950) was convinced that the sudden jump in pressure observed with squall lines was a result of propagating gravity waves and he named these waves "pressure jump" lines. Most importantly, Tepper believed the propagating waves to be the cause, not the by-product, of the squall line. Similarly, Williams (1953) defined the term "elevation wave" to correspond to an observed pressure rise. These elevation waves were found to be present with the squall lines Williams studied during the 1948 Cloud Physics Project in Ohio. He noted that usually elevation waves were coincident with thunderstorm activity.

Classical analyses of "thunderstorm highs" were performed by Fujita (1955). A figure of his depicting the thunderstorm high as well as the trailing wake depression, which will be reviewed in the next subsection, is presented as Fig. 3 (from Fujita, 1955). Fujita concluded in a similar fashion to Levine (1942) and to the findings of the Thunderstorm Project (Byers, 1949) that the thunderstorm high was caused by the hydrostatic effect of high momentum air being cooled by evaporation and brought to the surface by downdrafts and forming a large cold pool. Also, in opposition to the theory stated by Tepper, Fujita argued the squall line produced the sudden pressure jump observed with these systems and not vice-versa. Among others, Fujita drew several conclusions from his analyses regarding the characteristics of the thunderstorm high. Primarily, the strength of the mesohigh is proportional to the intensity of the squall line. Furthermore, the mesohigh is immediately preceded by a tight pressure gradient commonly known as the pressure surge or jump. Fujita (1963) found the mean magnitude of the gradient to range from $1.2 - 3.1 \text{ mb km}^{-1}$ and for its horizontal speed to be as much as 22 m s^{-1} . Superimposed on the mesohigh is

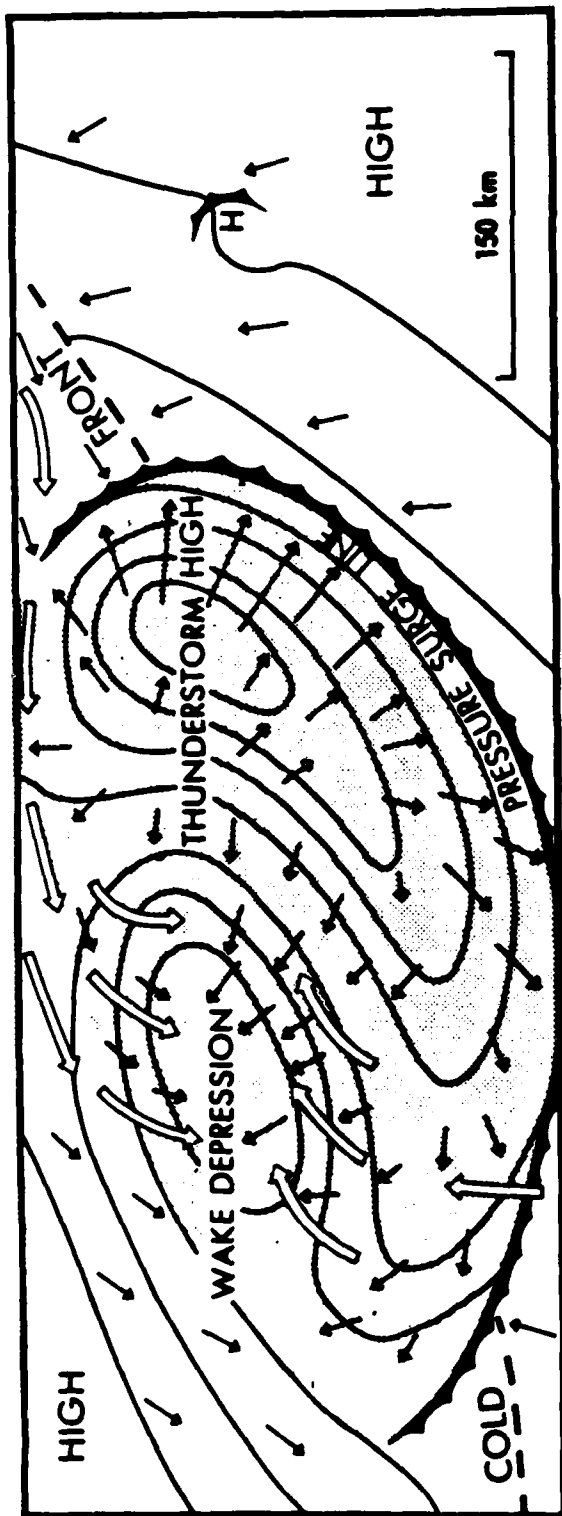


Fig. 3. Schematic section through a squall line illustrating the thunderstorm high and wake depression. Lines represent isobars. Wind vectors are illustrated with thin arrows while system relative flow denoted with open arrows. (from Fujita, 1955).

a pressure "nose" (Fujita, 1963) where the greatest pressure is found. The nose, up to 6 km in diameter, lies where the downdrafts impact the surface. Fujita also showed strong divergence ($50-100 \times 10^{-5} \text{s}^{-1}$) occurs within the thunderstorm high. Finally, Darkow and Livingston (1975) found the mesohigh to be responsible for triggering new convection.

2.2 The Wake Depression

Perhaps of most interest to this research is the study of the characteristics and cause(s) of the wake depression. A review of past and present ideas of this region of low pressure is presented here. As for the mesohigh, various terms have been and are being used to name this feature: depression wave (Williams, 1954), wake depression (Fujita, 1955), mesolow (Zipser, 1977) and most recently, wake low (Schaefer *et al.*, 1985) to name just a few.

Whereas Williams (1953) defined an elevation wave to represent a rise in pressure, he defined a depression wave to represent an analogous fall in pressure. Several depression waves were analyzed in association with squall lines passing over the Cloud Physics Network in Ohio. He found that despite the rapid pressure falls usually concurrent with their passage, the depression wave did not coincide with thunderstorm activity as did the elevation wave. Most importantly, Williams (1954) noted that the rain ceased as the wave passed. He concluded that there was a possible relationship between the depression wave and the elevation wave and that their coexistence may be related to squall line activity.

Fujita (1955) also studied the region of low pressure to the rear of the mesohigh and termed the feature a "wake depression" since, as he thought, it was due to the wake of the thunderstorm high (see Fig. 3). He envisioned the thunderstorm high to act as a barrier in a flowing fluid. Air flowing around the barrier would induce a wake downstream and result in lower pressure there. This feature also satisfies the definition of a "mesodepression" (Fujita, 1963) because a complete circulation is not observed with the wake depression. Additionally, Fujita (1955) showed the thunderstorm high developing first and the wake depression forming later as the squall line matured. Furthermore, as the thunderstorm high dissipated he showed the wake depression to persist for several hours and even deepen. Later, Fujita (1963) concluded that the low pressure region could not be a result of the

barrier effect because the horizontal dimensions of the thunderstorm high were so large. He decided that the term "wake depression" should then "be abolished". Because it is presently common to refer to the environment following the convective line as the wake of the squall line, we find the term "wake depression" adequate to describe the feature.

Additional research of squall lines and its near environment revealed a pocket of warm, dry air at low levels below the trailing anvil. Many authors have referenced and explored this phenomenon in both tropical and midlatitude squall lines (Williams, 1963; Zipser, 1969, 1977; Miller and Betts, 1977; Brown, 1979; Ogura and Liou, 1980). The cause of the warm air has been attributed to mesoscale descent under the trailing anvil (Williams, 1963; Zipser, 1977; Miller and Betts, 1977; Brown, 1979). The creation of the wake depression was then linked to this warm air by hydrostatic processes.

Williams (1963) researched the wake depression and the "warm wake" which accompanied a thunderstorm event during the National Severe Storms Project (1961) and found the warm air aloft (a result of subsidence) to hydrostatically account for the low pressure. He noted that the warm air was extensive above but only local at the surface. Only rarely does the warm air penetrate to the surface and produce a warm wake. He also summarized that the wake depression is more pronounced during the dissipating stage of the thunderstorm.

A question to be answered here is what is or are the mechanism(s) causing this mesoscale sinking and resultantly the warming. Zipser (1969, 1977), drawing upon his analyses of tropical squall lines, concluded that evaporation of anvil precipitation was the responsible mechanism for the observed subsidence. Miller and Betts (1977) modelled the updraft-downdraft trajectories of tropical squall lines and found the intense downdrafts at the convective line to accelerate rearward of the storm as a concentrated current close to the ground and subsequently force or "suck" downward the air above the lowest 50-100 mb. The air would then warm adiabatically. They concluded more research was required to ascertain the effect of stratiform precipitation from the anvil falling into the previously sinking air. In an effort to test whether or not evaporative processes, as proposed by Zipser, can account for the mesoscale unsaturated downdraft, Brown (1979) modelled

tropical squall lines. He summarized that evaporation is probably the primary mechanism for the subsidence but stated that the warm, dry air found to the rear of the squall line suggests another cause. Brown concluded however that the warming may simply result from "continued subsidence in the presence of decreased evaporation." Clearly the debate continues as to the cause of the mesoscale subsidence observed under the trailing anvil which results in warming and has been linked to the formation of the wake depression. Our research into this issue has led us to propose another mechanism for consideration.

2.3 The Pre-Squall Mesolow

Perhaps the most comprehensive study of this pressure feature was accomplished by Hoxit *et al.*, (1976). The evidence which they and others present attributes the presence of the mesolow to subsidence warming in the upper troposphere and lower stratosphere ahead of the convective activity (Hoxit *et al.*, 1976; Schaefer *et al.*, 1985). This is illustrated in Fig. 4 (from Hoxit *et al.*, 1976). Subsidence in the range of a few tens of cm s^{-1} can produce pressure falls of sufficient magnitude to cause the pre-squall mesolow (Hoxit *et al.*, 1976). Finally, they hypothesized the sinking motion described above may inhibit new convection in front of the convective line until the gust front forces the air upward releasing its convective instability.

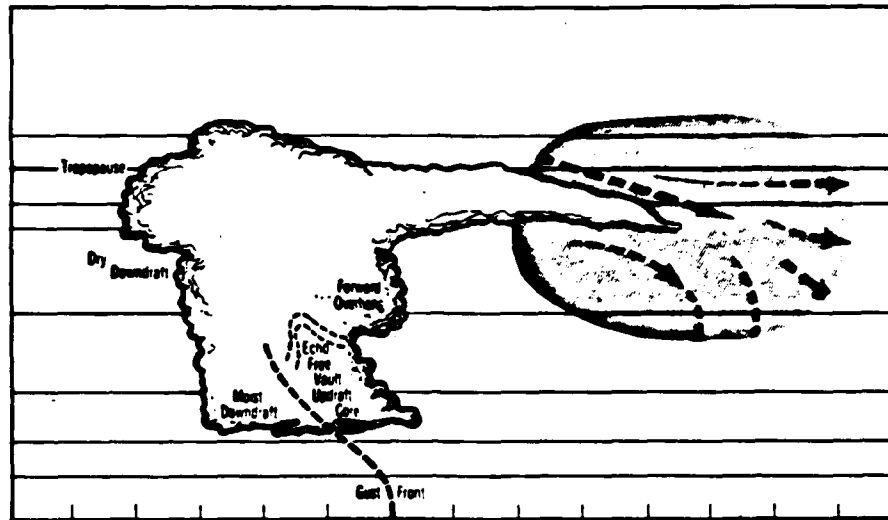


Fig. 4. Illustration of a cumulonimbus cloud and vertical motion downwind of cloud. Dashed arrows were based on calculations. Shaded area denotes region of subsidence. (from Hoxit *et al.*, 1976).

Chapter 3

OKLAHOMA-KANSAS PRE-STORM

3.1 Data Sources

Field experiments designed to explore the mesoscale structure of tropical and mid-latitude convective storms have been conducted worldwide over the past several decades: The Thunderstorm Project (1946-47); The Cloud Physics Project (1948); National Severe Storms Project (1961); Line Island Experiment (1967); VIMHEX (1972); GATE (1974); SESAME (1979); CCOPE (1981); and most recently, OK PRE-STORM (1985). These experiments primarily used surface networks and/or rawinsondes to obtain observations.

The Oklahoma-Kansas Preliminary Regional Experiment for STORM-Central (OK PRE-STORM) was held 1 May - 27 June 1985 in the south central plains of the United States. Its purpose was to provide a base for testing new sensing and observing equipment and for collecting surface and upper atmospheric data in the vicinity of mesoscale convective systems (MCS) to heighten our knowledge of these storms. A total of eighty automated surface observing systems were arranged in approximately a 350 by 450 km array over the states of Kansas and Oklahoma (Fig. 5). The northernmost forty stations were NCAR Portable Automated Mesonet (PAM) instruments while the southernmost forty stations were NSSL Surface Automated Mesonet (SAM) instruments. Two PAM stations were colocated with two of the SAM stations for comparative purposes. The PAM and SAM instruments collected five standard meteorological parameters: u and v wind components, dry temperature, wet-bulb temperature, rainfall, and atmospheric pressure at five minute intervals throughout the course of the experiment. In addition to the surface mesonet, twenty-seven upper air stations were located throughout the network with fifteen of them being pre-existing NWS rawinsonde sites and the remainder

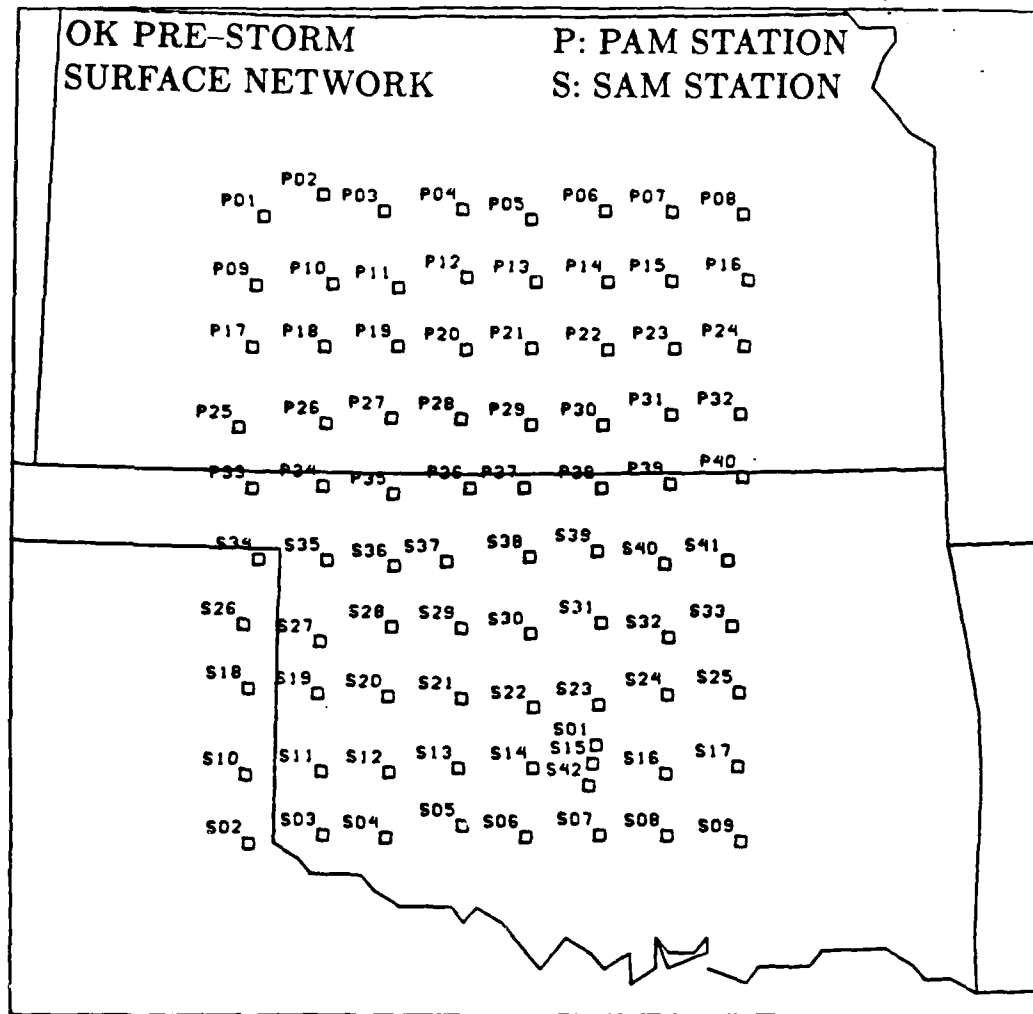


Fig. 5. The OK PRE-STORM surface mesonet showing the positions of the eighty automated surface observing stations.

being supplemental PRE-STORM sites. Figure 6 shows the locations of the rawinsonde sites in the immediate PRE-STORM area. The overall quality of the PRE-STORM sounding data set is good but occasionally errors are present within individual soundings. These errors have been attributed to the age of the sounding equipment and to the meteorological variations being measured (Showell,1986). Examples of erroneous data include incorrect heights, temperatures and winds at various levels. For some of the problems, tentative corrections were made available to the users of the data set. Attempts to correct for mistakes in the sounding data set are underway.

During the two months of the PRE-STORM experiment, volume scan radar data was digitized at seven NWS WSR-57 radar stations in and around the network. A large collection of digitized radar data is available. Composites of radar reflectivity patterns can be produced using the digitized data from several radar sites allowing for detailed analyses of precipitation patterns associated with mesoscale convective systems. Volume scans were digitized at 2 degree increments up to a maximum of 22 degrees. Reflectivity measurements are grouped into 15 levels. In addition to the surface, upper air and conventional radar networks, two dual-Doppler sites and three atmospheric wind profilers were operational during PRE-STORM. Furthermore, two P-3 aircraft flying a total of 195 hours were used to complete the observing network.

3.2 Data Analysis Procedures

Extensive quality control of the PRE-STORM PAM data set was accomplished by NCAR and Colorado State University and the results show the data set to be of high quality. Suggested corrections to the PAM pressure data were developed in response to routine calibration checks of the PAM instruments which revealed an error in the pressure instrumentation. Using smoothed analyses of monthly mean pressure and sensor calibrations, pressure adjustments for each PAM site were obtained and are reported in Johnson and Toth (1986). The NSSL PRE-STORM SAM data set has not been fully examined for quality and reliability at this time. Surface pressure adjustments, similar to those developed for the PAM stations, have not been obtained for the SAM stations.

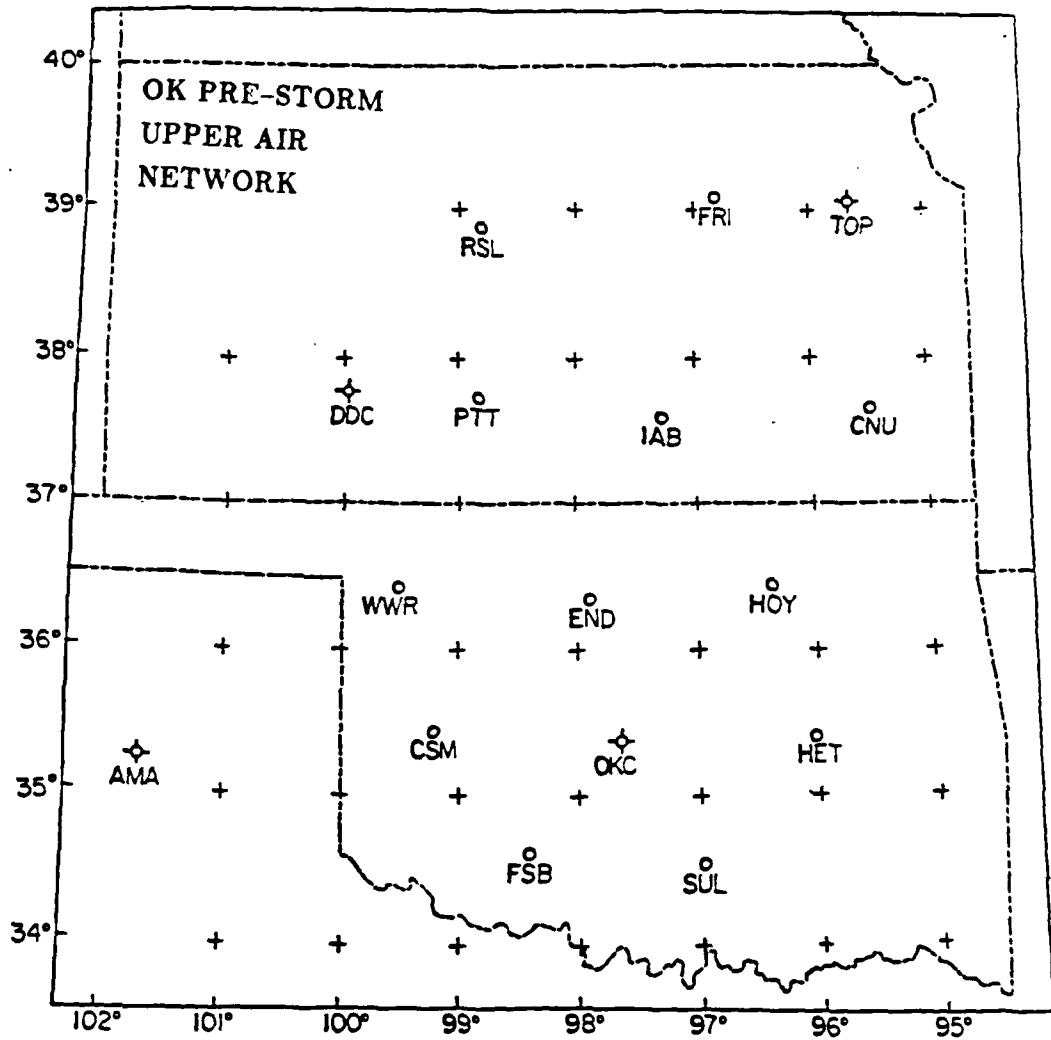


Fig. 6. Locations of the rawinsonde stations in the immediate OK PRE-STORM network. Plain circles represent supplemental stations while others represent National Weather Service stations.

Table 1 lists the estimated PAM pressure adjustments for 10–11 June 1985. These values differ by -0.7 mb from those published by Johnson and Toth (1986) but prove to be better for the 10–11 June case. No corrections were possible for the SAM stations.

In order to eliminate the effect of varying topography in the pressure analyses, the pressure data was reduced to a common level of 518 m ASL using standard reduction methods. This level was chosen because it represents the mean elevation of the 40 PAM stations. Currently, the elevations of the SAM stations are questionable and so the mean of the PAM station elevations was retained for the reduction level.

The final manipulation of the data was to eliminate the tidal oscillation due to diurnal fluctuations of the pressure. Diurnal pressure curves representing the mean daily fluctuations of June 1985 pressures were calculated for several NWS stations in and near the PRE-STORM network. Because these curves varied slightly for each station, a mean curve was used to obtain numerical adjustments. These adjustments were then made to both the PAM and SAM pressures. The maximum amplitude of adjustment in the positive direction was $+1.3$ mb and -0.4 mb in the negative direction.

The upper-level figures and vertical cross sections in this thesis were created by compositing numerous PRE-STORM soundings. This procedure provided an easy way for obtaining additional data to allow for more detailed analyses at selected levels. Data values from various soundings were advected forward or rearward at 14 m s^{-1} from the northwest (310°). To obtain composites centered around 0600 GMT, those soundings launched between 0430–0745 GMT on 11 June 1985 were used. Specifically, two soundings from Wichita, Kansas (IAB) at 0624 and 0430 GMT and three from Russell, Kansas (RSL) at 0430, 0555 and 0745 GMT. These soundings lie approximately on a line perpendicular to the squall line.

Table 3.1: ESTIMATED PRE-STORM PAM ELEVATION AND PRESSURE ADJUSTMENTS FOR 10-11 JUNE 1985

Site	Elev (m)	P. Adjust (mb)	Site	Elev (m)	P. adjust (mb)
1	799	+0.6	22	407	-1.4
2	651	+0.2	23	418	-0.4
3	575	-1.2	24	336	-1.1
4	540	-1.9	25	769	-0.6
5	484	-0.7	26	625	-0.7
6	404	-0.8	27	625	-0.8
7	452	+0.1	28	530	-2.5
8	461	-1.3	29	434	+0.7
9	791	-0.9	30	387	+0.1
10	653	-1.0	31	407	+0.7
11	613	-0.9	32	320	-1.0
12	545	+0.4	33	786	-0.8
13	479	0.0	34	628	-0.4
14	467	-2.9	35	546	-0.7
15	403	+0.3	36	379	-0.5
16	371	-0.5	37	356	-0.2
17	821	-0.8	38	330	-0.5
18	725	-0.8	39	374	+1.3
19	632	-0.3	40	300	+0.4
20	561	-0.9	41	414	-1.4
21	472	-0.3	42	480	-0.5

Chapter 4

SYNOPTIC OVERVIEW

During the span of OK PRE-STORM, numerous MCSs were probed and monitored. In the June phase of the experiment, some nineteen systems in formative, mature and dissipative stages passed over the mesonet network. A depiction of the approximate tracks of these storms is presented as Fig. 7. This research focuses on the intense squall line which traversed portions of Kansas and Oklahoma on 10-11 June 1985.

The squall line of 10-11 June possessed all the aforementioned characteristics. The storm had well defined front-to-rear and rear-to-front mesoscale "jet" features (Houze and Rutledge, 1986; Augustine and Zipser, 1986; Smull and Houze, 1986b, Moncrieff, 1986). A fierce line of convection led the system which tracked southeastward across the PRE-STORM network at approximately 14 m s^{-1} . Following the leading line, a distinct transition zone and a widespread region of stratiform precipitation are evident predominantly during the mature stage of the storm's life. The surface pressure field was characterized by an intense mesohigh, a long lived wake depression, and also a pre-squall mesolow.

Prior to an in-depth discussion of the 10-11 June squall line, a brief overview of the synoptic setting leading to the storm's formation is beneficial. At 1200 GMT on 10 June, some seven hours before the first sign of convection in association with the squall line under study, a southerly flow of warm, moist air prevailed over Kansas and Oklahoma. Visible and IR satellite images taken at 2100 GMT on 10 June 1985 are presented as Fig. 8 and show the initial line of convection forming over southwestern Kansas and the Oklahoma panhandle. The development pattern of this particular squall line matched that of the broken line category as defined by Bluestein and Jain (1985). A 2100 GMT

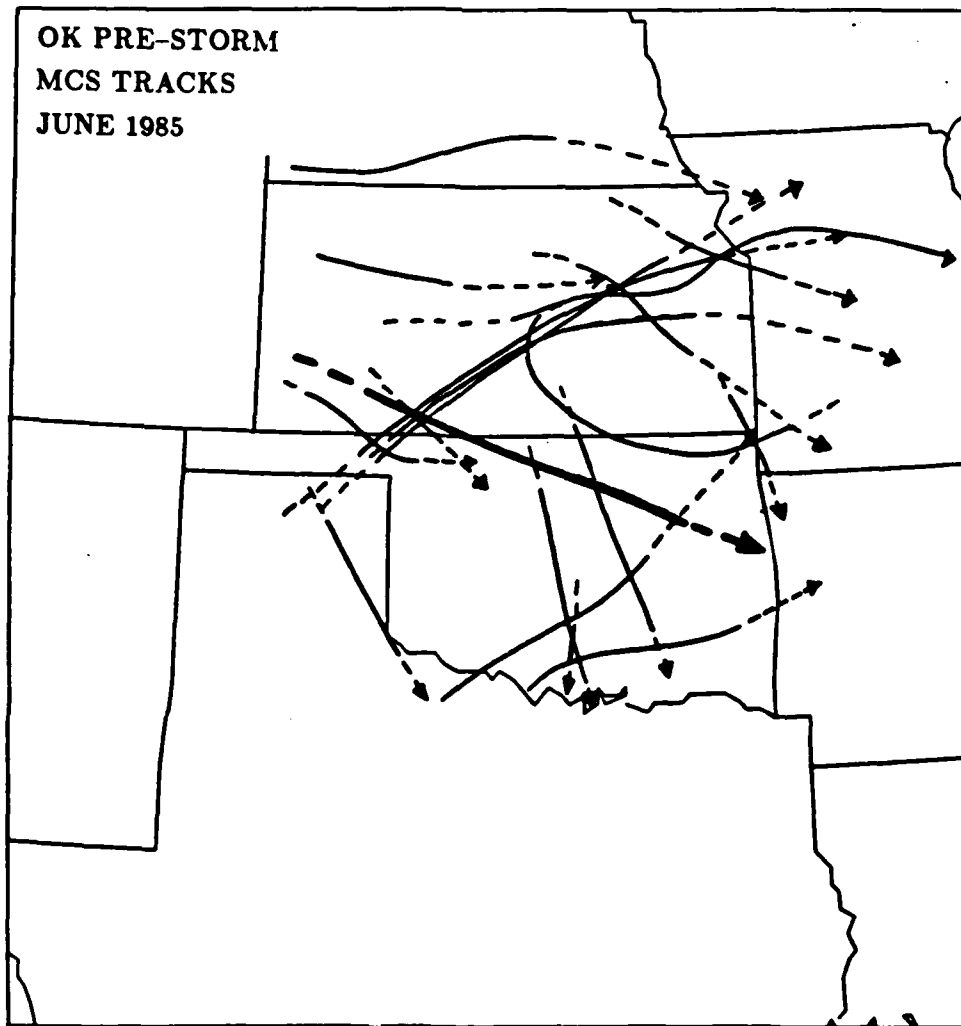


Fig. 7. Approximate tracks of the 19 MCSs which passed over the OK PRE-STORM mesonetwork in June 1985. Dashed line depicts the formative and dissipative stages of the MCS. Solid line depicts mature stage.

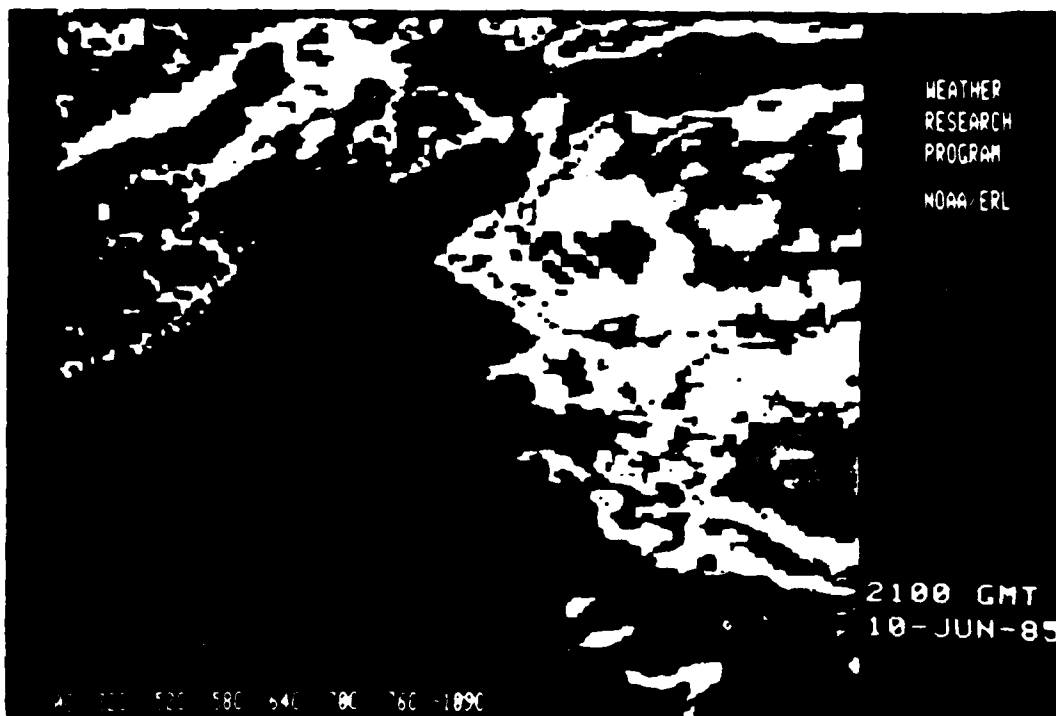
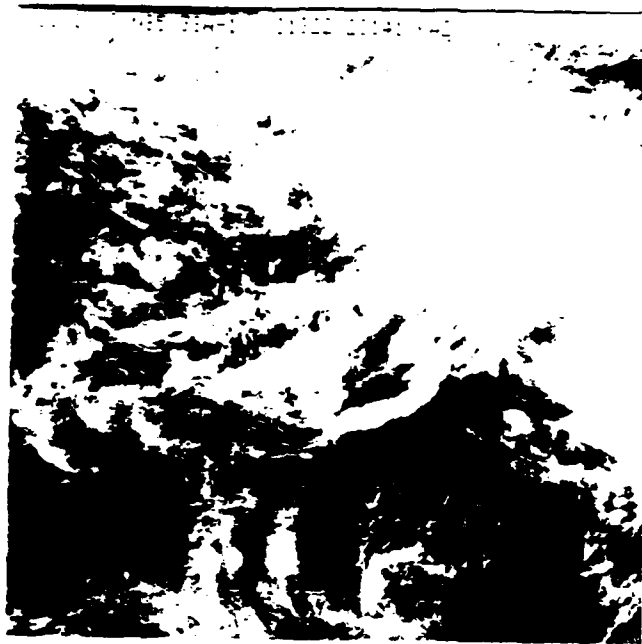


Fig 8. Visible (upper) and IR (lower) images of the forming squall line at 2100 GMT, 10 June 1985. In the IR image, green and yellow denote the most intense areas of convection.

mesoanalysis of the U.S. central plains along with the radar reflectivity pattern is shown in Fig. 9. The radar pattern was obtained from smoothed nephanalysis by the NMC (National Meteorological Center). A weak stationary front meandered across the border of Oklahoma and Kansas and rainfall was widespread over Kansas, eastern Colorado and parts of Nebraska. South of the front warm and moist conditions prevailed with dewpoints exceeding 18°C. Winds were predominantly from the southeast. North of the front surface conditions were cooler and slightly drier primarily in response to a dissipating MCS over eastern Kansas (see reflectivity pattern in Fig. 9). This system developed several hours earlier over Arkansas and subsequently built rearward into parts of Oklahoma and Kansas. Also, there is a strong northwesterly flow bringing cool and very dry air into western Nebraska.

Figure 10 shows NMC upper air analyses for 0000 GMT at four standard levels: 850, 700, 500, and 300 mb. At 850 mb a broad low is centered over New Mexico with a 20 kts (10 m s^{-1}) southerly flow over the PRE-STORM region. This low is evident in the previous surface mesoanalyses. The predominant feature at upper levels is a strong short wave trough pushing into western Kansas and Oklahoma. This feature is supported by a thermal trough evident at 500 mb and a 90 kts (45 m s^{-1}) jet maximum entering the trough upstream at 300 mb. The development of the squall line is tied closely to the progression of this short wave.

A sounding taken in advance of the developing squall line at 2330 GMT on 10 June is illustrated in Fig. 11 to show the pre-squall environment. Fairly moist conditions exist below 800 mb with drying gradually occurring with increasing altitude. Strong wind shear exists from the surface to 700 mb which favors intense convection. The freezing level is found near 600 mb. This sounding is similar to the composite soundings for the broken line category compiled by Bluestein and Jain (1985) except it is significantly more moist below 400 mb.

With a blanket of warm, moist and unstable air covering the network, a flow of cool and dry air entering Nebraska and an upper level short wave trough, the stage was set for explosive development of the squall line. The squall line would develop rapidly and move

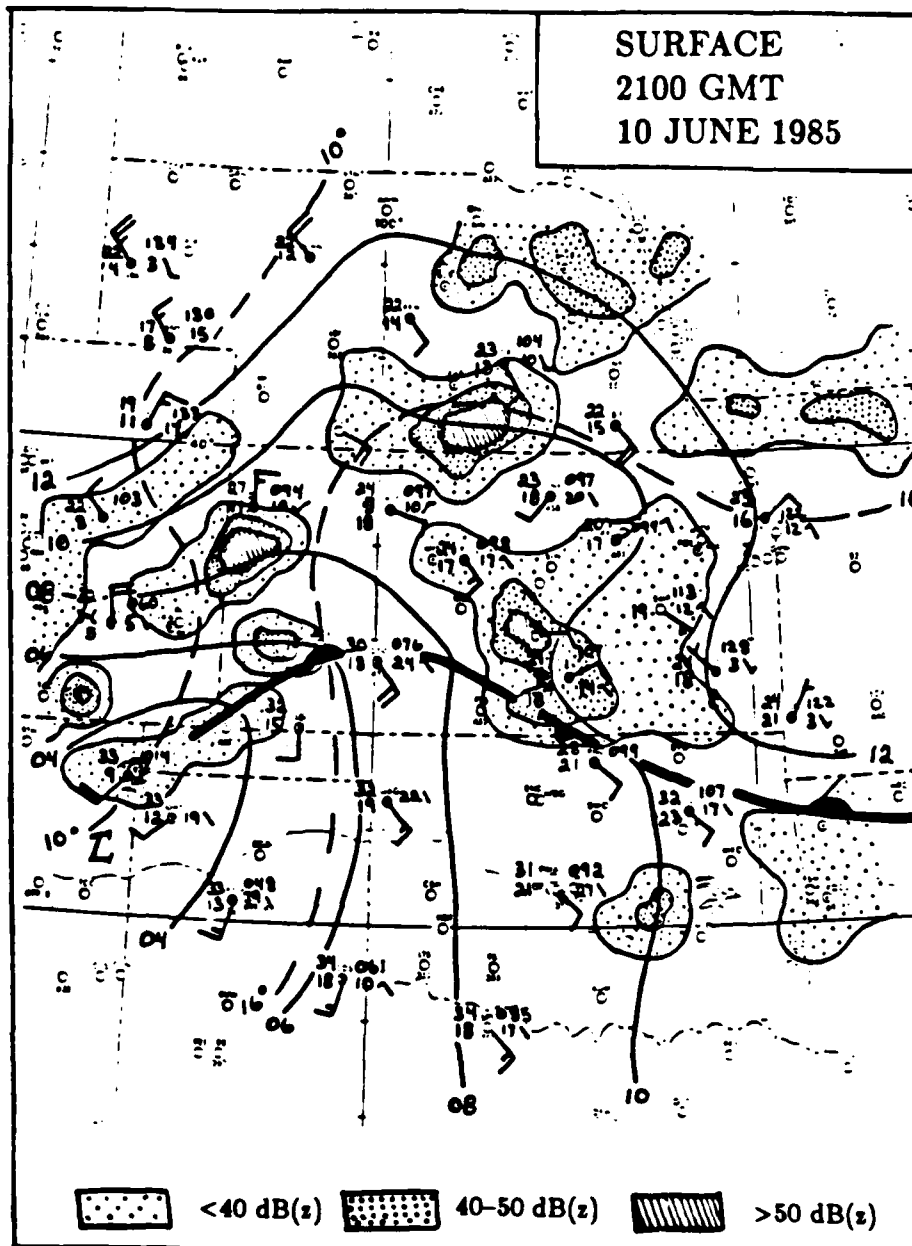


Fig. 9. Surface mesoanalysis at 2100 GMT, 10 June 1985. Solid lines denote isobars (mb), dashed lines denote isodrosotherms (C). Hatched and stippled areas represent intensity of rain echoes. Bold broken line depicts frontal boundary.

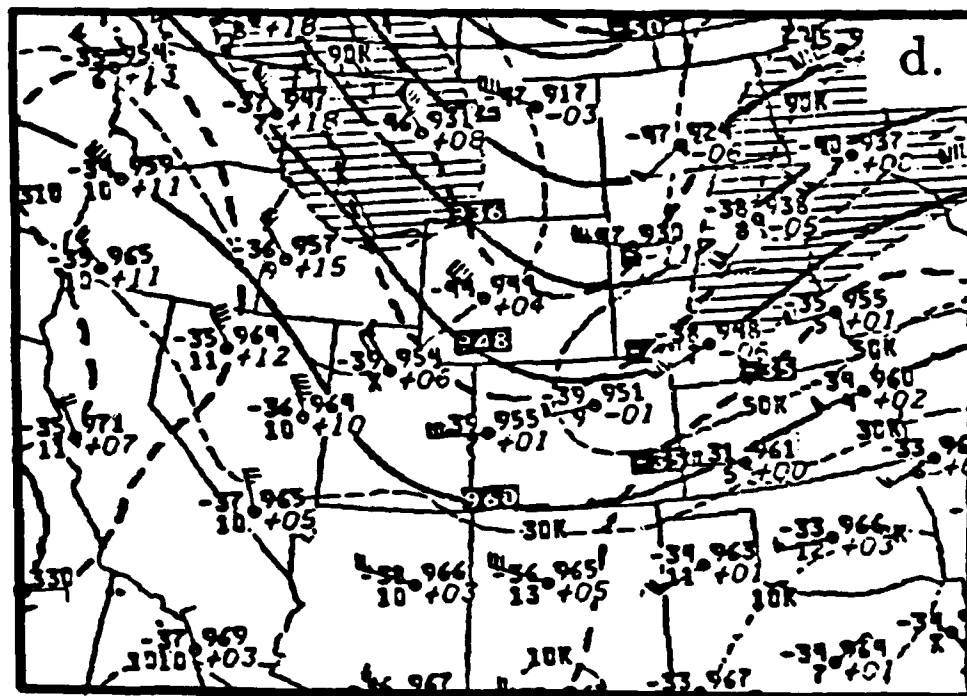
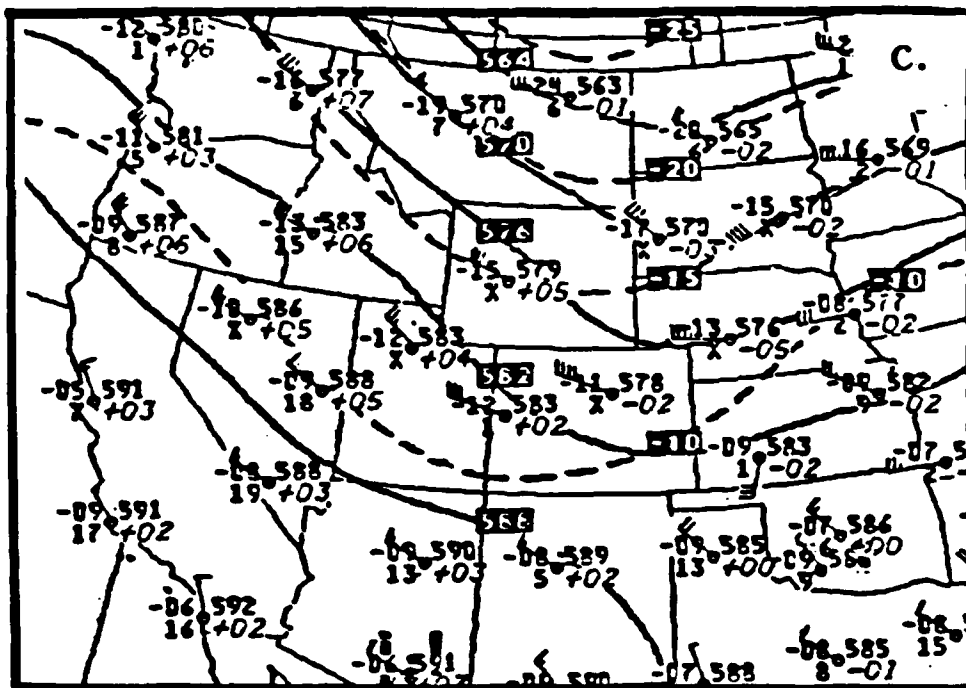


Fig. 10. Continued.

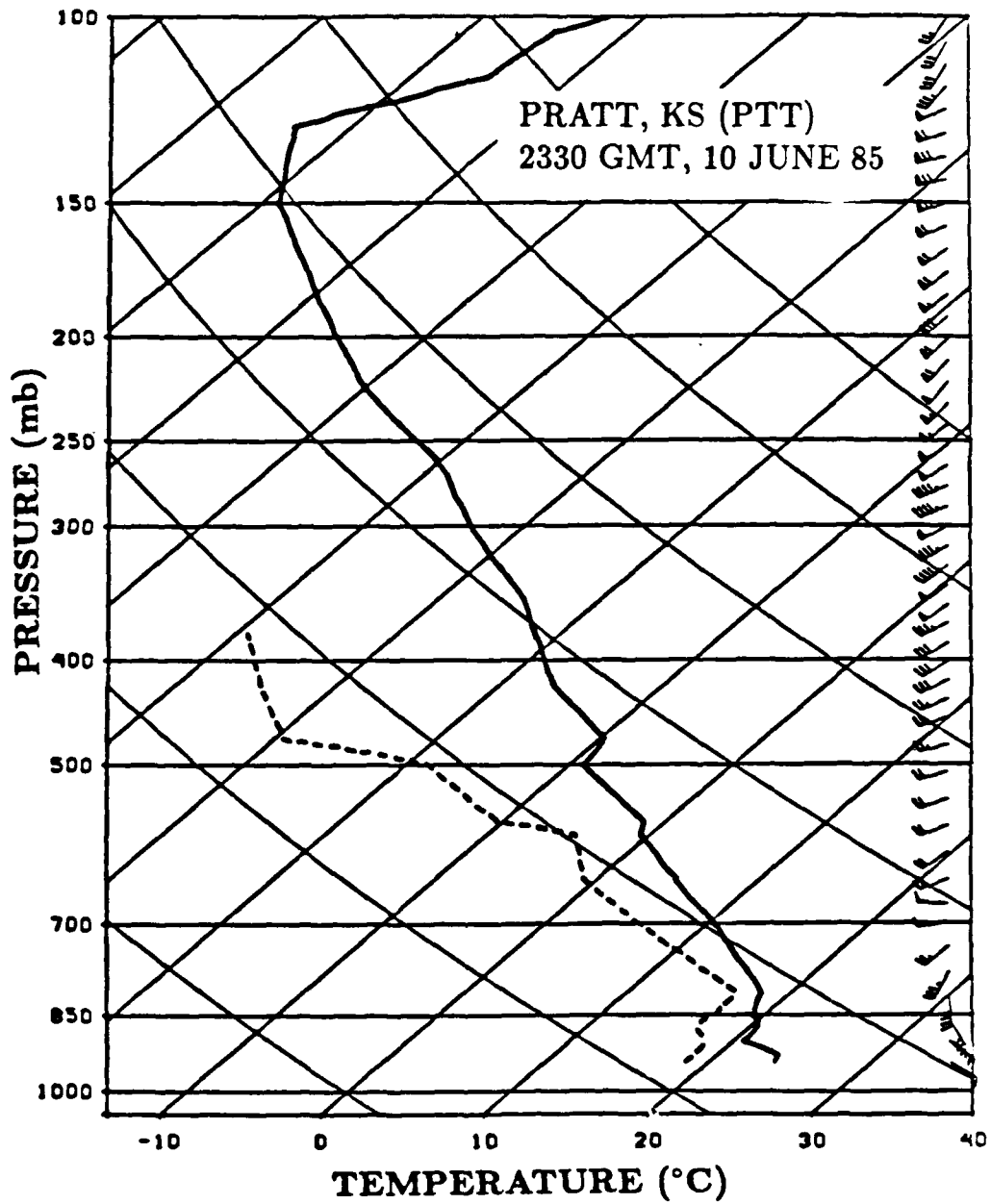


Fig. 11. Pre-squall sounding from Pratt (PTT), KS at 2330 GMT, 10 June 1985. Temperature and dewpoint traces are denoted with solid and dashed lines, respectively. Winds are plotted on the right (a full barb equals 5 m s^{-1} and a flag equals 25 m s^{-1}).

southeastward over the two state region reaching maturity around 0300 GMT on 11 June (see Fig. 12). The storm would dissipate and move into Missouri, Arkansas, and southeast Oklahoma near 0900 GMT.

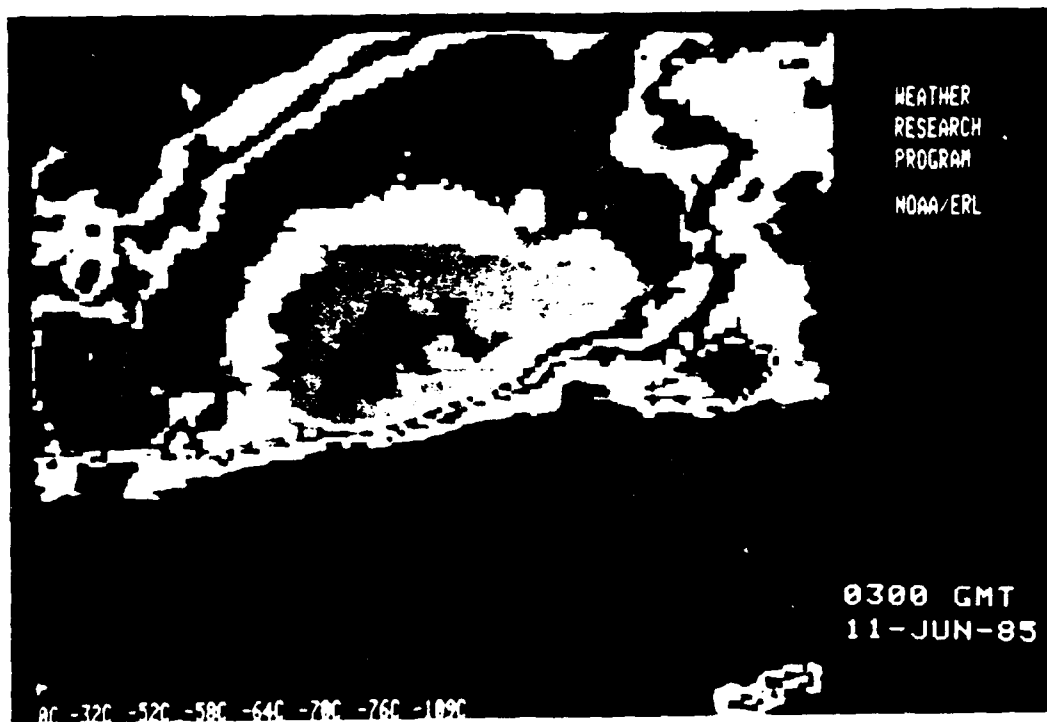


Fig 12 IR image of mature squall line at 0300 GMT, 11 June 1985. Red denotes the most intense areas of convection.

Chapter 5

RESULTS OF SURFACE ANALYSES OF THE 10-11 JUNE SQUALL LINE

In this section, mesoanalyses of the 10-11 June squall line which passed over the OK PRE-STORM network are presented. The intent is to examine on a mesoscale the surface characteristics of this particular squall system and draw general conclusions regarding the surface structure of midlatitude squall lines. Four areas will be discussed in particular: precipitation, temperature and dewpoint, pressure, and potential temperatures.

5.1 The Storm's Precipitation Pattern

As mentioned previously, the 10-11 June 1985 squall line was characterized by three distinct precipitation zones: the convective line, a transition zone and the trailing stratiform region. This squall line developed a widespread and "uniform" shield of stratiform rainfall which formed several hours after the initial convection and persisted for several hours. Houze (1977); Zipser (1969, 1977); Leary and Houze (1979) and Leary (1984) found similarly that with tropical mesoscale convective systems the initial convection led the appearance of the stratiform precipitation by typically four to eight hours. Also, the full extent and intensity of this precipitation shield occurred approximately two to three hours after the convective line began to dissipate. This lag in the growth of the stratiform region in relation to that of the convective line has been observed and documented by Leary and Houze (1979) in their study of tropical squall systems during the GATE experiment. Figure 13 shows the system's low-level reflectivity pattern at hourly intervals from 2300 GMT on 10 June to 0800 GMT on 11 June 1985. The radar composites illustrated in the figure were created using digitized radar data from the Wichita, KS (ICT); Oklahoma City, OK (OKC); and Amarillo, TX (AMA) National Weather Service radar sites. Data from the Garden City, KS (GDC) site was not available. The composites selected depict

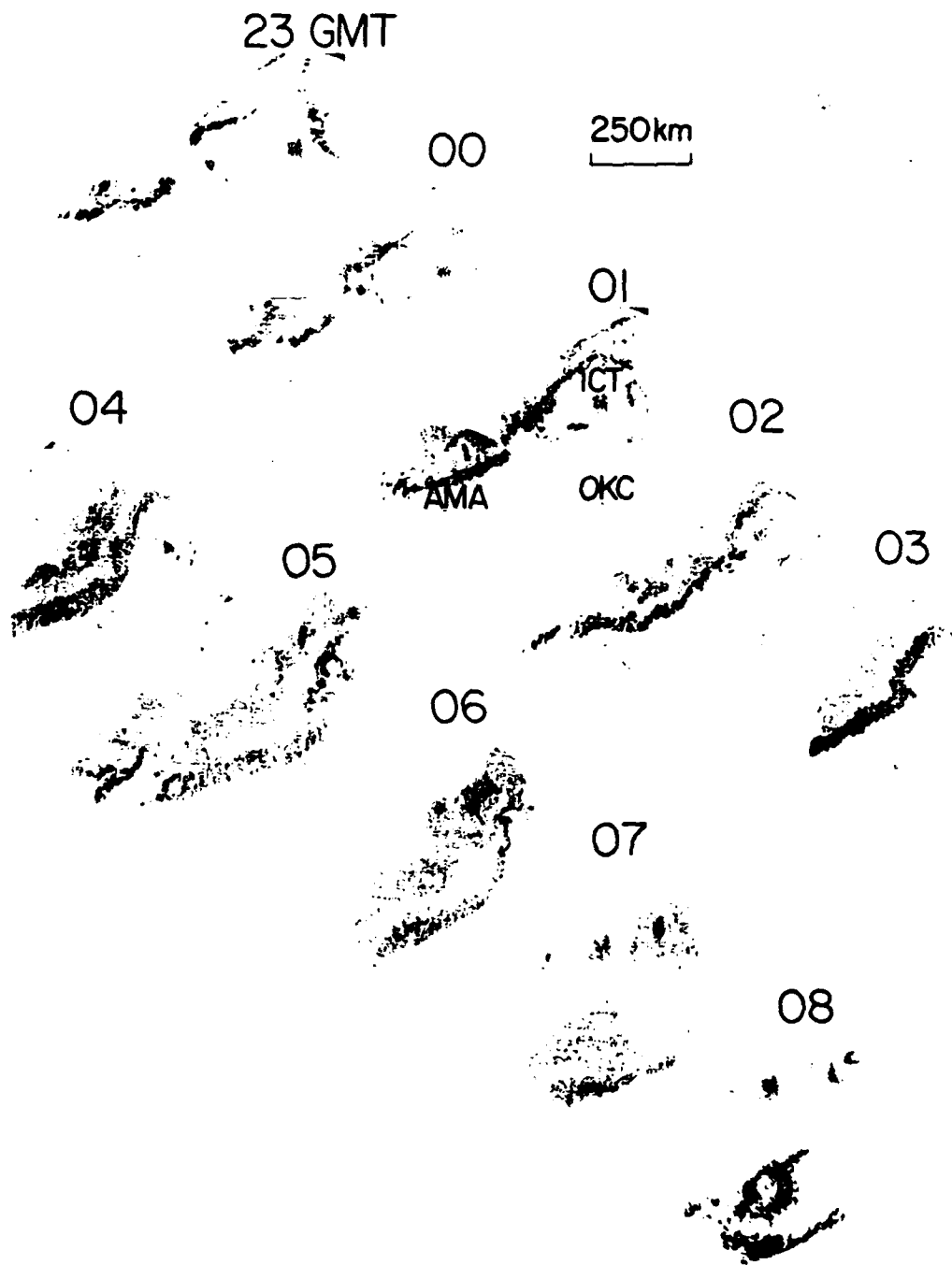


Fig. 13. Diagonal displays of composited low-level reflectivity at hourly intervals. Upper diagonal from 2300-0300 GMT and lower diagonal from 0400-0800 GMT. Reflectivity values from lightest to darkest shading are 15, 25, 35 and 50 dB(z). Locations of Amarillo, TX (AMA); Wichita, KS (ICT) and Oklahoma City, OK (OKC) are given

the evolution of the squall line as it passed over the PRE-STORM network. In the figure, the composites are arranged along two diagonals; the top from 2300-0300 GMT and the lower from 0400-0800 GMT.

At 2300 GMT the line is maturing and taking the classical linear shape to the west and northwest of the ICT and AMA sites, respectively. With time the line continues to strengthen and cover a larger area as it approaches Wichita, KS from the northwest (310 degrees) at 14 m s^{-1} . At 0200 GMT the full length of the convective line is evident extending over 700 km from the Texas panhandle to northeastern Kansas.

The line reached full maturity around 0300 GMT (see Fig. 13) and was directly overhead at ICT. At this time, the stratiform precipitation covered over 80% (over 72,000 km^2) of the storm's reflectivity field compared with 20% (18,000 km^2) for the convective line. Within the convective line individual echos exceeded 50 dB(z) while to the rear within the stratiform region echos ranged from 15-25 dB(z). Most importantly at 0300 GMT is the initiation of "bowing" of the convective line and the formation of a transition zone between the leading line and the trailing stratiform region. Additionally, to the rear of this bow and in line with the storm's motion a "notch" appears in the stratiform field around 0230 GMT. This feature, along with the bowing, is depicted in Fig. 13.

This phenomenon of bowing in the convective line has recently been studied and documented by Fujita (1981). He defined this bow echo as "a bow-shaped mesoscale echo (and) a potential inducer of strong downbursts." Fujita's studies during project NIMROD (Northern Illinois Meteorological Research on Downburst) reveal that high and damaging winds are associated with this bow echo.

Smull and Houze (1985) in their investigation of the trailing stratiform region associated with a squall line which traversed the NSSL observational network on 22 May 1976 similarly observed a notch in the anvil rainfall echo pattern and an accompanying bowing of the convective line. They hypothesized that this strong mid-level inflow into the trailing anvil which "acted to evaporate precipitation particles at the rear edge of the stratiform rain area." Additionally, they believed the rear inflow of dry air to be linked with a relative-flow cyclonic vortex found in the stratiform region. As the notch evolved and

evaporated more precipitation, they observed a bulge or bowing of the leading convection and suggested a connection between the notch and subsequent changes in the shape and motion of the convective line. The genesis of the notch was found to precede the bowing by about one hour. These results by Smull and Houze are similar to those found for the 10-11 June case.

By 0500 GMT, the stratiform region had maximized its horizontal coverage surpassing some 140,000 km² and began to lose its uniformity. Significant regions of heavier rainfall (greater than 35 dB(z)) embedded within the broad extent of the stratiform precipitation appeared and became more apparent during the next three hours. The convective line, as well as the transition zone and the stratiform region, has increased its forward "bowing" at this time.

From 0600 to 0800 GMT the notch continues to enlarge and the bowing of the line increases until it breaks apart. At 0700 GMT the squall line has all but dissipated with the exception of the large stratiform region which has also separated into two distinct centers. Just to the northeast of the ICT radar station an interesting circular pattern of stratiform rain is observed with the reflectivity factor increasing inward and exceeding 35 dB(z) at its center. At 0800 GMT this feature is more pronounced and is rotating cyclonically as seen with radar time lapse photography (Peter Dodge, Hurricane Research Division, AOML, personal communication, 1986). This phenomenon is comparable to the comma echoes explained by Smull and Houze (1985) or to the rotating head echo defined by Fujita (1979). Smull and Houze believed this cyclonic echo to be a result of the breakup of the relative-flow vortex found within the stratiform region into several subvortices. Fujita, on the other hand, suggested this echo was a mesoscale circulation induced by the bowing of the convective line. After 0800 GMT the remaining stratiform region dwindled and moved out of the PRE-STORM area. An isochrone analysis showing the hourly movement of the gust front throughout the squall line's life is shown in Fig. 14.

Figure 15 presents analyses of the total measured rainfall from the squall line and the amount and percentage of that total due to stratiform precipitation. The tabulations of the total rainfall amounts were made using the 42 PAM stations (the northernmost

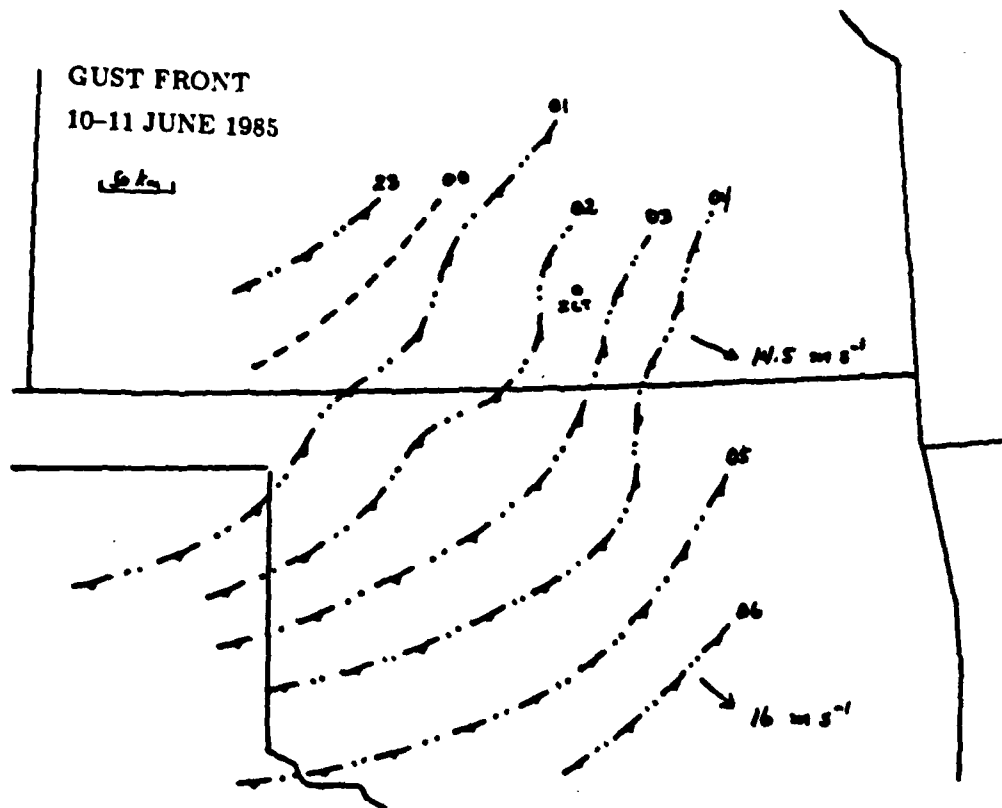


Fig. 14. Isochrone analysis of gust front position. Dashed line represents an estimated position. Arrows show direction and speed of movement of gust front.

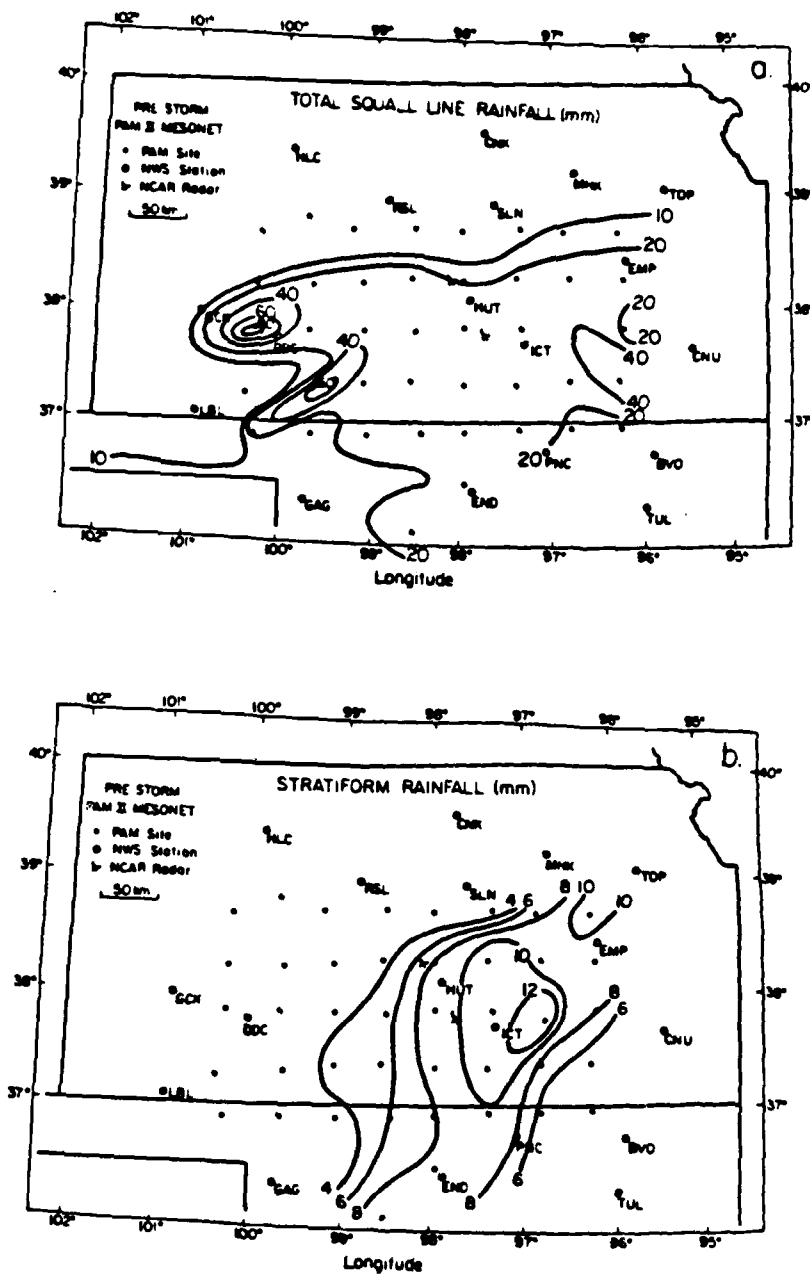


Fig. 15. Analyses of Total Rainfall (a), Stratiform Rainfall (b) and Stratiform Rain Fraction (c) for the 10-11 June squall line over the PAM network.

stations of the PRE-STORM network) and the surrounding NWS stations. Overall, Fig. 15a shows a majority of the area received in excess of 20 mm of rain. The western portion of the network received highly variable amounts exceeding 60 mm at some locations. The immaturity of the squall line during the time it traversed the western area can account for the variability. A rather uniform region of rainfall totals from 20 - 30 mm is seen over the central sections and moderate variability is again evident in the east as the system dissipated. Earlier, it was shown that the life cycle of the stratiform region lags that of the convective line. From this fact, we expect most of the stratiform rain in association with this squall line to fall over the eastern areas of the PRE-STORM network. This is indeed true as illustrated in Fig. 15b where a large portion of central and eastern Kansas and northern Oklahoma received well over 8 mm of stratiform rain or 20-40% of the total rainfall (see Fig. 15c). In northeastern Kansas, where the squall line arrived in a highly weakened state, some stations received 60% of their total rainfall from the anvil precipitation.

5.2 Temperature and Dewpoint Analyses

As reviewed in the synoptic overview, warm and moist conditions prevailed over the PRE-STORM network during the late afternoon hours on 10 June 1985. As the storm materialized and entered the western half of the network, significant disturbances in the temperature and dewpoint fields occurred. Substantial cooling at the surface results when cool air from within the convective towers descends through the downdrafts and spreads outward at the ground. The "temperature break" (Byers, 1949) corresponding to the boundary of the cold air dome, immediately follows the gust front at the surface (Fujita, 1963). Also, temperature falls are often observed well outside the region experiencing precipitation. Figures 16-18 illustrate the temperature and dewpoint fields at early (2300 GMT), mature (0300 GMT), and dissipative (0700 GMT) stages of the storm's life cycle over the PRE-STORM network. Contours are drawn at 2°C intervals.

At 2300 GMT (Fig. 16a) the cold pool associated with the convective line is shown over western Kansas. Dramatic temperature falls occurred with its arrival. Temperature

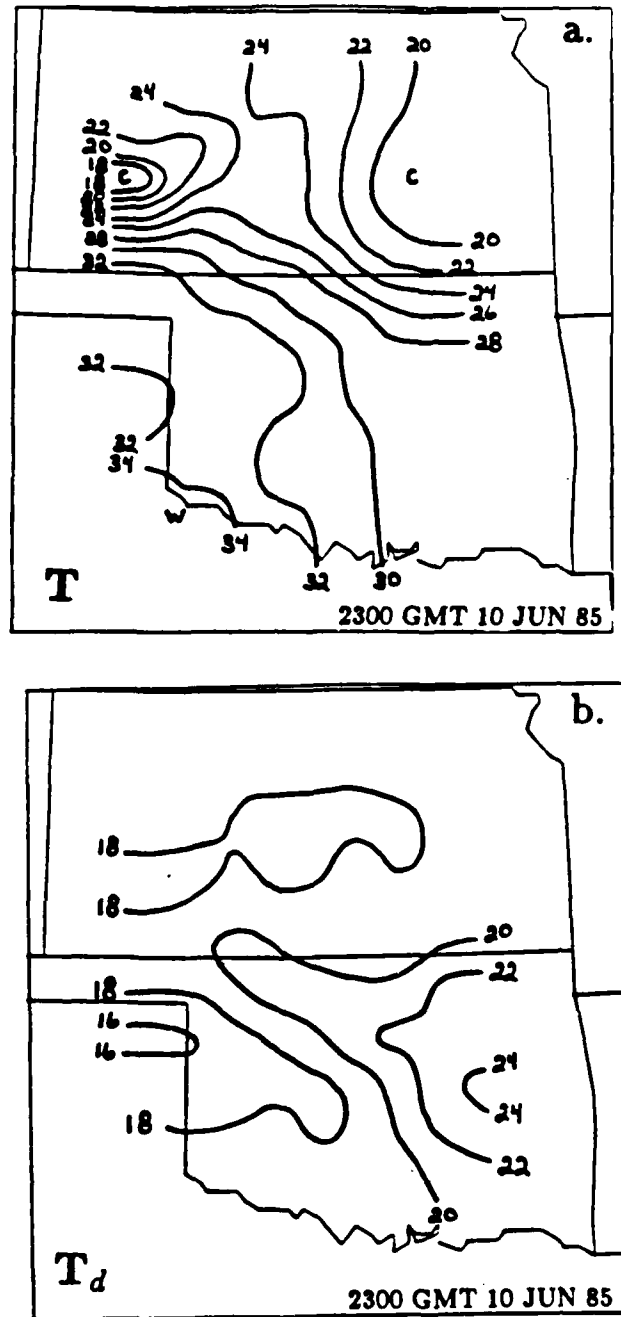


Fig. 16. Surface temperature (a) and dewpoint (b) analyses for 2300 GMT, 10 June 1985 over the PRE-STORM network. Warm and cool regions are labeled by W and C, respectively.

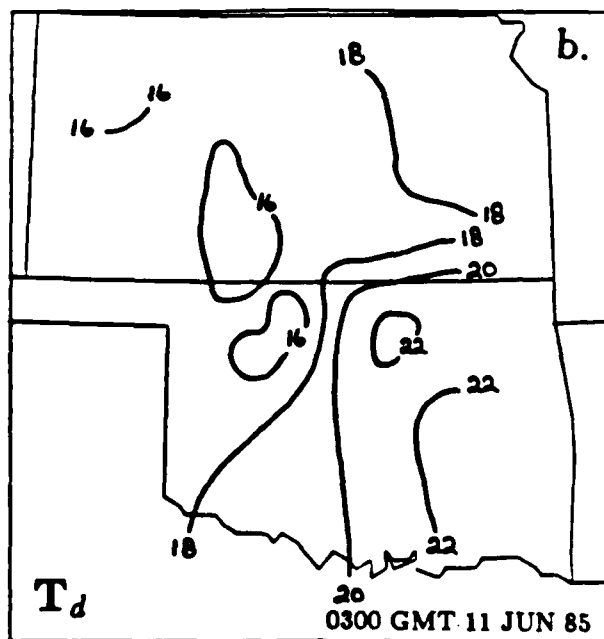
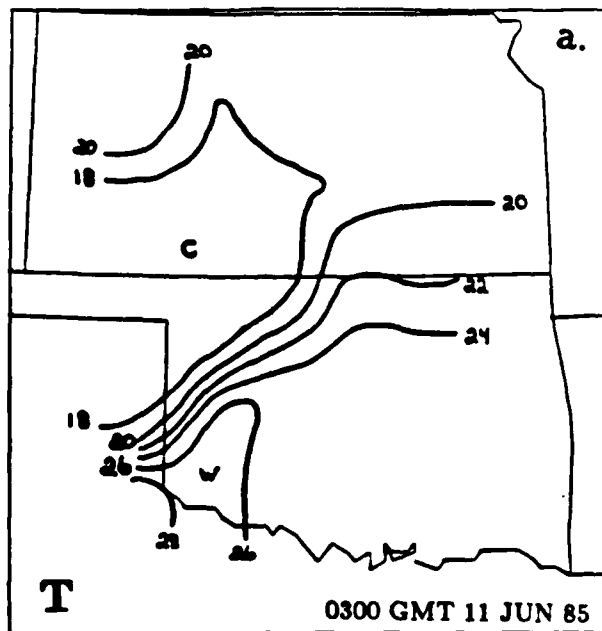


Fig. 17. As in Fig. 16 except for 0300 GMT, 11 June 1985.

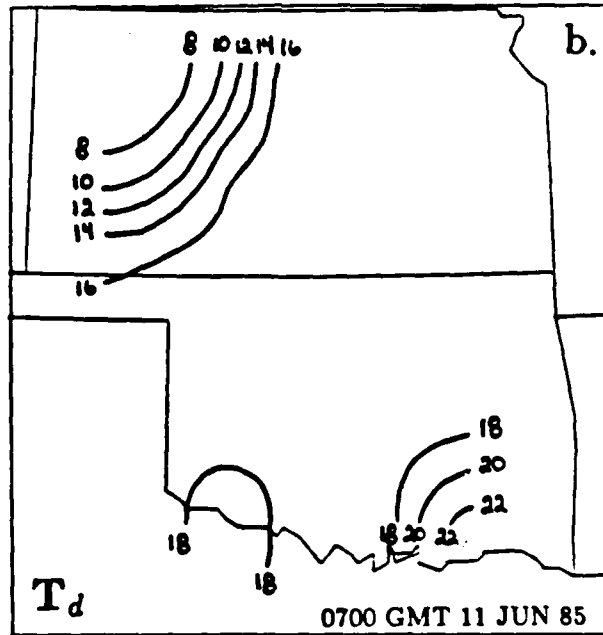
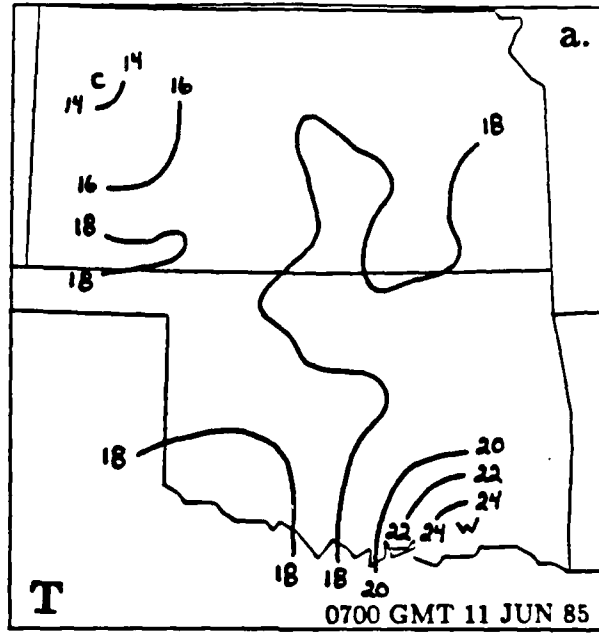


Fig. 18. As in Fig. 16 except for 0700 GMT, 11 June 1985.

drops averaging 9°C resulted from the passage of the gust front. In particular, PAM station 17 experienced a temperature drop of 10.5°C in just 1.5 hours. Immediately to the east of the cold dome and ahead of the gust front, temperatures were much warmer averaging around 25°C . In eastern Kansas, the surface cooling produced from the remnants of the previous MCS is seen with temperatures below 20°C . Hot conditions prevailed over southwestern Oklahoma. When the temperatures are compared with the corresponding dewpoints in Fig. 16b, a tongue of warm, moist air is observed to feed into the squall system from southeast Oklahoma. A pocket of relatively low dewpoint air appears over Kansas representing the drying of the boundary layer by the convective downdrafts.

At 0300 GMT (Figs. 17a and 17b) the convective line has fully matured and moved into central Kansas and northern Oklahoma. Figure 17a shows clearly that the effect of this squall line has been to significantly cool the boundary layer over a large area extending from northern Texas into central Kansas. Little if any temperature gradient exists in the immediate post-squall region. Temperatures throughout the wake area are near 17°C . The accompanying dewpoint analysis shows that collocated with this cold pool are two pockets of low dewpoint (below 16°C) indicating the air has low absolute humidity. A strong temperature gradient is analyzed over portions of Oklahoma marking the general position of the gust front and the convective line. Ahead of the system, in the "undisturbed" environment, a southwesterly flow of warm, moist air is seen and extends northward into the region previously under the influence of the other MCS.

At 0700 GMT during the dissipative stage of the squall line, the only remaining area of warm air (greater than 20°C) is found over extreme southeastern Oklahoma (Fig. 18a). With the exception of cooler air entering northwest Kansas, the temperature field at this time is fairly flat throughout the two state area with temperatures near 18°C . A look at the dewpoint field shows that a much drier air mass associated either with a pre-existing frontal system or with frontogenesis is entering Kansas. This dry air mass was located earlier in western Nebraska and is now, after the demise of the squall line, making its way into the PRE-STORM area.

5.3 Mesoanalysis of the Surface Pressure

The primary focus of this thesis is to investigate the nature, structure and possible forcing of the wake depression accompanying a midlatitude squall line. Over two decades have passed since Fujita (1963) and Williams (1963) performed detailed analytical studies of these mesoscale pressure features. Numerous mesoanalyses of surface pressure for the 10-11 June MCS depicting the evolution of the wake depression as well as the mesohigh and the pre-squall mesolow are presented.

The sources of the pressure data used in this section are the 80 aneroid barometers located with each PAM and SAM automated station. The data were collected at five minute intervals. During the course of this particular squall line, some of the SAM stations were not operational; however, the data coverage for this storm is excellent.

A series of nine pressure analyses is now presented beginning at 2300 GMT on 10 June 1985 and continuing until 0725 GMT the following day. The analyses are shown mainly at one hour intervals. In addition to the pressure contours, the temperature, dewpoint and wind data from each PAM and SAM station are given. Furthermore, to show the mesoscale pressure features as they relate to the storm's precipitation pattern the reflectivity field is superimposed onto each analysis. The reflectivity pattern closest to the time of the individual pressure analysis was used. It is appropriate to restate that the radar data from the Garden City, KS site was not available for this storm.

The first analysis is for 2300 GMT (Fig. 19). The contours are analyzed at 1 mb increments and are labeled as departures from 950 mb. A weak trough of low pressure is located about 75 km northeast of the ICT radar site. This appears to be the fading remnants of the wake depression produced by the MCS which passed over the mesonet network a few hours earlier. Some light precipitation with a few embedded heavier showers is falling in this vicinity. Temperatures are relatively cool in the trough. To the west is the early stage of a mesohigh taking form in conjunction with the developing squall line. The maximum pressure at this time is slightly over 950 mb. Immediately in advance of the surface gust front (denoted with a dashed and double-dotted line), a southwest to northeast oriented trough, roughly parallel to the early convective line, has formed.

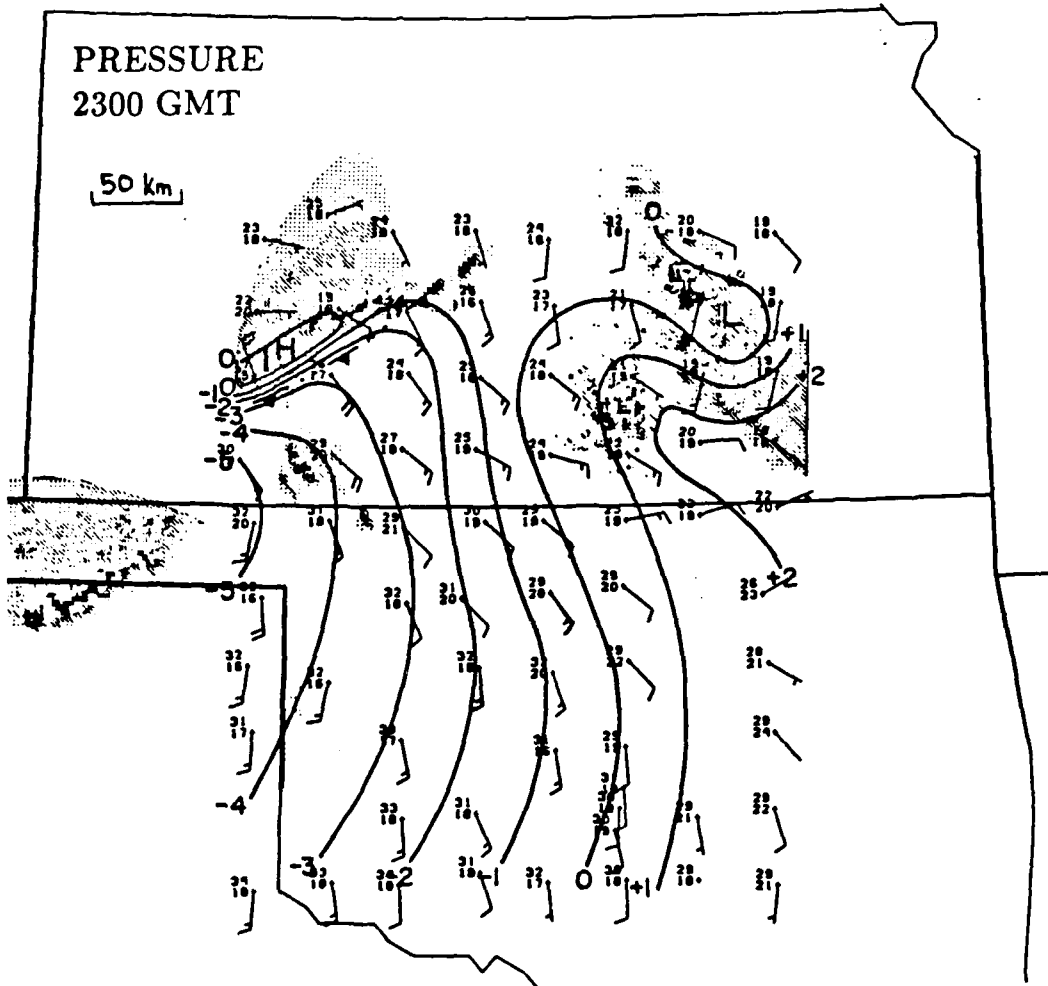


Fig. 19. Pressure analysis at 518 m ASL at 2300 GMT, 10 June 1985. Contours are departures from 950 mb. Reflectivity values from lightest to darkest shading are 15, 25, 35 and 50 dB(z). Dashed line represents the end of stratiform rainfall at the ground. Centers of high and low pressure denoted with H and L, respectively.

Along with high temperatures and high dewpoints, pressures within the trough range 1-5 mb lower than within the mesohigh. The surface wind field exhibits cyclonic turning as southerly winds prevail over Oklahoma but accelerate and become southeasterly as the wind flow approaches the gust front. To the rear of the convective line some light rainfall representing the very early stages of the stratiform precipitation is observed.

Advancing two hours to 0100 GMT on 11 June 1985 (Fig. 20), we see that the squall line has rapidly intensified and pushed farther into the PRE-STORM area. The most dominating feature is the very strong mesohigh located along the convective line just north of the Oklahoma-Kansas border. Pressures have increased over 4 mb in the mesohigh's center since 2300 GMT to about 954 mb. The analysis shows that the mesohigh is not a uniform, continuous feature along the convective line. In fact, its shape, size and strength varies considerably in the course of just 1/2-1 hour. It often takes the form of a "bubble high" with a defined center. Why would the mesohigh be so pronounced at the location shown in the figure? Obviously, the evaporative cooling which creates the high and cold dome is occurring all along the leading line. Possibly the mesohigh in the figure represents the locality of the most intense cumulonimbus cells which would maximize the evaporative cooling. However, as seen by the reflectivity pattern this does not appear to be the case for the 0100 GMT analysis. The most severe convection is situated on either side of the mesohigh.

It is suggested that the analyzed "bubble" mesohigh represents the current location of the initial cold dome which formed around 2200 GMT on 10 June with the initial convection. Visible satellite images from 2030 GMT on 10 June (not presented) show an intense convective cell over southwest Kansas (see Fig. 8a for 2100 GMT image). The cell was forming at the northernmost edge of the developing but still immature squall line. Observations from the local NWS station reported the presence of severe thunderstorms just northwest of Garden City at 2120 GMT. Figure 21 depicts the severe weather events which occurred with these early thunderstorms. There were numerous reports of hail in the Garden City to Dodge City, Kansas area ranging in size from marbles to ping-pong balls from 2125-2330 GMT. In addition, the NWS observing station at Garden City and Dodge

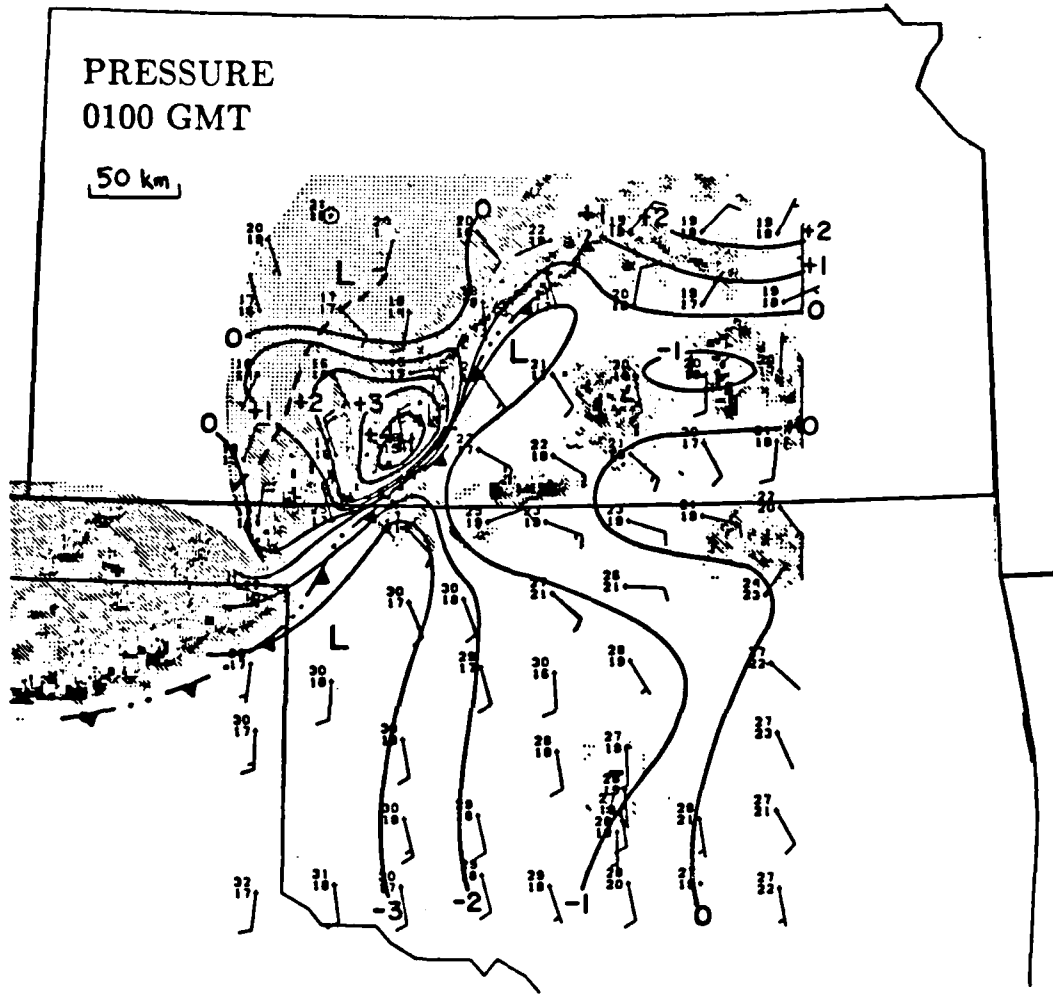


Fig. 20. As in Fig. 19 except for 0100 GMT, 11 June 1985.

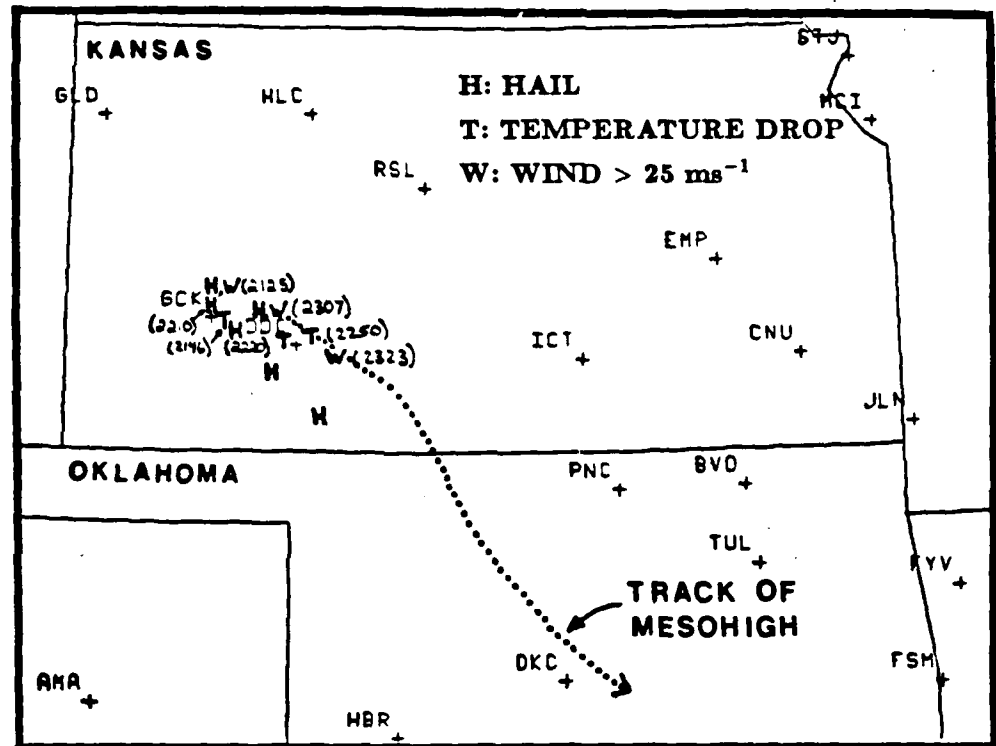


Fig. 21. Severe weather events in southwest Kansas during the late afternoon on 10 June 1985. Locations of large hail (greater than 2 cm), large temperature drops (greater than 10°C within an hour of the onset of rain) and high winds (above 25 m s⁻¹) are indicated. Times for these events are in GMT. Dotted line represents path of mesohigh.

City along with PAM station 17 observed a sharp temperature fall of 11°C within an hour of the onset of first rainfall from these storms. The combined effect of hail and intense rainfall rates led to the creation of a large cold pool in this area of southwestern Kansas. It is believed that this initial cold pool moved southeastward with the developing squall line and was intensified by additional evaporative cooling as the line strengthened. The formation of the mesohigh around 2300 GMT coincides well with the time and location of this early cold pool. The mesohigh analyzed at 0100 GMT reflects the presence of this cold dome and can be tracked through the course of the squall line into Oklahoma as shown in subsequent analyses.

In the two hours since the 2300 GMT analysis, the convective line has grown farther northward and interestingly so has the trough situated just ahead of the convection (Fig. 20). This implies a link between the convection and the formation of the trough or pre-squall mesolow (Hoxit *et al.*, 1976). This trough which parallels the leading line of convection would become more defined as the squall intensified. The wake depression with the previous storm is almost imperceptible but still exists over the eastern network. Behind the convective line underneath the area of increasing stratiform precipitation, first signs of a wake depression are observed at 0100 GMT. Note the lag in the wake depression's maturity as compared to the mesohigh. No closed contour of low pressure has yet formed. The dashed line in the region of stratiform precipitation represents the end of rainfall at the surface as determined from five minute PAM/SAM station data.

At 0200 GMT (Fig. 22) the three pressure features frequently observed with midlatitude squall lines are well pronounced: the pre-squall mesolow, mesohigh, and the wake depression to the rear of the line. The trough preceding the gust front has grown in areal coverage and advanced to the southeast. The old wake depression shown in the previous figure appears to have merged with the pre-squall trough (or vice-versa) and this may account for the 949 mb closed contour near Wichita, KS. The mesohigh has also enlarged but its maximum strength has diminished by a millibar to 953 mb. Possibly the greatest pressure is between PAM stations and therefore not observed. A strong pressure gradient defines the mesohigh's leading boundary with a pressure difference of 5 mb over a 40 km

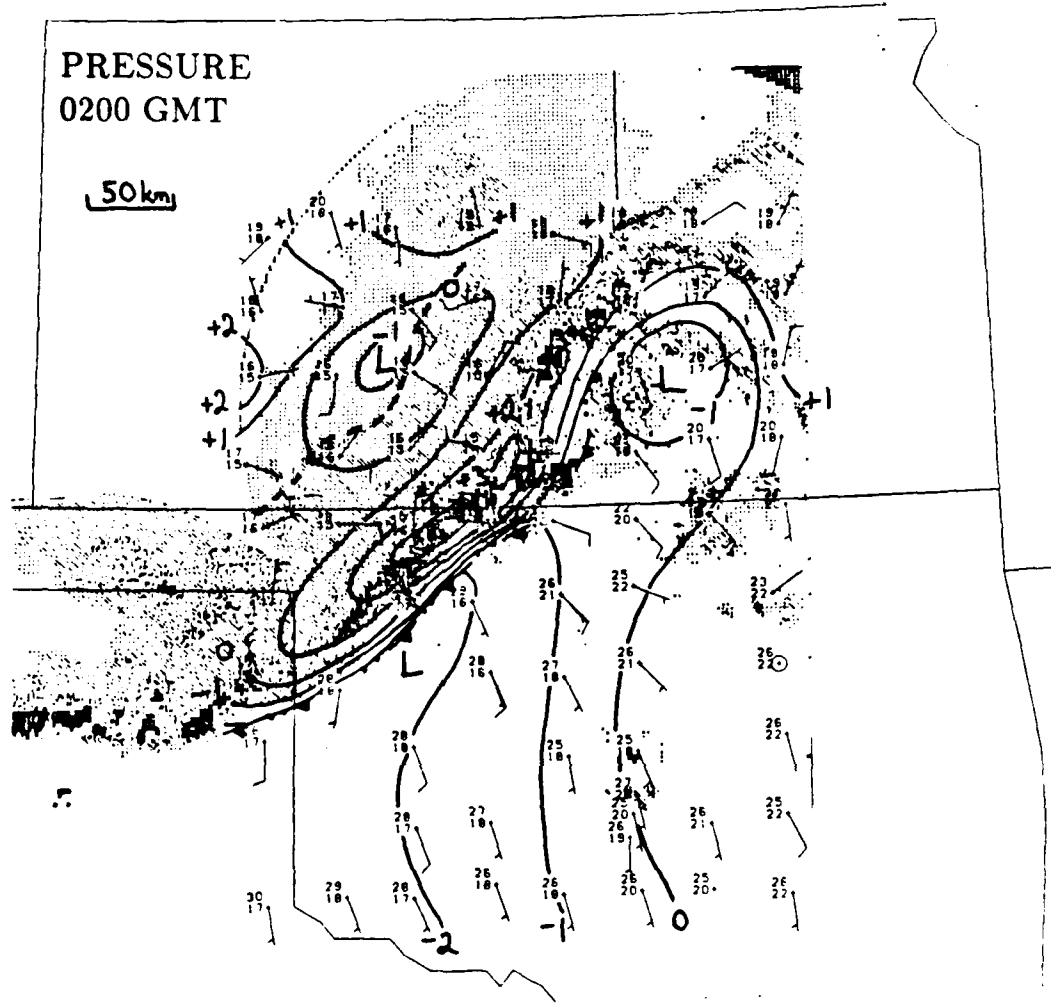


Fig. 22. As in Fig. 19 except for 0200 GMT, 11 June 1985.

distance. To the rear of the mesohigh's center, the pressure gradient is noticeably weaker as the pressure decreases towards the wake depression. At this hour, the wake depression has formed with the lowest pressure near 949 mb. A pressure difference of 4 mb exists between the centers of the wake depression and the mesohigh. The maximum dimension of the wake depression at this early stage is about 150 km which agrees with Schaeffer *et al*, (1985). The axis of the wake depression coincides with the line delineating the end of stratiform precipitation at the ground. A final observation at 0200 GMT is that the wake depression develops prior to a well defined transition zone in the reflectivity field.

The squall line acquired its greatest intensity near 0300 GMT and Fig. 23 illustrates the pressure and reflectivity pattern for this time. Although the convective line stretches from northeast Kansas to the Texas panhandle, the highest pressure (about 954 mb) is confined to the mesohigh located now over northern Oklahoma. Strong convective activity is found in the high's vicinity. The most significant change in the pressure field lies with the growing wake depression. The wake has deepened to 948 mb and has assumed an elliptical shape with the major and minor axes approximately 200 km and 80 km in length, respectively. Again, the major axis of the wake depression lies at the back edge of where the stratiform rainfall reaches the ground. The superimposed wind field reveals that the wind in the vicinity of the wake depression overshoots the axis of lowest pressure. The wind does not flow into the center of the low from all directions and there is no circulation around it. This satisfies well the definition of a mesodepression defined by Fujita (1963). In fact, Fujita later chose to adopt this nomenclature for the wake depression. As the figure shows, the air converges with the environmental air at the back edge of the wake depression. This phenomenon will be discussed further in a later section. The difference in pressure from the mesohigh to the wake depression at 0300 GMT has increased to 6 mb. Fujita (1955, 1963) found similar pressure drops from the mesohigh to the wake depression of 6-8 mb with mid-western squall lines. The wake depression appears to be strongest in the vicinity of the notch in the reflectivity pattern.

At 0400 GMT (Fig. 24) the stratiform precipitation region is nearing maturity and a transition zone is becoming more defined. Over Oklahoma the convective line is observed

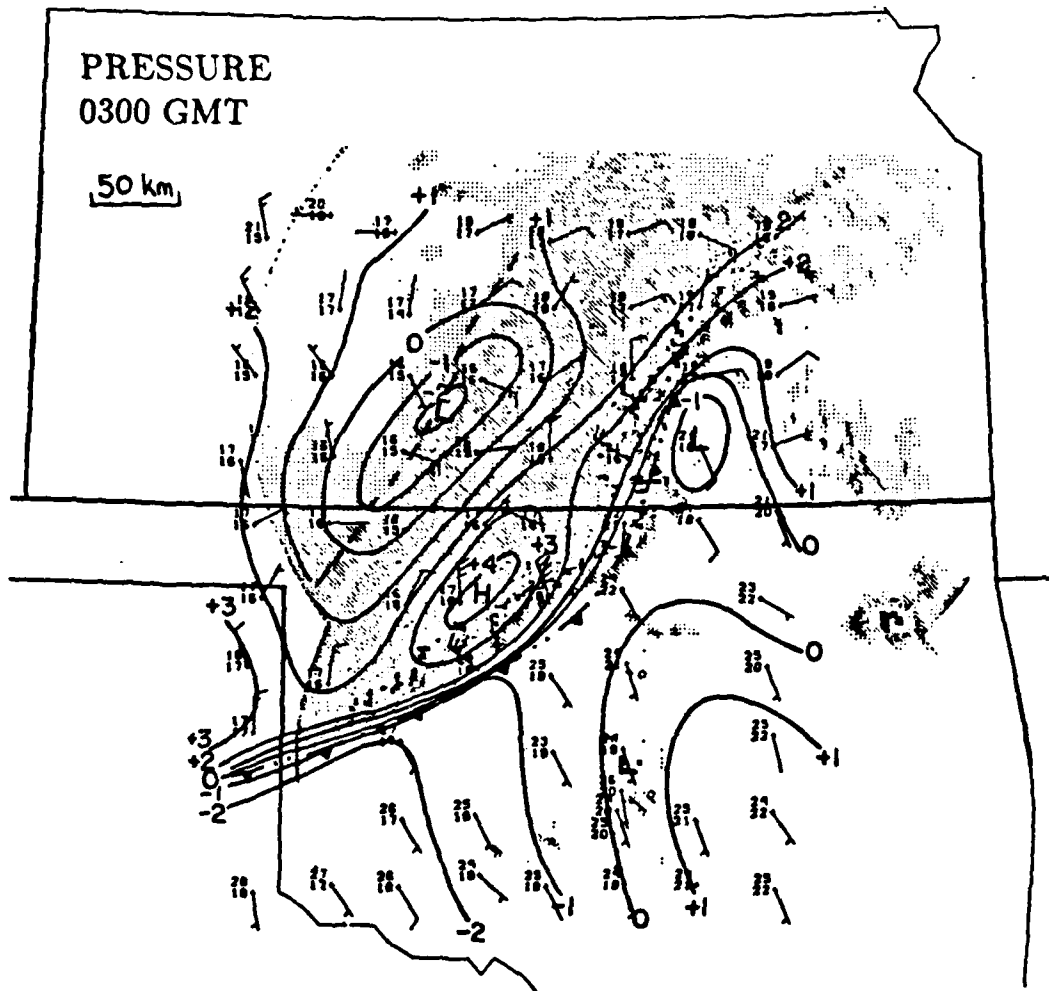


Fig. 23. As in Fig. 19 except for 0300 GMT, 11 June 1985.

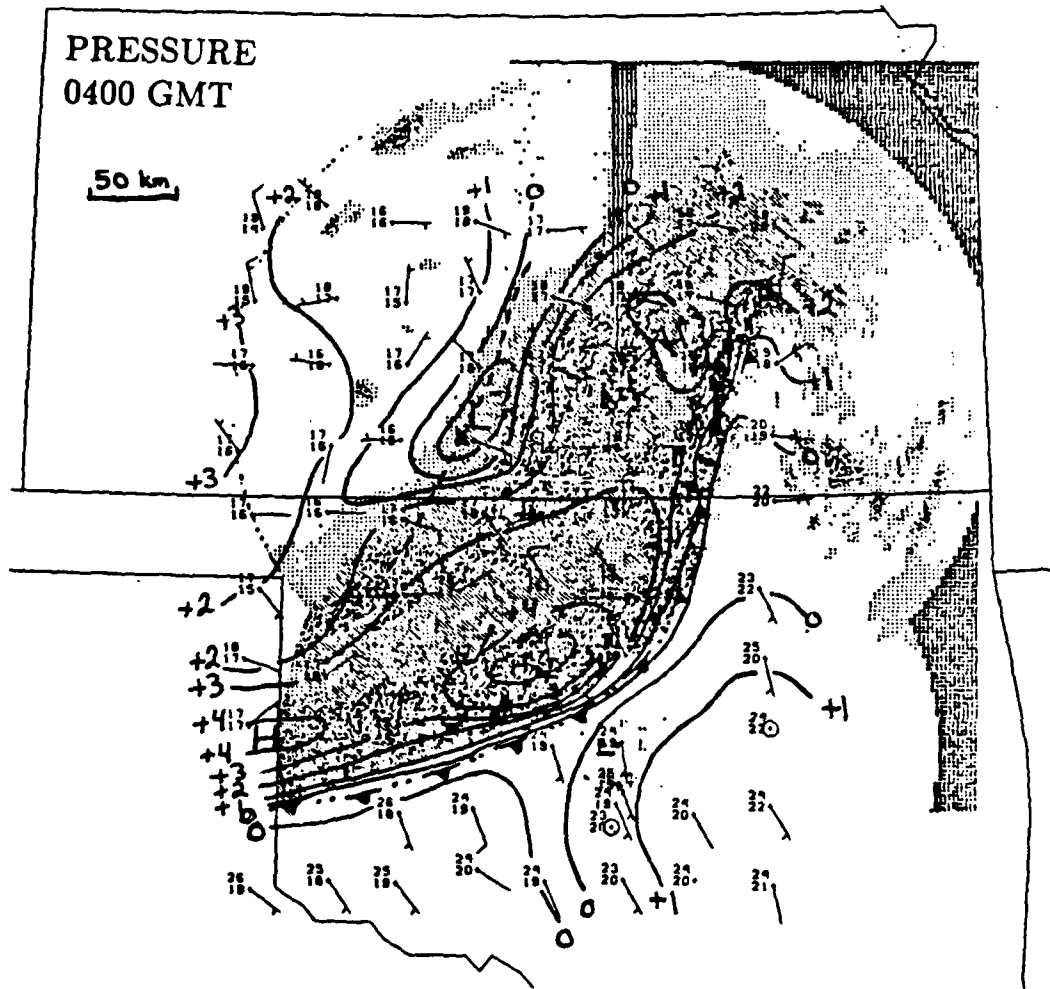


Fig. 24. As in Fig. 19 except for 0400 GMT, 11 June 1985.

to bow or bulge. Three "bubble highs" are now apparent in the figure with the more predominant being the same mesohigh tracked from southwestern Kansas. The other two mesohighs, located in Kansas and along the Texas-Oklahoma border, are transient features and will not appear in the analysis an hour later. Intense cells along the northern section of the convective line may explain the brief existence of the small mesohigh in Kansas. The bulging of the convective line is occurring in the vicinity of the main mesohigh. A maximum temperature gradient of 8°C exists from the center of the cold dome associated with the main mesohigh to the undisturbed air ahead. To the rear of the mesohigh, the wake depression has changed in shape and is slightly weaker than in the previous analysis but possibly the lowest pressures are between the PAM stations. As seen in the previous figures, the wake depression consistently lies along the back edge of where the stratiform rainfall reaches the ground.

The analysis for 0500 GMT (Fig. 25) shows the continued bowing but weakening of the convective line over Oklahoma. The mesohigh in this region remains strong. Again, the most significant change from the last analysis is with the wake depression. There appears to be a splitting of the wake depression into two parts with the most dominant mesolow in Kansas. As discussed in section 5A, the notch appears in the reflectivity field to the rear of the bow in the convective line. The two parts of the wake depression are positioned on either side of the notch in the stratiform region. The total length of the wake depression at this time is over 300 km.

Figure 26 illustrates that at 0600 GMT the mesohigh over Oklahoma has moved steadily southeastward and weakened slightly to 954 mb. Much of the PRE-STORM network is in the post-squall environment but the stratiform region is still causing significant precipitation in the east. The two wake depressions analyzed in the figure are now separate features with the strongest over Kansas just outside of Wichita. The Oklahoma low is very weak at best. The wind is again observed to blow through the axis of lowest pressure. To the west, northwesterly winds bringing cooler air and higher pressures are seen to invade the network.

By 0700 GMT (Fig. 27), the squall line has greatly diminished and moved out of the network with the exception of the stratiform rainfall region. A small, weak mesohigh still

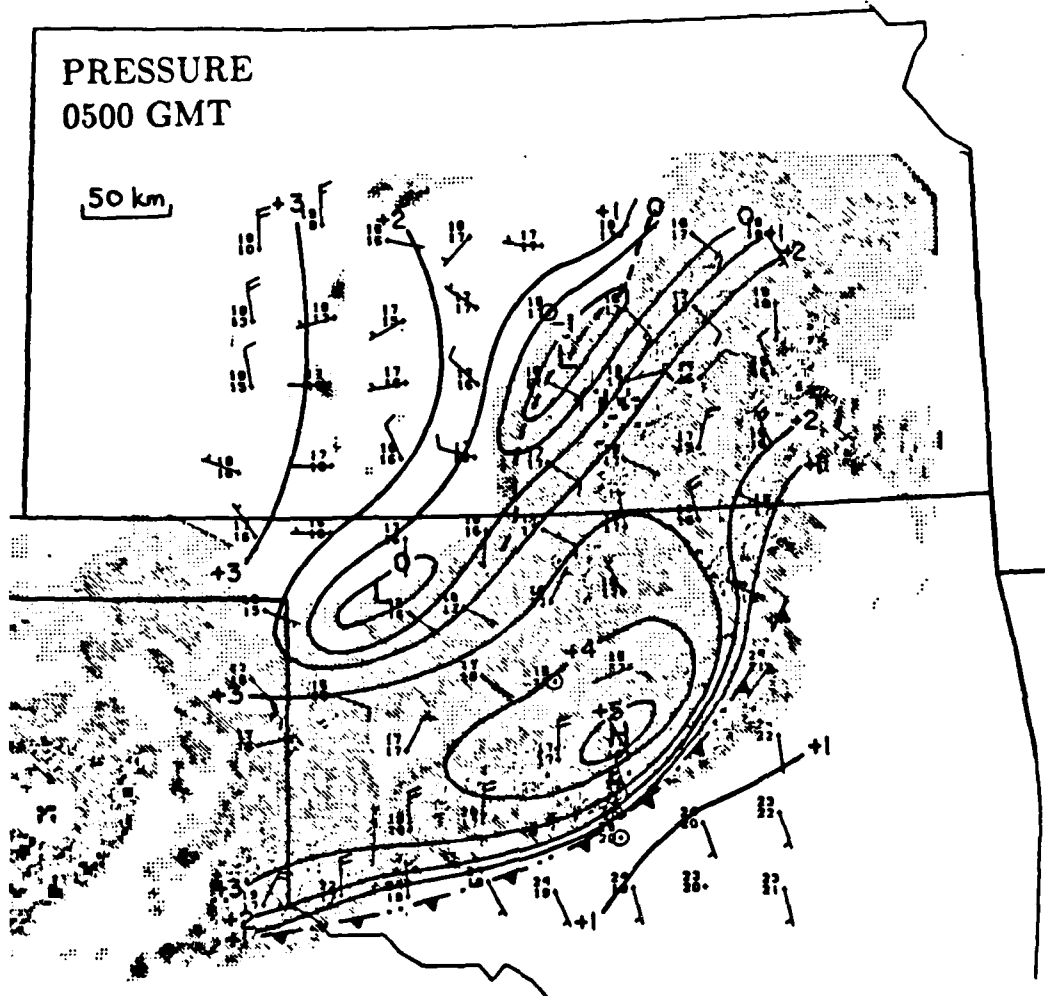


Fig. 25. As in Fig. 19 except for 0500 GMT, 11 June 1985.

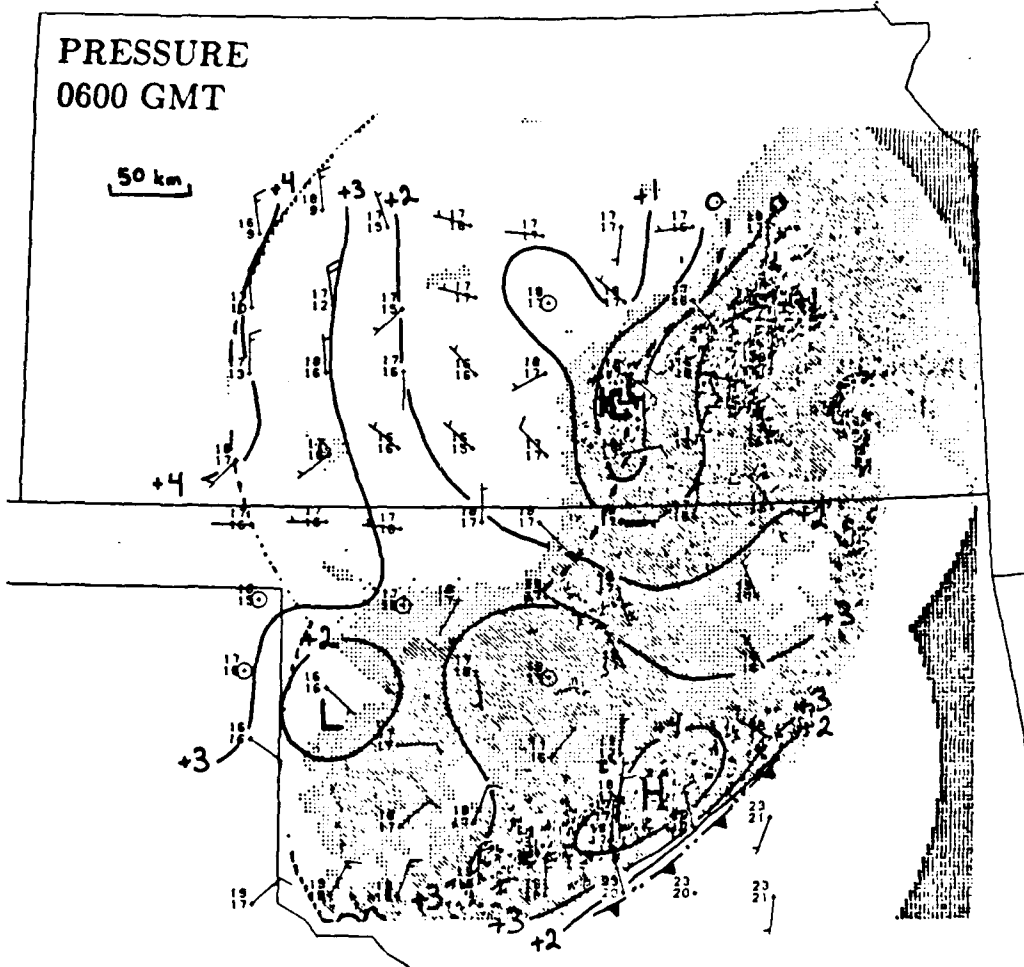


Fig. 26. As in Fig. 19 except for 0600 GMT, 11 June 1985.

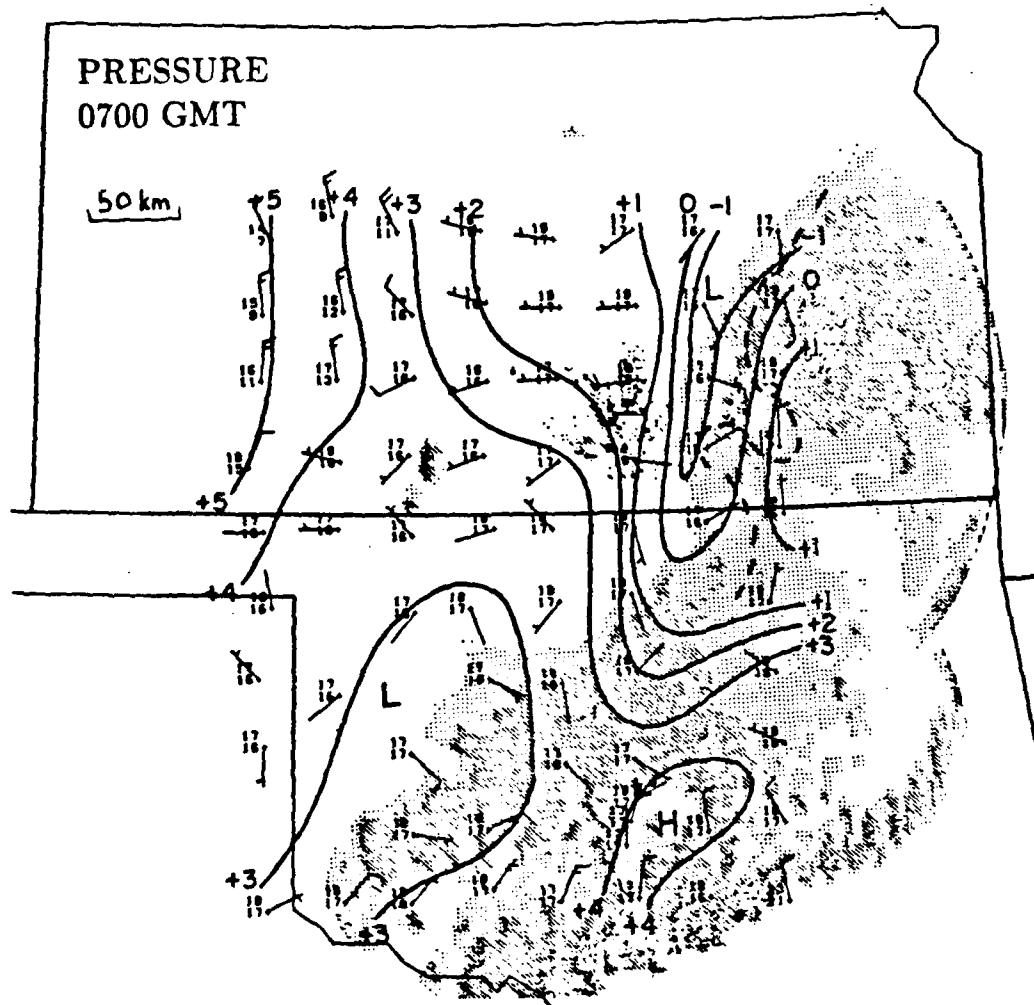


Fig. 27. As in Fig. 19 except for 0700 GMT, 11 June 1985.

exists over southern Oklahoma. The two wake depressions, however, are still well defined with the Kansas low assuming a long and narrow shape situated just behind the intense stratiform echo. Higher pressures associated with the new airmass are still advancing into the western network. The most interesting event observed with the wake depression associated with the 10-11 June squall line begins near 0700 GMT.

During the next 25 minutes, the Kansas low begins a sudden and most interesting intensification. At PAM station 23, located in the eastern Kansas portion of the PRE-STORM network, the pressure fell 2.2 mb from 0700 to 0725 GMT as a small but deep low pressure center developed overhead (Fig. 28). The analysis at 0725 GMT shows clearly the well defined wake over eastern Kansas. The wake depression located over southwest Oklahoma at 0700 GMT has now faded from the analysis. Notice that even with the relatively strong low over Kansas the winds blow through its center and converge at the back edge where a strong pressure gradient exists (about 5 mb/50 km). Figure 29 presents a divergence analysis at 0720 GMT in the vicinity of the wake depression. Convergence is occurring all along the back edge of the wake and not in its center while divergence is observed to the east of the wake in response to strong surface outflow from the convective line. After forming over PAM station 23, this small-scale low pressure center, roughly 50 km in width, moved northeastward arriving at PAM station 16 at 0750 GMT while the broader wake depression moved to the east. From this observation, it is assumed that the small low is a transient feature embedded within the overall wake depression. Therefore, the wake depression appears to possess small scale elements.

In summary, Fig. 30 illustrates the tracks of both the mesohigh and the wake depression with this MCS. Immediately, it is apparent that these two pressure features did not follow the same path across the PRE-STORM network. The mesohigh steadfastly tracked southeastward while the wake depression moved to the east. Note how the wake depression, more so than the mesohigh, changed shape during its existence.

A final observation of the wake depression concerns the temperature and moisture changes following its passage. As reviewed in chapter 2 of this thesis, the wake depression is attributed to a pocket of warm, dry air found below the rear anvil of the squall line

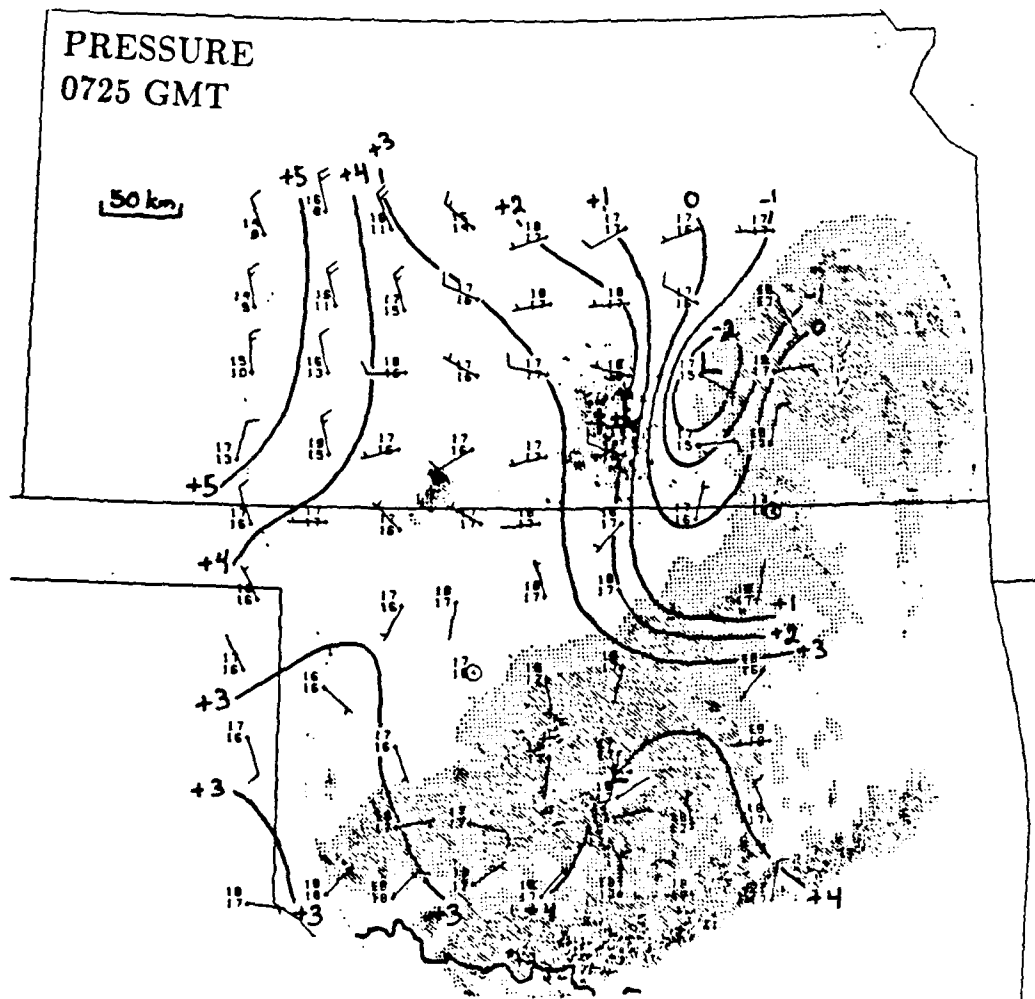


Fig. 28. As in Fig. 19 except for 0725 GMT, 11 June 1985.

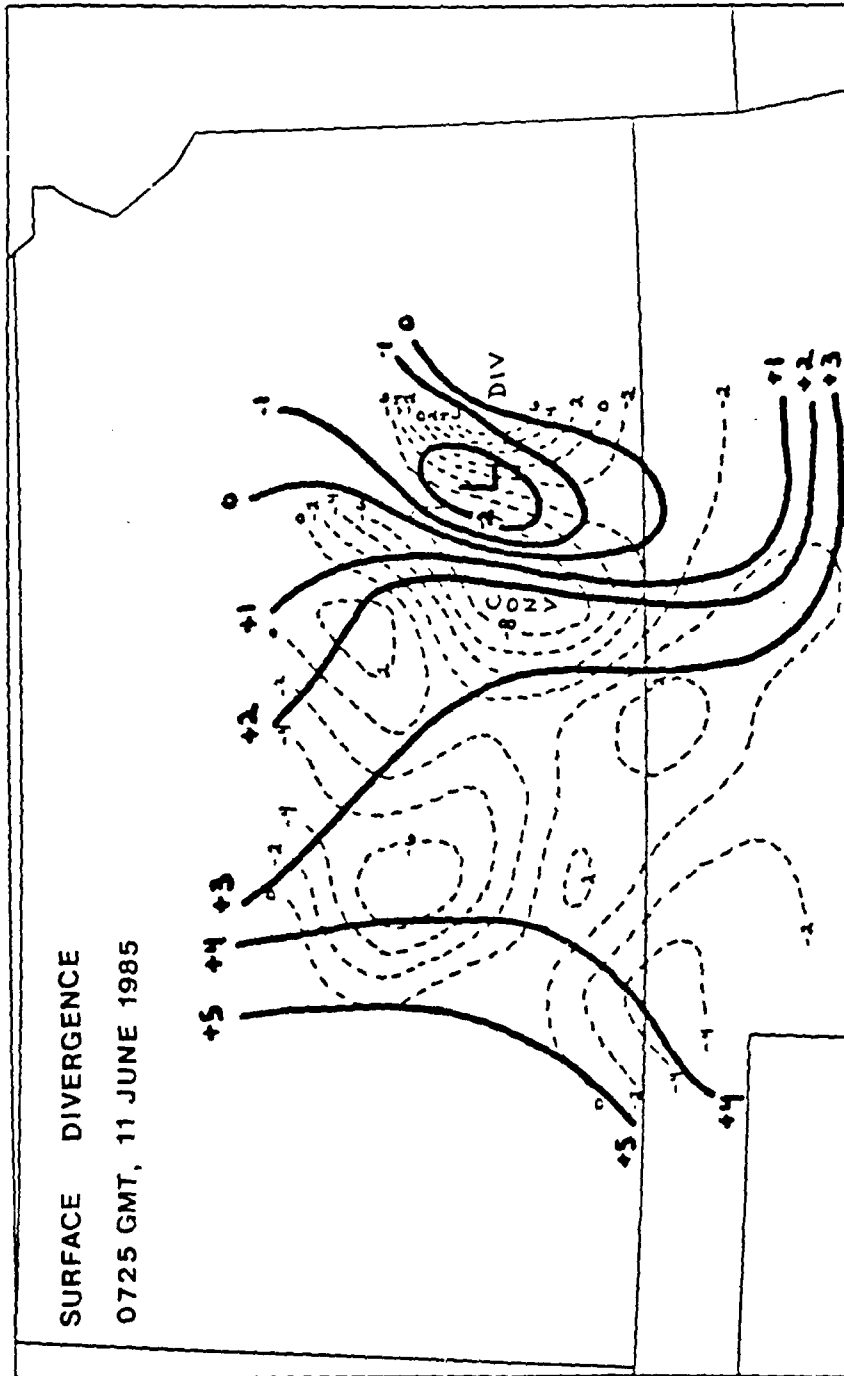


Fig. 29. Surface divergence field ($\times 10^{-5} \text{ s}^{-1}$) over PAM network at 0725 GMT, 11 June 1985. Solid contours represent isobars (mb) for same time. Center of wake depression labeled as L.

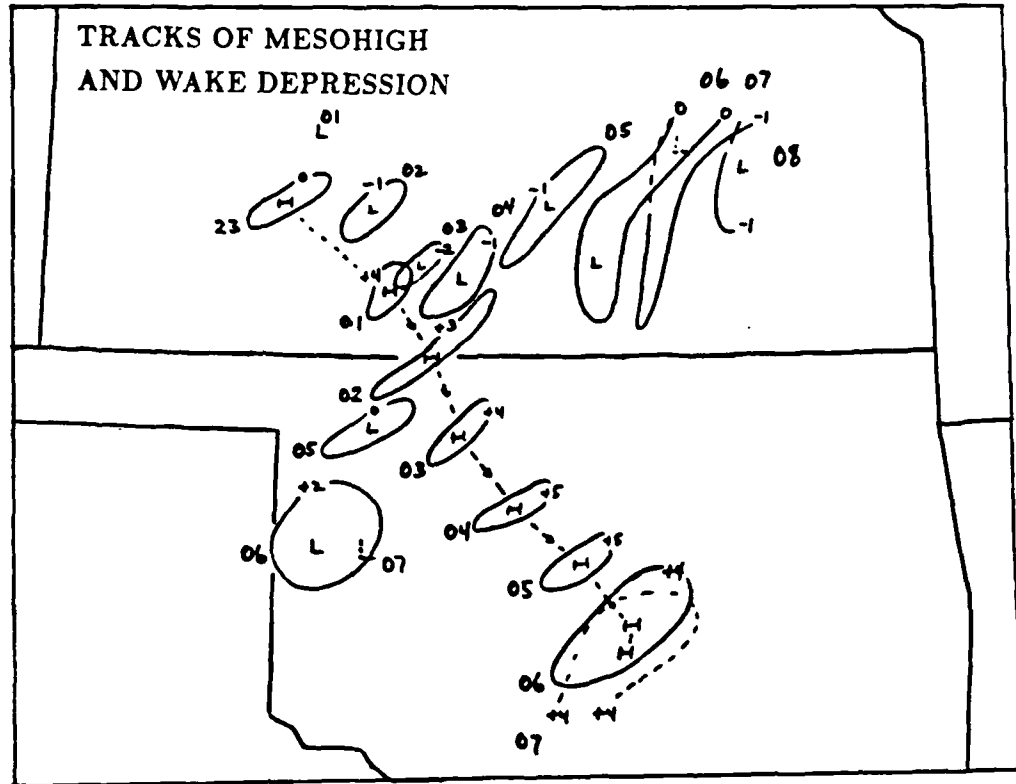


Fig. 30. Tracks of surface mesohigh (H) and wake depression (L). Times in GMT. Contours labeled as departures from 950 mb.

but above the ground. From examination of the network database, no significant surface warmings occurred during or after the passage of the wake depression implying that little, if any, of the warm, dry air aloft penetrated to the surface. At PAM station 23 where the wake passed overhead, a slight warming of 1.5°C and a simultaneous drop in relative humidity of 14% did occur, however, after passage. Williams (1963) noted surface warmings are possible though following the passage of thunderstorms. Most of the temperature rises were small averaging less than 5.5°C but a few exceeded 8°C. Johnson (1983) documented several cases of surface "heat bursts" following squall lines. No such heat bursts were observed with this particular storm. Zipser (1977) observed the "mesolow" to coincide with minimum surface dewpoints which implies downward mixing of drier air from aloft. From the analyses presented in this section, the wake depression does appear to be located with relative dewpoint minima; however, the lowest dewpoints in the network were frequently found just outside the wake depression or within the mesohigh.

5.4 Surface Analyses of Potential and Equivalent Potential Temperatures

Potential temperature analyses give the analyst another tool to interpret the effects of squall lines on the environment. Three analyses each of potential and equivalent potential temperatures have been prepared for the early, mature and dissipative stages of the squall line (2300 GMT, 0230 GMT, and 0725 GMT, respectively). Figures 31a and b illustrate the fields of these parameters at the surface for 2300 GMT on 10 June with the pressure analyses superimposed for easier interpretation. Much of the surface in eastern Kansas has been cooled at this time by the effects of the earlier MCS. Some convective activity remains however, and so added evaporative cooling produces the relatively low values of potential temperature (θ) in this area. Across the state in western Kansas a small band of low θ indicates the presence of the squall line. This band correlates well with the position and size of the mesohigh from the line. Over the remainder of the network, fairly high temperatures exist with a strong gradient of potential temperature ahead of the developing squall line. The field of equivalent potential temperatures (θ_e) is complicated with numerous regions of high and low values. One θ_e minimum is found in eastern Kansas

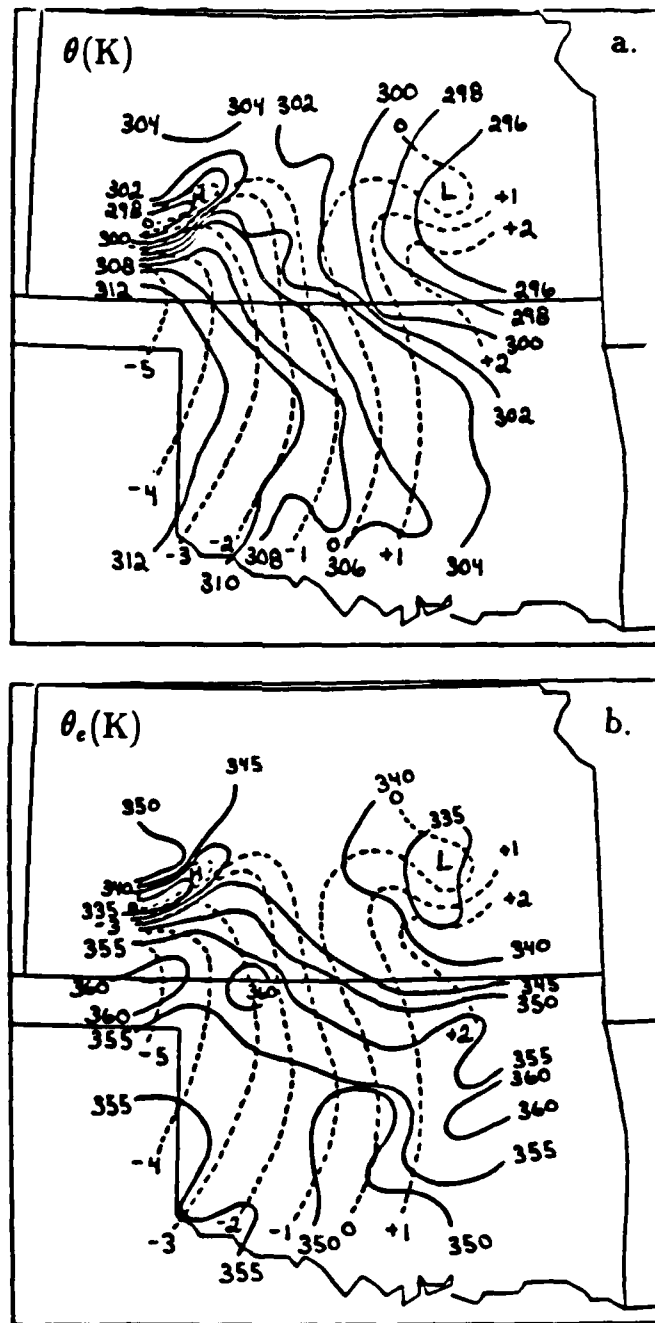


Fig. 31. Analyses of potential temperature (a) and equivalent potential temperature (b) at 2300 GMT, 10 June 1985. Temperature contours (K) are solid and pressure contours (mb) are dashed lines.

in association with the rain showers there and another in western Kansas with the squall line. Prior to the arrival of the squall line, pre-existing values of θ_e generally exceeded 345K below 800 mb in the western portion of the network. The low surface values of θ_e (about 333K) observed later with the squall line in Fig. 31b could only have come from aloft since the only previous source of low θ_e was above 700 mb. Therefore, the region of minimum equivalent potential temperature implies descending motion. The cold dome shown in the vicinity of the squall line also represents the early location of the initial cold dome which formed as a result of the hail and heavy rainfall over western Kansas (see section 5c). This cold dome will subsequently expand and track southeastward with the mesohigh. A band of rather high θ_e extends across the network from the Oklahoma panhandle to eastern Oklahoma with two centers of greater than 360K.

Similar analyses are presented as Figs. 32a and b for 0230 GMT on 11 June near the storm's maturity. A large area of the network has been cooled due to the rainfall and cool downdrafts from the convective cells. Rather uniform potential temperatures averaging 295K cover much of Kansas and some of northern Oklahoma behind the convective line. The lowest temperatures, about 293K, are found to coincide with the location of the surface mesohigh. In the vicinity of the weak but strengthening wake depression we see no signs of warming at the surface in association with the warm air above the mesolow. The trough parallel to and in advance of the convective line coexists with a tongue of relatively high θ air streaming northward from southwestern Oklahoma. Quite a strong gradient of potential temperature exists in the vicinity of the convective line. With the corresponding analysis of equivalent potential temperatures, many of the same features are observed. Low values are again found in the vicinity of the mesohigh and show the effects of cool convective downdrafts.

At 0725 GMT (Figs. 33a and b), during the weakening stage of the MCS but the mature stage of the wake depression, the potential temperature field is very flat with only minor fluctuations observed across the network. This time period was chosen to illustrate once again that even during the most intense stage of the wake depression no high values of θ are observed. Williams (1963), pointed out that such occurrences are rare.

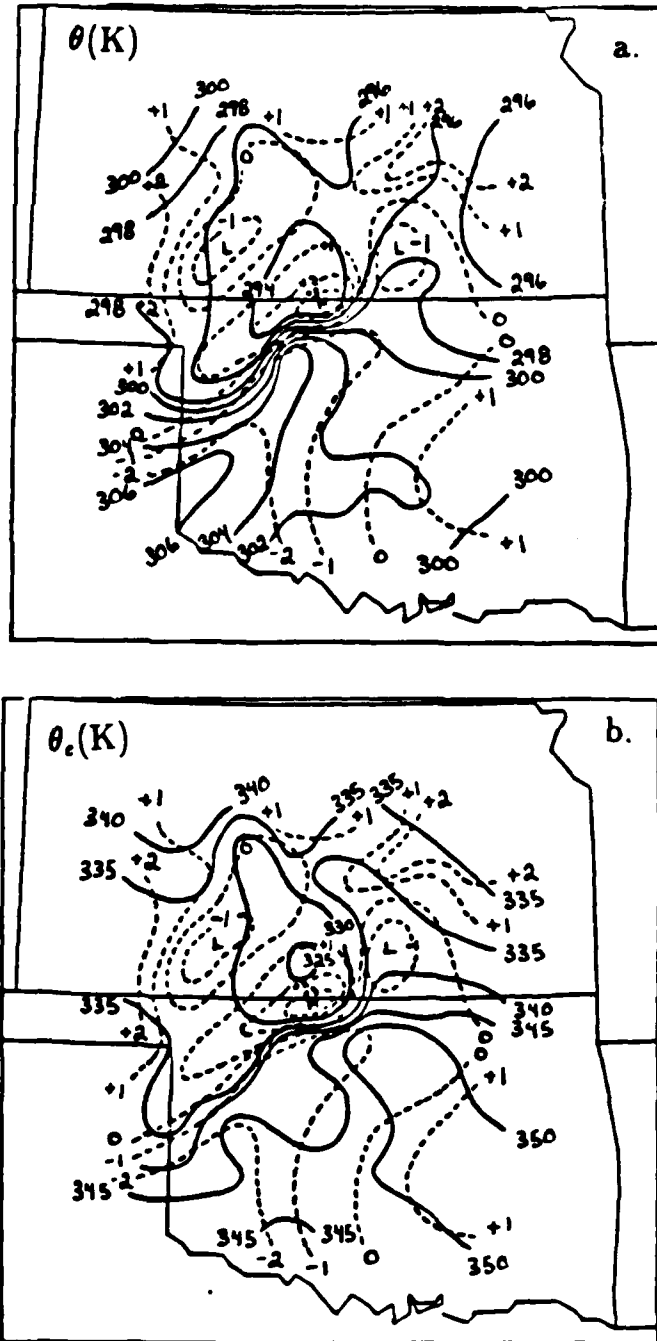


Fig. 32. As in Fig. 31 except for 0230 GMT, 11 June 1985.

The equivalent potential temperature analysis for this time shows the wake depression is centered in a relatively low region of θ_e but this may not be significant. Again the field is flat. The large change noticed with this analysis is the tight gradient of θ_e seen over the northwestern portion of the network associated with the approaching cold and dry air mass.

Chapter 6

TIME SERIES FOR SELECTED PAM STATIONS

Time series plots were prepared for three PRE-STORM PAM stations affected in some way by the squall system of 10-11 June 1985. These series show well the changing meteorological conditions associated with the passage of a midlatitude squall line. Figures 34 and 35 illustrate the time traces of surface pressure, rainfall amount, temperature and dewpoint for PAM stations 10 and 41, respectively. In both figures, the upper time series depicts the change in pressure and rainfall amounts while the lower series depicts the variability of temperature, dewpoint and pressure. Each time series begins at 2000 GMT on 10 June and continues to 1000 GMT on 11 June. Significant events along each trace are labeled.

For station 10, in the western region of the PRE-STORM network, evidence of the storm's passage and the arrival of a frontal system are clear in Fig. 34. The squall line was in the developing stage as it passed this station possessing both a weak mesohigh and an even weaker wake depression. The pressure trace shows that a small pressure jump and an accompanying weak mesohigh occurred shortly after 2220 GMT on 10 June. The immaturity of the convective line at this time explains the shallowness of the mesohigh. A few minutes after the pressure surge, heavy precipitation began. The rainfall trace shows the initial burst of rain from the convective line started near 2230 GMT and amounted to nearly 23 mm. A transition zone had not developed at this time but the figure shows a flattening of the rainfall trace indicating the rainfall abated some but never ceased. A secondary rain event, amounting to only 5 mm, followed at 2315 GMT with the onset of the lighter stratiform region. Indications of a wake depression on the pressure trace are weak at best because of the early stage of the squall line. The pressure fall evident

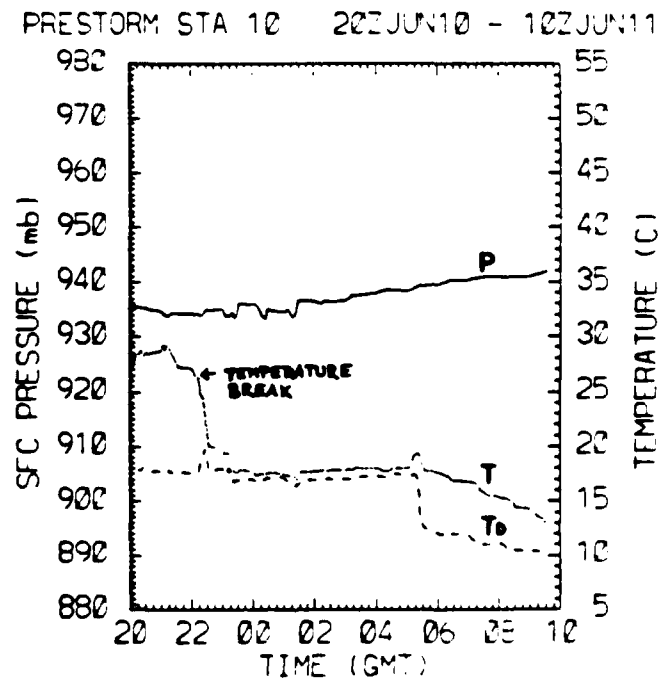
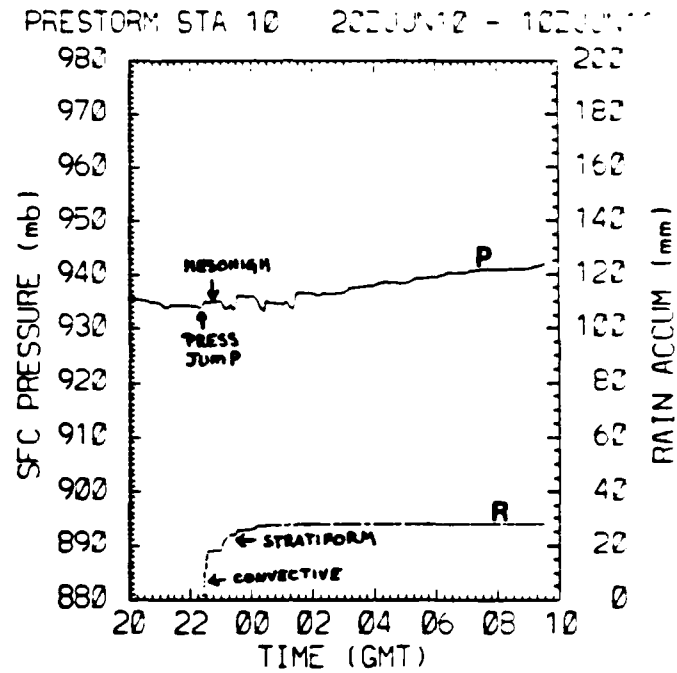


Fig. 34. Time series of pressure (mb) and accumulated rainfall (mm) in (a) and pressure, temperature (C) and dewpoint (C) in (b) at PAM station 10.

after the mesohigh is largely due to the passage of the mesohigh. The temperature and dewpoint traces show that in addition to a sharp cooling of 7°C within 15 minutes of the leading line's arrival, a moistening to nearly saturated conditions took place. From 0200 GMT and beyond, a steady rise in pressure was observed due to the approach and passage of a frontal system which later caused a substantial drying of the lower boundary layer.

Station 41, located in north central Oklahoma, was struck by the mature line. This station was affected by a strong mesohigh but not by a strong wake depression. Beginning with the pressure trace in Fig. 35, a small decrease in surface pressure is present just before the pressure jump indicating the passage of the pre-squall mesolow. Immediately this decrease is followed by a rapid pressure jump of 4 mb with higher pressures observed with time as the center of the mesohigh passed. The trace clearly shows the great magnitude of the mesohigh which persisted at the station for nearly 2.5 hours. Subsequently, a pressure drop and a weak wake depression are seen in the pressure trace. As shown in the pressure analyses in the previous section, the lowest pressures found with the wake depression did not pass this station but remained north in Kansas. The pressure at station 41 never fell to those observed in the pre-squall environment. All three precipitation regions discussed in section 5A are conspicuous in the rain accumulation trace. Fifteen minutes after the initial pressure jump, heavy rain from the deep convection began and amounted to 19 mm. This downpour was followed by a transition zone which was becoming visible in the reflectivity pattern (see Fig. 24). Additionally, the stratiform rain fell from 0350 to 0555 GMT provided 9 mm or 32% of the total rainfall. Soon after the pressure jump there was an 8°C temperature break along with a pronounced decrease in dewpoint. With the onset of precipitation the surface quickly reached near saturation.

The next time series plot presented is for PAM station 23 situated in the eastern portion of the PRE-STORM network within Kansas. This station was also affected by the mature squall line but unlike stations 10 and 41 an intense wake depression followed the mesohigh. Figure 36 illustrates this time series plot providing traces for surface pressure, rainfall amounts and maximum wind speed. Time extends from 0000 1200 GMT on 11 June 1985. As in the previous plots, significant events are labeled. As was seen for station

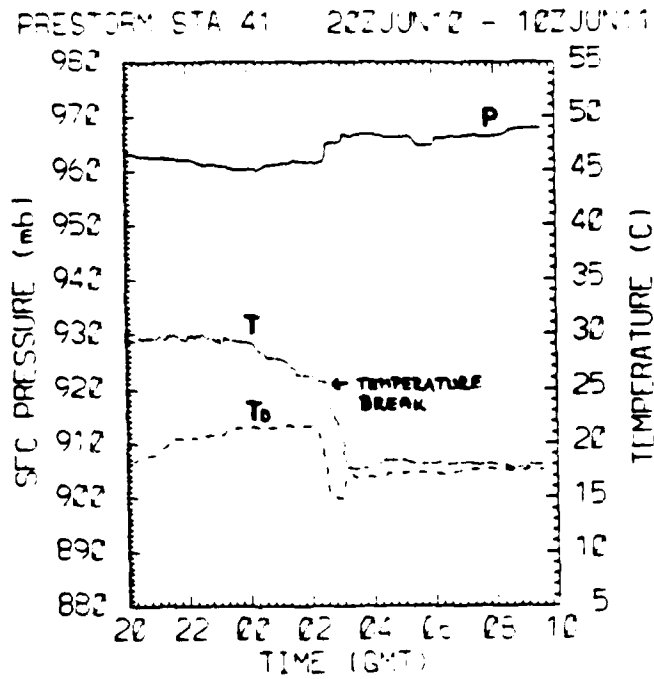
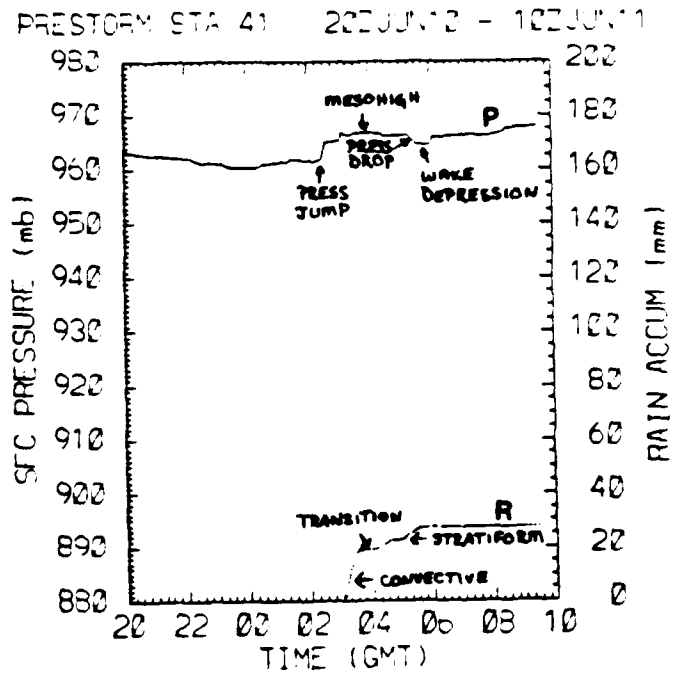


Fig. 35. As in Fig. 34 except for PAM station 41.

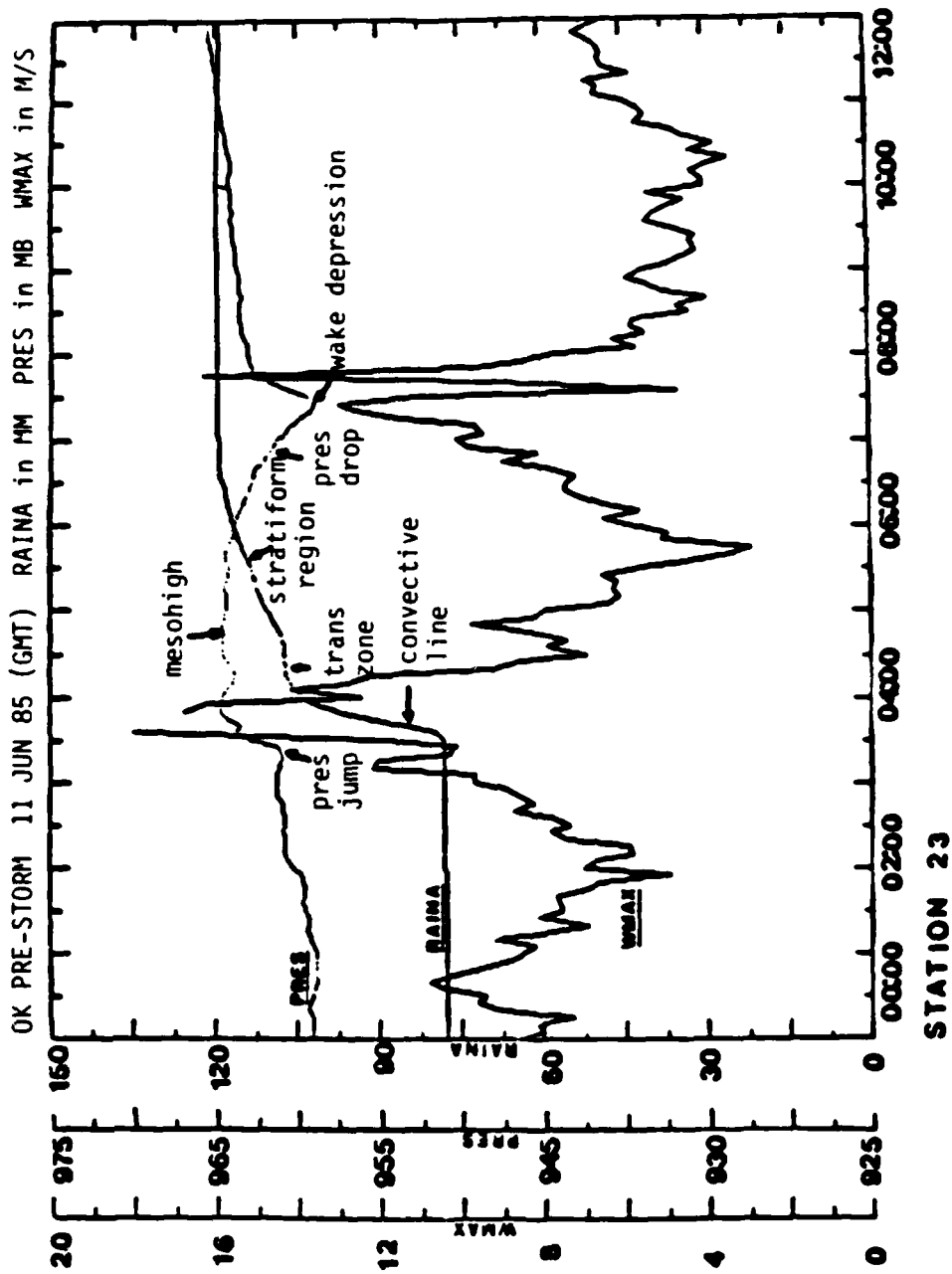


Fig. 36. Time series of maximum wind gust ($m s^{-1}$), pressure (mb) and accumulated rainfall (mm) at PAM station 23.

41, the pre-squall mesolow is evident in the pressure trace as a small pressure decrease preceding the pressure jump. A jump of almost 4 mb was observed with the arrival of the mesohigh and the convective line at 0330 GMT. Concurrent with the pressure surge is an abrupt wind gust associated with the convective downdrafts diverging at the surface. The initial burst of precipitation occurs a few minutes after the pressure surge and the wind gust. About 28 mm of rain fell from passage of the convective line. The mesohigh is clearly depicted in Fig. 36 as a large dome of high pressure which corresponds to the large cold dome. Succeeding the convective line is the transition zone noted in the rainfall trace. A long period of stratiform rainfall began at 0420 GMT and continued steadily until 0705 GMT. This illustrates the size of the stratiform region during the mature stage of the squall line. Thirteen millimeters of stratiform rain fell which is substantially greater than with stations 10 and 41. Note the much calmer winds during the stratiform period.

Some 3.5 hours after the initial pressure jump the pressure dropped to the pre-squall value at 0700 GMT. Thereafter, the pressure fell further as the strengthening wake depression approached. The trace indicates that a sharply defined and intense mesolow passed this station at 0725 GMT on 11 June. The pressure in the wake's center was roughly 2.2 mb below the pre-squall value. The difference between the maximum pressure in the mesohigh and the minimum in the wake depression was about 6 mb. As stated in section 5°C, the wake depression is positioned at the back edge of where the stratiform precipitation reaches the ground. The pressure trace in Fig. 36 confirms this observation. Soon after the passage of the wake depression, an abrupt rise in pressure occurs along with a second wind maximum. It is believed that this second strong gust is a result of the strong pressure gradient found at the back edge of the wake depression (see Fig. 28). Not all stations reported double wind maxima with the passage of this squall line, most only observed a single gust event.

Chapter 7

RESULTS OF LOWER TROPOSPHERIC ANALYSES FOR THE 10-11 JUNE SQUALL LINE

To further investigate the structure of the trailing region of this squall system as well as the mesoscale features found there, in particular the wake depression, analyses of potential and equivalent potential temperatures and relative humidity were prepared for 850 mb (about 1.0 km AGL). These analyses, along with the surface analyses already presented, provide a vertical view through the wake region. To summarize this section, a composite vertical cross-section of the trailing region is presented.

To begin, two upper air profiles are presented. The first following the MCS which traversed the network earlier on 10 June and the second following the 10-11 June squall line. These soundings illustrate well the "onion" or "diamond" shaped profile occasionally found in the wake region of both mid-latitude and tropical squall systems (Zipser, 1977; Ogura and Liou, 1980). Both soundings were launched at Wichita, Kansas. Figure 37 represents a vertical profile of temperature and dewpoint from the surface to the upper troposphere at 2100 GMT (1500L) on 10 June. This particular sounding was launched to the rear of the convective line of the MCS which passed Wichita, Kansas earlier on 10 June (not the squall line of focus in this report). Surface conditions are moist and nearly saturated although not as moist as have been observed. Immediately above the surface a thick layer of warm, dry air is present and above this layer the sounding is once again nearly saturated indicating the rawinsonde has most likely penetrated cloud base. The strong inversion between ground level and 911 mb separates the cool, moist conditions at the surface from the warm, dry conditions aloft. The temperature within this inversion increases slightly by 1.5°C from the surface value of 20.0°C, revealing the

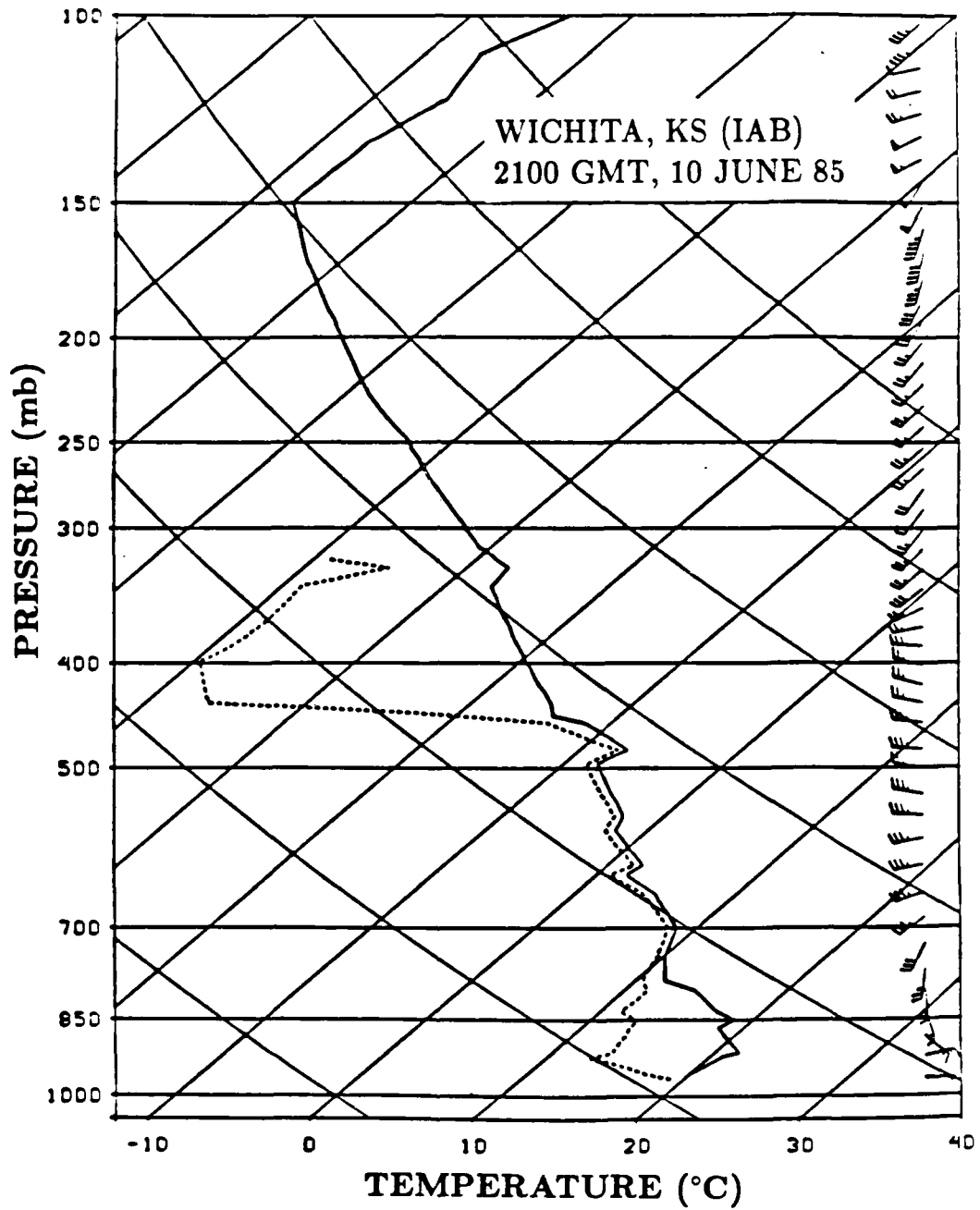


Fig. 37. Wake region "onion" sounding from Wichita (IAB), KS at 2100 GMT, 10 June 1985. Temperature and dewpoint traces are denoted with solid and dashed lines, respectively. Winds are plotted on the right (a full barb equals 5 m s^{-1} and a flag equals 25 m s^{-1}).

inversion is weak; however, the dewpoint decreases abruptly by 5.5°C to the inversion top. The maximum separation of temperature and dewpoint in the lowest levels of the troposphere is 8.1°C , found a little below the inversion top at 920 mb. Relative humidities in this vicinity averaged 60%. To the right, winds are observed to veer with height from the surface where outflow from the convective line is seen.

Figure 38 shows a sounding profile on a similar thermodynamic diagram but for 0624 GMT (0024L) on 11 June following the severe squall line discussed in this thesis. As with the previous sounding, this one was launched in the post-squall or wake region of the system following the precipitation. Overall, this profile differs little from the previous figure except the layer of warm, dry air is much more pronounced as is the "onion" shape. The surface air is relatively cool (18°C) and nearly saturated with the relative humidity at 98%. The intense rainfall from the squall's passage has left the ground wet and the adjoining air moist. Also, easterly surface winds at 7 m s^{-1} indicate persistent outflow from the convective line which passed some three hours earlier. As was the case with the previous sounding, a deep layer of warm, dry air is found just above the surface to 700 mb, about 2.7 km thick. Above 700 mb the sounding is moist again most likely indicating rear anvil cloud. The warmest temperature in this layer is 19°C at 850 mb which is a slight increase of 1°C from the surface value. The dewpoint clearly takes a dramatic drop of 11°C from the surface to near 850 mb resulting in lowest relative humidities around 45%. The maximum separation of temperature and dewpoint in this layer is found around 1 km AGL (850 mb) and measured 12°C . These observations are similar to those found by Ogura and Liou (1980) in their investigation of an onion sounding following a midlatitude squall line. Zipser (1977), in his study of tropical squall lines, also found the maximum separation of temperature and dewpoint to be located approximately 1 km AGL (900 mb) but was somewhat greater in magnitude at 15°C .

As for the wind profile, there is backing of winds with height. This differs from the previous sounding but must be interpreted cautiously since the winds may be largely ageostrophic in the vicinity of the squall lines; however, it could be an indication of cold air advection. A surface cold front and an upper level short wave is approaching the network as reviewed in the synoptic overview.

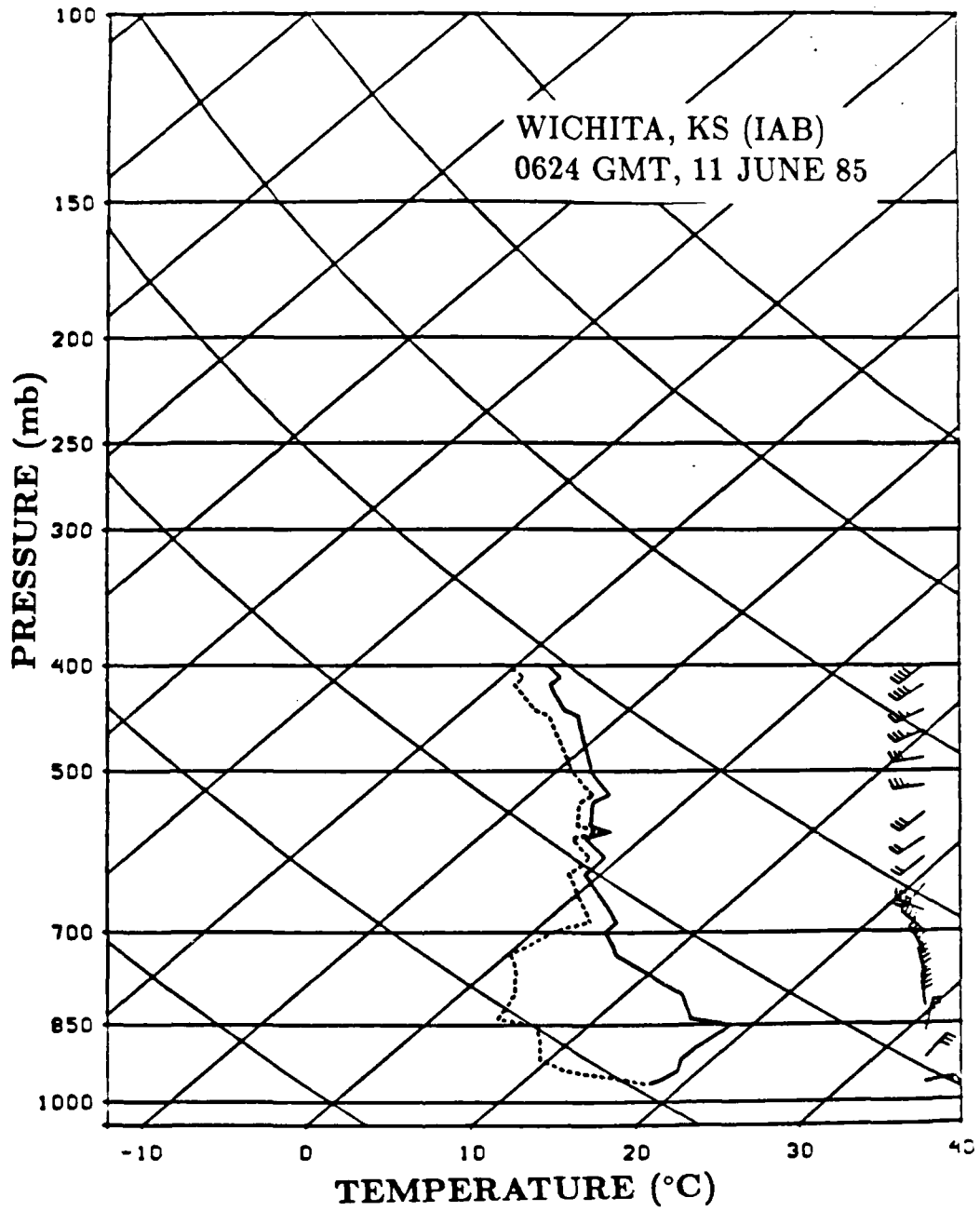


Fig. 38. As in Fig. 37 except for 0624 GMT, 11 June 1985.

Williams (1963) stated that the "warm wakes" which he observed in squall lines during the National Severe Storms Program were more extensive aloft than at the surface. In some cases, Williams observed a warming and drying at the surface following the convection indicating that some of the warm, dry air aloft had penetrated to the surface. From the sounding in Fig. 38 and the PAM/SAM data given in the analyses in section 5, it does not appear that the warm, dry air ever reached the surface for the 10-11 June storm. Likewise, for tropical systems, Zipser (1977) stated that it was "highly implausible" for the warm, dry air to penetrate to the surface. He observed that this air may reach within 100 m or so of the ground. Furthermore, Williams concluded that the warm, dry region located above the surface to the rear of the convection (as seen in Figs. 37 and 38) was a result of subsidence which was a typical feature with thunderstorm wakes. Other authors also reached a similar verdict saying the warming and drying of the air was a result of a mesoscale downdraft which is established underneath the rear anvil of the squall system (Houze, 1977; Zipser, 1977; Brown, 1979). It is widely acknowledged now that this layer of warm air is hydrostatically responsible for the observed wake depression.

The following three figures (Figs. 39-41) depict composites of relative humidity, potential and equivalent potential temperatures (with low-level reflectivity superimposed) at 850 mb centered about 0600 GMT on 11 June. This time was selected to permit an observation of the above parameters during the maturity of the wake depression. From the relative humidity composite (Fig. 39), moist air (greater than 90% relative humidity) indicating the position of the convective line is seen in Oklahoma and eastern Kansas. The dashed and double-dotted line shows the position of the surface gust front at 0600 GMT. To the rear of the convective line, in the proximity of the squall line wake, much drier air is observed with a broad band of below 60% relative humidity paralleling the leading convection. A pocket of quite dry air (less than 50% relative humidity) is located above the Wichita, Kansas station and coincides both with the dry layer evident in the Wichita sounding in Fig. 38 and the position of the surface wake depression. To the rear, a tongue of nearly saturated air is present with some humidities approaching 100%. The reflectivity pattern reveals the presence of some shower activity in this region of high moisture.

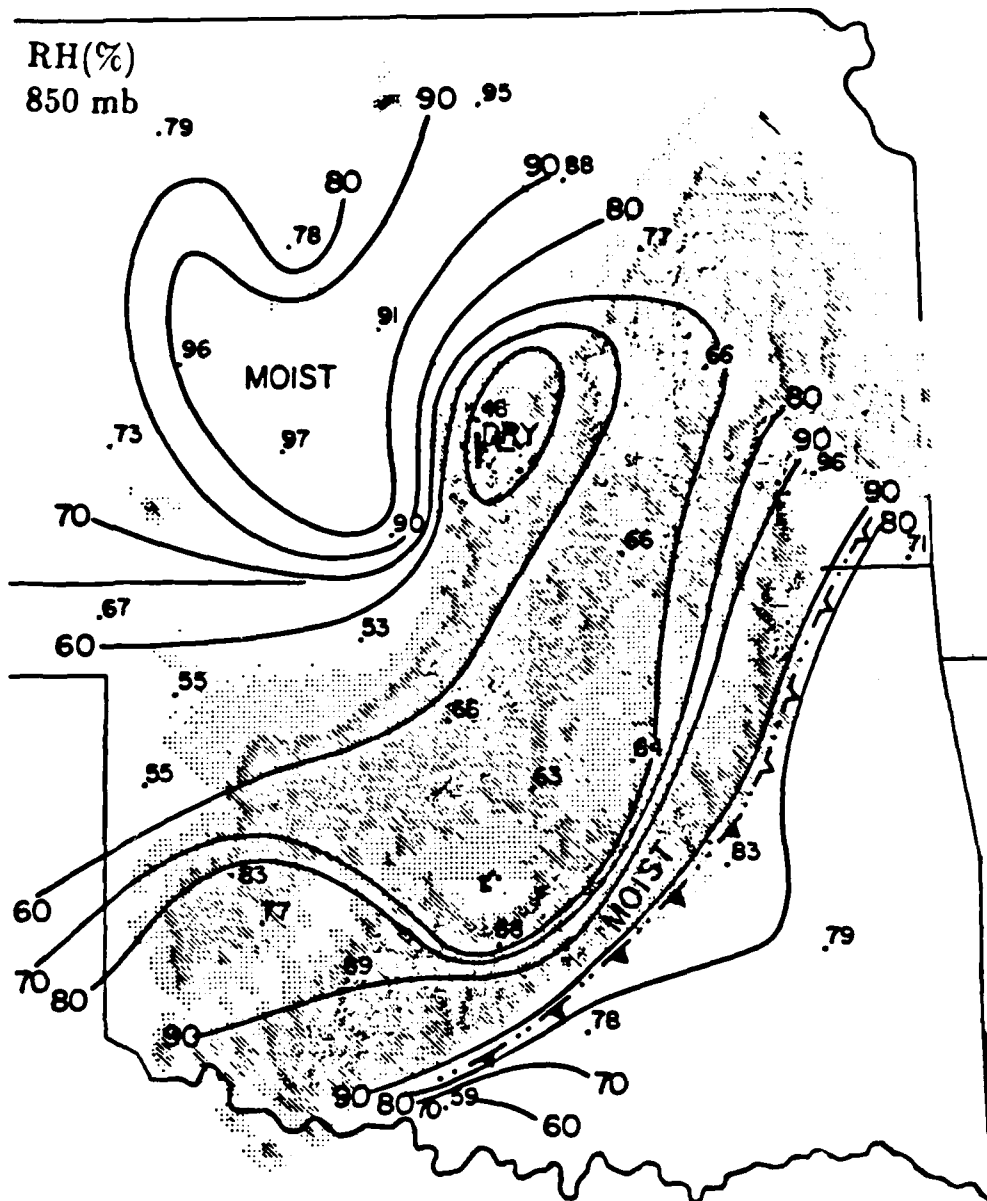


Fig. 39. Composite 850 mb relative humidity (%) with reflectivity at 0600 GMT, 11 June 1985. Reflectivity values from lightest to darkest shading are 15, 25, 35, 50 dB(z). Surface position of gust front denoted by dashed double-dotted line.

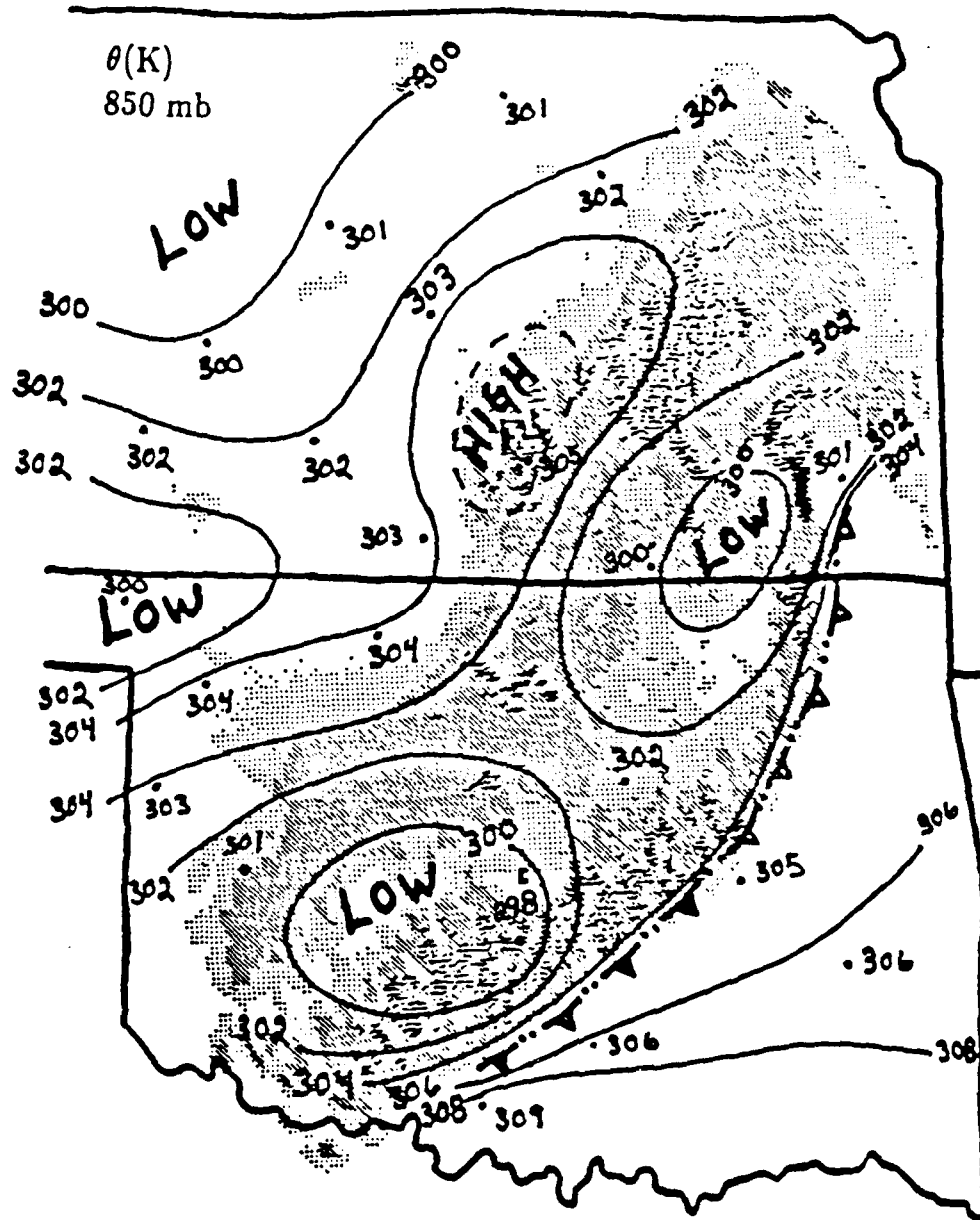


Fig. 40. Same as Fig. 39 except for potential temperatures (θ). Maxima and minima labeled High and Low, respectively. Contour values have been truncated to nearest whole number.

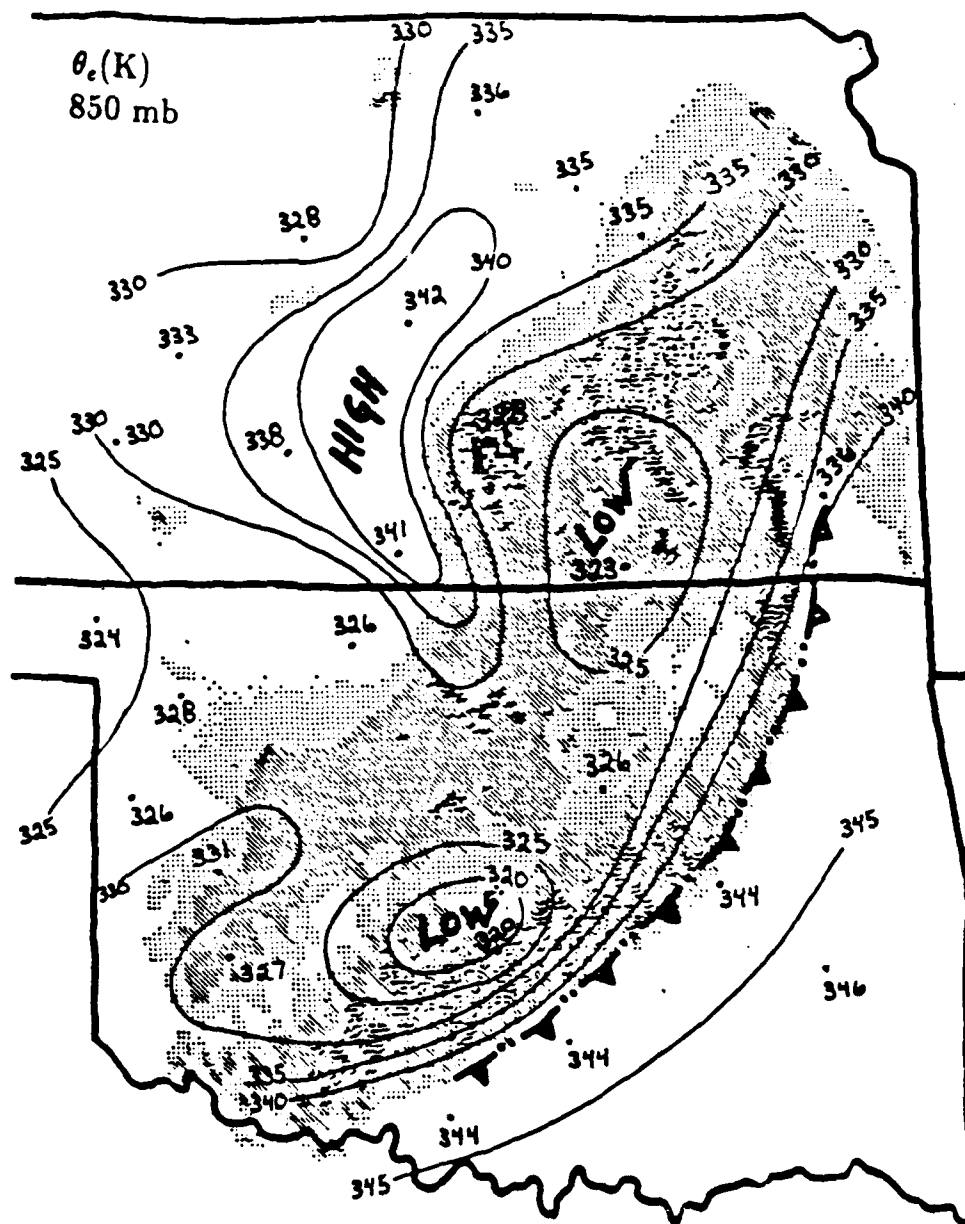


Fig. 41. Same as Fig. 40 except for equivalent potential temperatures (θ_e).

Figure 40 shows a composite of potential temperatures (θ). Two minima are found in the vicinity of the convective line, a result of evaporative cooling in the convective downdrafts, while a band of high potential temperature is analyzed farther to the rear with a center found over south Kansas near Wichita. As mentioned in section 5a in the discussion of the storm's reflectivity pattern, the convective line broke apart or split into two portions. The low θ centers in the composite coincide generally with the location of the two regions of deep convection after the split. The location of the split is observed to lie between the two low centers when the reflectivity pattern is superimposed onto the composite. Also, the notch seen in the echo pattern (thought to be related to the bowing and splitting of the leading line) is seen in the vicinity of a band of maximum potential temperatures. This maximum is located in the wake of the squall line and coincides with the dry pocket shown in the relative humidity composite. The high value shows the air to be relatively warm but also indicates the air is likely sinking in this locality. Relatively high values of θ are believed to be introduced at 850 mb from higher levels via subsidence. This subsiding, warm and dry air is manifested as the warm, dry layer in the "onion" sounding in Fig. 38. Vertically-pointing Doppler radar data reported by Houze, Rutledge and Biggerstaff (personal communication) substantiate the inference of subsidence. A figure illustrating this subsidence will follow later.

The next figure (Fig. 41) shows a composite of the equivalent potential temperatures (θ_e) in the PRE-STORM network. Again, two low centers are found in the vicinity of the convective line. This is reasoned by downward motion in a convectively unstable atmosphere where θ_e decreases with height. Farther rearward, a pronounced region of high values of θ_e were observed. Recall that this region of the network was also nearly saturated at 850 mb as seen in the relative humidity composite. When examining the streamlines both below and above 850 mb (not shown), convergence is seen at 900 mb in the area of the high equivalent potential temperatures, but divergence exists aloft at 800 mb. This implies that warm, moist air from near the surface is being lifted to the 850 mb level resulting in the high values of equivalent potential temperatures. As mentioned earlier, precipitation echos are seen in this region of moist air. If the vertical distribution of

θ_e is computed in this area, it is seen that above the 850 mb level the equivalent potential temperatures are decreasing with height to about 650 mb. This results in convective instability and hence can explain partially the presence of the precipitation echos.

A composite of relative humidity at 700 mb is presented as Fig. 42. As before, a band of high moisture is seen along the line of convective activity. When compared with the humidity analysis at the lower level, the moisture in this band extends in some places a little more rearward. This shows the convective line is tilting rearward with height. The dry band of relative humidities less than 60% is clear at 700 mb but is situated farther to the northwest away from the convective line. The secondary maximum of moisture found over west central Kansas also has tilted with height similar to the preceding dry band. Very dry air is intruding into the extreme northwestern corner of Kansas. The notch in the precipitation which is a region of enhanced rear inflow as found by Houze and Biggerstaff (personal communication, 1986) matches precisely with the shape and location of the dry tongue analyzed at 700 mb over the border region of Kansas and Oklahoma.

To show more evidence of subsidence in the vicinity of the wake depression, a composite analysis of potential temperature surfaces and relative humidity is shown as Fig. 43. This cross-section was chosen because it passes through the vicinity of the wake depression. A word of caution to the reader, the composite is highly compacted in the horizontal and stretched in the vertical and therefore must be viewed carefully. The most interesting feature is a pocket of dry air with relative humidity less than 50% (relative humidities are drawn with bold lines) seen above IAB at 0624 GMT. This dry air coincides with the dry layer shown in Fig. 38. The isentropic surfaces (shown with thin lines) reveal a moderately deep layer of near neutral stability at this station from 850-720 mb with potential temperature lines compacted below 850 mb indicating high stability. It can logically be inferred from these observations that subsidence warming and drying is occurring at this station. As stated before, it is this subsidence warming that causes a hydrostatic fall in pressure at the surface and subsequently the wake depression. The rear anvil of the squall line is seen in the composite as a moisture maximum above the two IAB stations. Humidities in this area exceed 90% which is generally regarded as an indication of cloudy

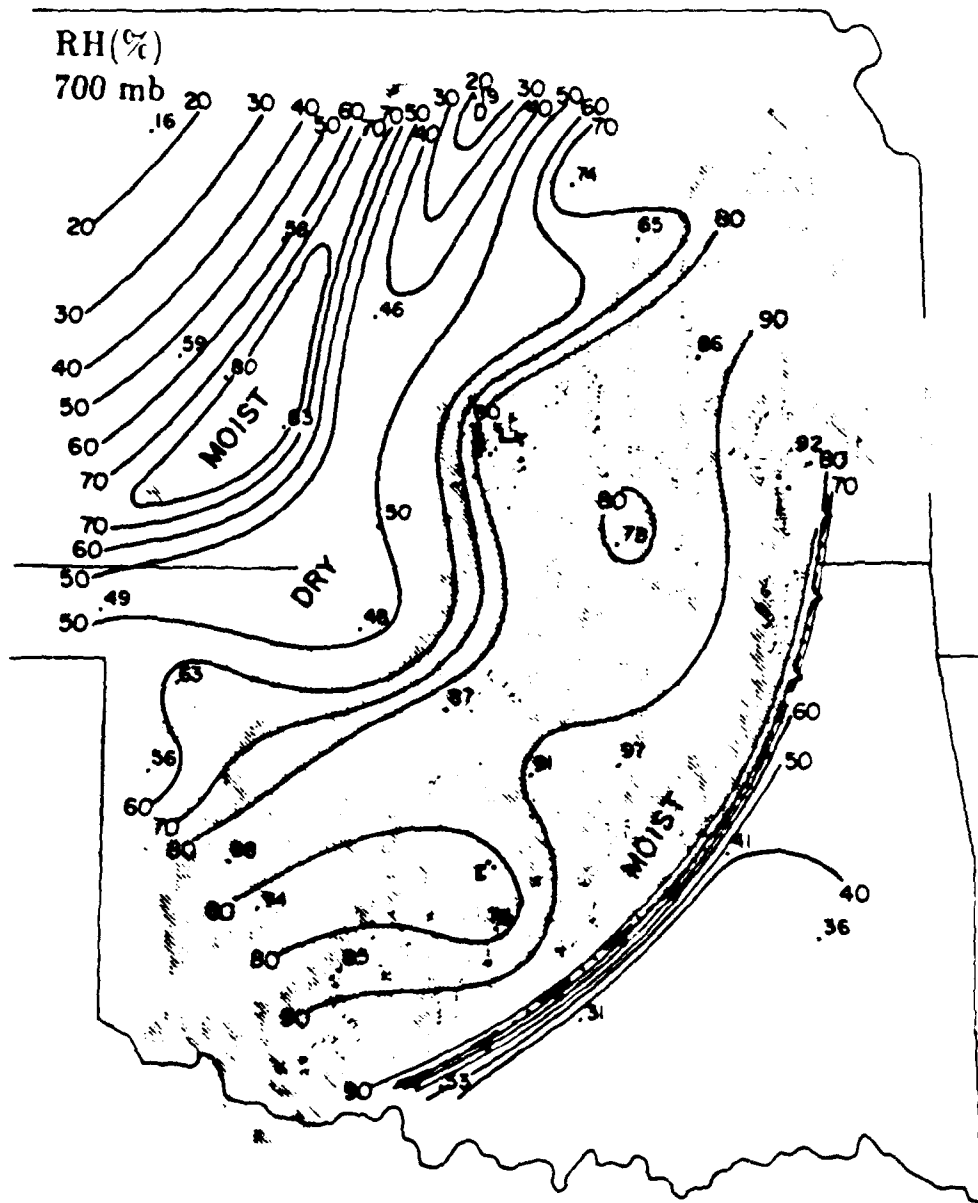


Fig. 42 Composite 700 mb relative humidity (%) with reflectivity

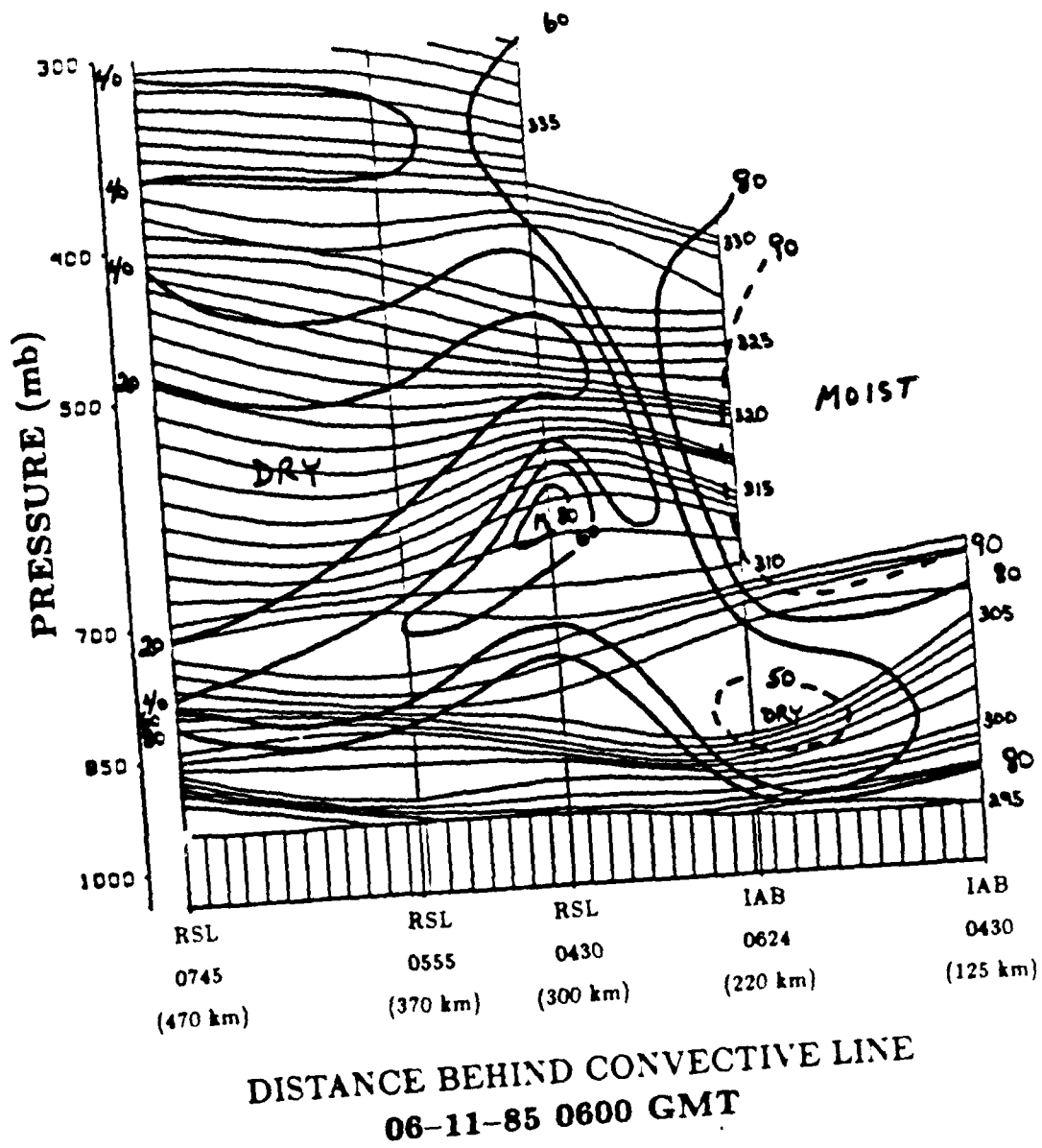


Fig. 43. Composite cross section of potential temperature (K) and relative humidity (%) at 0600 GMT, 11 June 1985. Isentropes are thin lines and isohumes are bold lines. Moist and dry regions labeled.

air. A secondary maxima of moisture is seen above RSL at 0430 GMT. The high values of equivalent potential temperature shown earlier in the 850 mb composite can be explained further by the presence of a vertical bulge of moisture (in excess of 80% RH) seen at RSL (0430 GMT). Also, between RSL (0745 GMT) and RSL (0555 GMT) and below 850 mb indications of a cold front are seen with the tightening of potential temperature lines sloping rearward with height from the surface. Finally, very dry air is seen aloft of RSL at 0555 GMT and 0745 GMT.

Following this discussion of the vertical distribution of potential temperature and relative humidity, it is appropriate now to discuss the vertical distribution of horizontal air flow relative to the moving squall line. Smull and Houze (1986b) constructed vertical cross sections perpendicular to the squall system of radar reflectivity and horizontal velocity for the 10-11 June case. Their cross sections are presented as Fig. 44. Panels (a) and (b) in the figure illustrate the reflectivity and velocity patterns, respectively, along 310 degrees azimuth for the far trailing section of the squall line. The stratiform region of precipitation is present as a band of relatively high dB(z) with a marked bright band at the melting level near 3 km. The corresponding velocity field shows clearly the rear inflow jet directed from left to right. Smull and Houze (1986b) found the inflow towards the convective line lies at the base of the trailing anvil which suggests the rear inflow evaporates substantially the stratiform precipitation which falls into it. Additionally, the rear inflow layer is seen to slope downward towards the convective line in panels (c) and (d). It is necessary to point out that the velocity panels represent horizontal velocities and hence do not explicitly show vertical velocities. However, vertical velocity calculations by Rutledge (personal communication, 1986) show that indeed the rear inflow jet descends from the trailing anvil region into the convective line.

To further examine how the rear inflow jet relates to the squall line as a whole, a composite vertical cross section similar to that prepared by Smull and Houze was constructed showing relative wind flow along the cross section and humidity (Fig. 45). The horizontal distance from station IAB (0431 GMT) to station RSL (0555 GMT) is approximately 280 km. Arrows assist in depicting the jet features. The reader should be aware that this is a

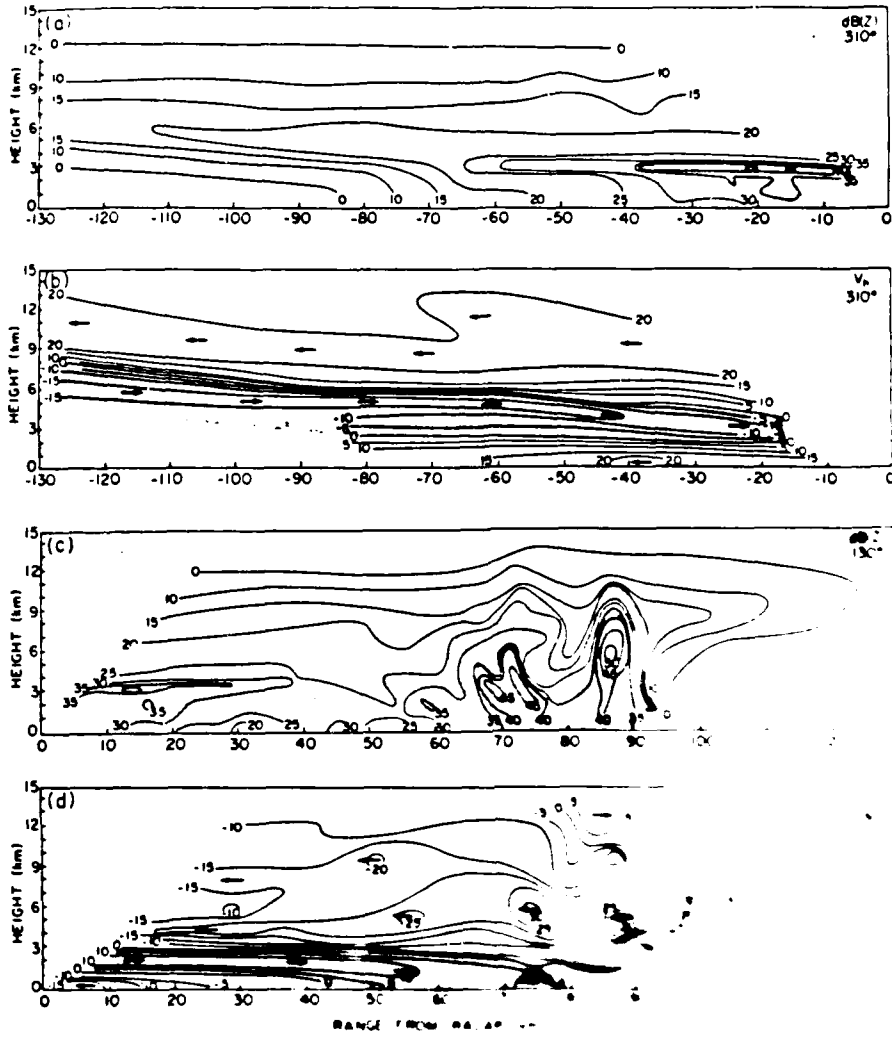


Fig 44 Vertical cross sections of
 0345-0353 GMT. The
 patterns contained in
 this figure are
 (a) and (d) are a
 reflection of the
 direction of the
 wind.

AD-A135 609

OBSERVATIONS OF A MIDLATITUDE SQUALL LINE BOUNDARY
LAYER WAKEUP AIR FORCE INST OF TECH WRIGHT-PATTERSON
AFB OH P HAMILTON 1987 AFIT/CI/NR-87-451

2/2

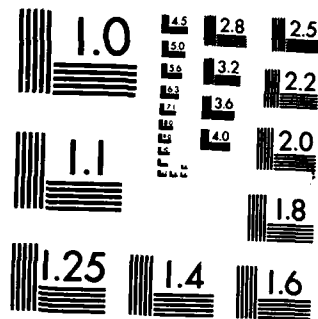
UNCLASSIFIED

F G 4/2

NL



END
DATE
FILMED
1-87



MICROCOPY RESOLUTION TEST CHART
NATIONAL BUREAU OF STANDARDS-1963-A

composite figure using soundings from various times centered about 0600 GMT and not an instantaneous look at the trailing region of the squall line. Also, some distortion may exist in the transition from RSL soundings to IAB soundings. High humidities characterize the trailing rear anvil (seen above the two IAB soundings) and the nearly saturated surface. This cross section shows the rear inflow jet to exist near the base of the anvil cloud as found by Smull and Houze. The strongest inflow is found above RSL (0430 GMT) in excess of 10 m s^{-1} . From there the rear inflow is observed to decelerate somewhat to $5\text{-}10 \text{ m s}^{-1}$ towards the convective line. Smull and Houze also showed a deceleration of the rear inflow from 15 m s^{-1} to about 10 m s^{-1} . The reason for the discrepancy in wind speeds is probably due to the different times for each cross section. Perhaps most revealing is the apparent correlation between the descending rear inflow and the downstream pocket of dry air observed above IAB (0624 GMT). As the rear inflow descends under the anvil, individual air parcels both within and below the jet may also descend and subsequently should warm and dry via adiabatic processes. From the surface pressure analyses, the location of the wake depression coincides with the warm, dry air observed aloft of IAB at 0624 GMT in Fig. 38 and in this cross section. This warm, dry pocket does not extend farther towards the convective line because the stratiform precipitation from the anvil (which is reaching the ground) is negating any warming which could be realized by the subsidence. Therefore, it is not surprising that the wake depression is consistently observed to lie at the back edge of the stratiform rainfall as seen in the pressure analyses in Section 5.3. Perhaps the warming of the air needed to hydrostatically explain the wake depression is a result of the subsidence driven by the rear inflow.

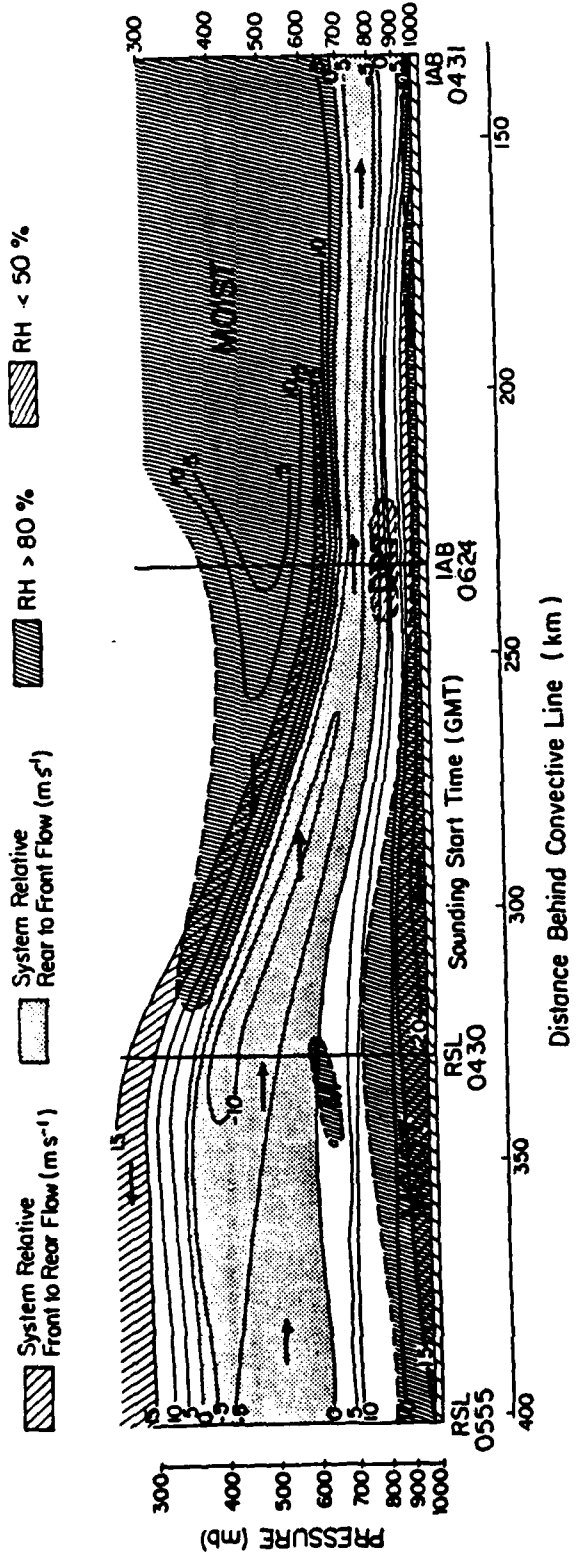


Fig. 45. Vertical composite cross section of system relative flow ($m s^{-1}$) and relative humidity (%) at 0600 GMT, 11 June 1985. Only that flow away from the convective line (front-to-rear jet) in excess of $15 m s^{-1}$ has been hatched. Arrows assist in depicting "jet" features.

Chapter 8

SUMMARY AND DISCUSSION

This thesis presented a thorough observational study of the surface and lower tropospheric features found with an intense midlatitude squall line which traversed the OK PRE-STORM mesonet network during 10-11 June 1985. The focus of the research was to investigate the horizontal and vertical characteristics, structure and lifecycle of the three mesoscale pressure perturbations frequently observed with these mesoscale convective systems: the mesohigh, wake depression and the pre-squall mesolow. In addition, how these pressure features related to other meteorological parameters such as precipitation, temperature (including potential temperatures), moisture, surface and upper level wind flow were explored. Many of the characteristics of this squall line, both at the surface and aloft, were similar to those discussed by earlier authors; however, new ideas regarding in particular the surface pressure field were reached via this research.

Several relationships between the reflectivity field and the surface pressure field were noted. The stratiform region of this squall line lagged the development of the convective line which reached maturity some two hours before the stratiform part. Similarly, the wake depression was observed to lag the maturation of the mesohigh with the mesohigh developing rapidly in response to evaporative cooling from the deep convective towers. However, the wake depression did appear to precede the appearance of the transition zone in the storm's reflectivity field. Furthermore, the squall line exhibited "bowing" which began near the time the squall reached greatest intensity. This bowing, as discussed by Smull and House (1985), is perhaps in response to the developing "notch" at the rear side of the stratiform region. This notch is a region of enhanced rear inflow into the system (House and Biggerstaff, 1986). The wake depression interestingly seemed to split into

two regions: one much more intense in Kansas while the other was weak and located to the south in Oklahoma. It seems from the analyses of surface pressure, reflectivity, and potential temperatures that the wake depression split in response to the splitting of the convective line and the two wake depressions analyzed were positioned to the rear of the two convective segments of the decaying squall line. On some pressure analyses, it was observed that the lowest pressures in the wake depression were found in the vicinity of "notch". Consistently, the wake depression was situated at the back edge of where the light stratiform rainfall reached the ground.

From early analyses of pressure and temperature and a review of the severe weather events which occurred with the early stages of this squall line, it is suggested that an initial cold pool was established in the western section of the PRE-STORM network and developed in response to intense convection and subsequent widespread hail and heavy precipitation. Furthermore, the mesohigh which developed with the squall system formed along with this cold pool. A single strong mesohigh could be tracked southeastward across the network and it is suggested that this was in response to the movement and intensification of this early cold pool.

Several other characteristics of the wake depression were noted from the research. This mesolow can undergo sudden intensification as seen in the analyses of pressure from 0700 to 0725 GMT on 11 June. It appears that the wake depression is not a smooth, uniform area of lower pressure but may have small scale features embedded within. With the passage of the wake low a second wind maximum was observed and is attributed to the tight pressure gradient and convergence analyzed at the rear edge of the wake depression. The surface winds are not observed to flow into the center of this low pressure feature even during its most intense stage. The air flows through the wake low and converges at the back edge with the surrounding environment.

Occasionally, "heat bursts" are observed at the surface in response to the passage of squall lines. This may be in response to the warm air found below the trailing anvil which might penetrate to the ground (Williams, 1963). For this squall system, no heat bursts were observed. It does not appear that any significant warming or drying at the

surface occurred in response to the passage of the wake depression. In addition, the lowest dewpoints were not found to coincide with the wake depression as was observed with tropical squall lines by Zipser (1977). With regard to the movement of the mesoscale pressure features, the path taken by the wake depression and the mesohigh differed by about 45 degrees.

From composite analyses of potential temperatures and relative humidity along with upper air profiles, it was concluded that the air is sinking adiabatically in the vicinity of the wake depression which accounts for the warming and drying observed above this feature. From upper air analyses of relative wind flow, the rear inflow jet and the front-to-rear jet was clearly seen to exist with this squall line as similarly found by Smull and Houze (1986). Furthermore, it was stated that research by other authors observed the rear inflow jet to descend towards the convective line. It was mentioned earlier in this thesis that the debate continues as to the cause of the subsidence found under the trailing anvil cloud of the squall line. Clearly, evaporative cooling from anvil rainfall may be a driving factor in the subsidence as concluded by Zipser (1977) and Brown (1979) among others; however, as Miller and Betts (1977) concluded, this phenomenon may in part be dynamically driven. It is suggested that the wake depression frequently observed at the surface behind the stratiform region of midlatitude squall lines is in part a manifestation of the descending rear inflow jet. In the cross section (Fig. 45), the dry pocket found over IAB (0624 GMT) does not exist farther towards the convective line even though the jet is still descending. This can be explained through the effects of the stratiform rain falling from the anvil base to the ground. Any warming gained from descent in the rear inflow is offset by evaporation of this precipitation. This explains why the wake depression at the surface is observed to "hug" the back edge of the stratiform precipitation.

During the OK PRE-STORM field experiment it was observed that occasionally a successive series of MCS developed and passed over the same region one following the other. Further research is needed to explore the possibility that the convergence observed at the rear edge of the wake depression may in part trigger new convection behind the MCS with which the wake is associated.

REFERENCES

- Atkinson, B.W., 1981: *Meso-scale Atmospheric Circulations*, Academic press, 495 pp.
- Augustine, J.A., and E.J. Zipser, 1986: The use of wind profilers in a mesoscale experiment. *Bull. Amer. Meteor. Soc.*, **68**, 4-17.
- Bluestein, H.B., and M.H. Jain, 1985: Formation of mesoscale lines of precipitation: Severe squall lines in Oklahoma during the spring. *J. Atmos. Sci.*, **42**, 1711-1731.
- Brown, J.M., 1979: Mesoscale unsaturated downdraft driven by rainfall evaporation: A numerical study. *J. Atmos. Sci.*, **36**, 313-338.
- Byers, H.R., and R.R. Braham, 1949: *The Thunderstorm*, U.S. Weather Bureau, Washington, D.C., 287 pp.
- Cheng, C. and R.A. Houze, 1979: The distribution of convective and mesoscale precipitation in GATE radar echo patterns. *Mon. Wea. Rev.*, **107**, 1370-1381.
- Darkow, G.L., and R.L. Livingston, 1975: Hourly surface static energy analysis as a delineator of thunderstorm outflow areas. *Mon. Wea. Rev.*, **103**, 817-822.
- Fujita, T., 1955: Results of detailed synoptic studies of squall lines. *Tellus*, **4**, 405-436.
- Fujita, T., 1963: Analytical mesometeorology: A review. *Meteor. Monogr.*, No. 27, 77-125.
- Fujita, T., 1979: Objectives operation, and results of Project NIMROD. Preprints 11th Conf. Severe Local Storms, Kansas City, MO, Amer. Meteor. Soc., 259-266.

- Fujita, T., 1981: Tornadoes and Downbursts in the context of generalized planetary scales. *J. Atmos. Sci.*, **38**, 1511-1534.
- Houze, R.A., Jr., 1977: Structure and dynamics of a tropical squall- line system observed during GATE. *Mon. Wea. Rev.*, **105**, 1540- 1567.
- Hoxit, L.R., C.F. Chappell and J.M. Fritsch, 1976: Formation of mesolows or pressure troughs in advance of cumulus clouds. *Mon. Wea. Rev.*, **104**, 1419-1428.
- Humphreys, W.J., 1929: *Physics of the Air*, McGraw Hill, 339 pp.
- Johnson, B.C., 1983: The heat burst of 29 May 1976. *Mon. Wea. Rev.*, **111**, 1776-1792.
- Johnson, R.H., and J.J. Toth, 1986: Preliminary data quality analysis for May-June 1985 Oklahoma-Kansas PRE-STORM PAM II Mesonet network. Atmospheric Science Paper No. 407, Colorado State University, Dept. of Atmos. Sci., Fort Collins, CO, 41 pp.
- Leary, C.A., and R.A. Houze, 1979: Melting and evaporation of hydrometeors in precipitation from the anvil clouds of deep tropical convection. *J. Atmos. Sci.*, **36**, 669-679.
- Leary, C.A., 1984: Precipitation structure of the cloud clusters in a tropical easterly wave. *Mon. Wea. Rev.*, **112**, 313-325.
- LeMone, M.A., 1983: Momentum transport by a line of cumulonimbus. *J. Atmos. Sci.*, **40**, 1815-1834.
- LeMone, M.A., G.A. Barnes and E.J. Zipser, 1984: Momentum flux by lines of cumulonimbus over the tropical oceans. *J. Atmos. Sci.*, **41**, 1914-1932.
- Levine, J., 1942: The effect of vertical accelerations on pressure during thunderstorms. *Bull. Amer. Meteor. Soc.*, **23**, 52-61.

- Maddox, R.A., 1983: Large-scale meteorological conditions associated with midlatitude, mesoscale convective complexes. *Mon. Wea. Rev.*, **111**, 1475-1493.
- Miller, M.J., and A.K. Betts, 1977: Traveling convective storms over Venezuela. *Mon. Wea. Rev.*, **105**, 833-848.
- Newton, C.W., 1966: Circulations in large shared cumulonimbus. *Tellus*, **18**, 699-713.
- Ogura, Y., and M. Liou, 1980: The structure of a midlatitude squall line. *J. Atmos. Sci.*, **37**, 553-567.
- Roux, F., 1987: Characteristics of the west-African squall lines observed during COPT81, Extended Abstracts of the 17th Conference on Hurricanes and Tropical Meteorology, April 7-10, 1987, Miami, FL, 67-70, Amer. Meteor. Soc., Boston, MA.
- Sawyer, J.S., 1946: Cooling by rain as a cause of the pressure rise in convective squalls. *Quart. J. Roy. Meteor. Soc.*, **72**, 168.
- Schaefer, J.T., L.R. Hoxit and C.F. Chappell, 1985: Thunderstorms and their mesoscale environment. In *Thunderstorm Morphology and Dynamics*, E. Kessler, Ed., University of Oklahoma Press, 113-131 pp.
- Showell, L., 1986: Rawinsonde processing techniques at the National Severe Storms Laboratory for the 1985 PRE-STORM data set. Informal Report, National Severe Storms Laboratory, Norman, OK.
- Smull, B.F., and R.A. Houze, Jr., 1985: A midlatitude squall line with a trailing region of stratiform rain: Radar and satellite observations. *Mon. Wea. Rev.*, **113**, 117-132.
- Smull, B.F., and R.A. Houze, Jr., 1986a: Dual-Doppler radar analysis of a mid-latitude squall line with a trailing region of stratiform rain. *J. Atmos. Sci.*, (Submitted for publication).

- Smull, B.F., and R.A. Houze, Jr., 1986b: The rear inflow jet in mesoscale convective systems, Preprints of the 23rd Conference on Radar Meteorology and Conference on Cloud Physics, September 22-26, 1986, Snowmass, CO, J163-J166, American Meteorological Society, Boston, Mass.
- Storm Data, 1985, Vol. 27, No. 6, p. 14. NOAA/National Climatic Data Center, Asheville, NC, 28801.
- Tepper, M., 1950: A proposed mechanism of squall lines: The pressure jump line. *J. Meteor.*, **7**, 21-29.
- Williams, D.T., 1953: Pressure wave observations in the central midwest, 1952. *Mon. Wea. Rev.*, **81**, 278-298.
- Williams, D.T., 1954: A surface study of a depression-type pressure wave. *Mon. Wea. Rev.*, **82**, 289-295.
- Williams, D.T., 1963: The thunderstorm wake of May 4, 1961. Nat. Severe Storms Project Rep. No. 18, U.S. Dept. of Commerce, Washington, D.C., 23 pp.
- Zipser, E.J., 1969: The role of organized unsaturated convective downdrafts in the structure and rapid decay of an equatorial disturbance. *J. Appl. Meteor.*, **8**, 799-814.
- Zipser, E.J., 1977: Mesoscale and convective-scale downdrafts as distinct components of squall-line structure. *Mon. Wea. Rev.*, **105**, 1568-1589.

LMED
88